THESIS APPROVAL

GRADUATE SCHOOL, KASETSART UNIVERSITY

Master of Science (Metrology)
DEGREE

Metrology
FIELD

Physics
DEPARTMENT

TITLE: Measurement of Rotation Rate by Using Fiber Optic Gyroscope

NAME: Mr. Korsakul Punyavardhana

THIS THESIS HAS BEEN ACCEPTED BY

B. Panacharoensawad **THESIS ADVISOR**
(Associate Professor Bancha Panacharoensaward, Dr.Ing.)

S. Kyl. **COMMITTEE MEMBER**
(Captain Sahapong Kruapech, M.S.E.E.)

Teerasak Veerapaspong **COMMITTEE MEMBER**
(Mr. Teerasak Veerapaspong, Dr.Eng.)

E. Hoonnivathana **DEPARTMENT HEAD**
(Mr. Ekachai Hoonivathana, M.S.)

APPROVED BY THE GRADUATE SCHOOL ON 23/02/2006

Vinai Artkyo **DEAN**
(Associate Professor Vinai Artkongharn, M.A.)

THESIS

MEASUREMENT OF ROTATION RATE BY USING FIBER OPTIC GYROSCOPE

KORSAKUL PUNYAVARDHANA

A Thesis Submitted in Partial Fulfillment of
the Requirements for the Degree of
Master of Science (Metrology)
Graduate School, Kasetsart University
2006

ISBN 947-16-1141-2

Korsakul Punyavardhana 2006: Measurement of Rotation Rate by Using Fiber Optic Gyroscope. Master of Science (Metrology), Major Field: Metrology, Department of Physics. Thesis Advisor: Associate Professor Bancha Panacharoensawad, Dr.Ing. 104 pages.
ISBN 974-16-1141-2

Fiber optic gyroscope is an instrument to measure angular displacement or rotation rate. Sagnac effect occurs when two counter propagation beams, (one clockwise, CW, and another counter clockwise, CCW) arising from the same source, propagate inside a fiber optic coil along the same closed path. If rotation occurs, the CW and CCW beams experience a relative phase different which is proportional to the rotation rate. Therefore, the change of rotation, perpendicular to the plane of the path of the light source, can be determined. The objectives of this experiment are: (a) to build prototype fiber optic gyroscope, (b) to study Sagnac effect in fiber optic and (c) to analyze the relationship between rotation rate and output signal from fiber optic gyroscope. The experiments were performed at 5 different rotation rates (i.e. 0.00, 0.13, 0.16, 0.24 and 0.38 radian/s) both in counter clockwise and clockwise directions.

The results of measurement show that the output signal from fiber optic gyroscope agrees with rotation rate. The higher rotation rate, the greater change of output voltage is obtained. The variation of output voltage definitely depends on the direction of rotation.

K. Punyavardhana.
Student's signature

B. Panacharoensawad
Thesis advisor's signature

16 / 2 /2006

ACKNOWLEDGMENTS

I would like to express my sincere gratitude and deep appreciation to my advisor, Associate Professor Dr. Bancha Panacharoensawad for his initiative idea, encouragement and always available answers. Grateful acknowledgments are likewise extended to my committee members, Dr. Teerasak Veerapaspong, Captain Sahapong Kruapech for their precious suggestion, insight and support.

For much needed technical support and guidance in the theory, photonic experiment and parts development, I would like to thank Mr. Kanokpot Areekul and. Flight Sergeant First Class Kittisak Nugkim. My gratitude is extended to all of kind-hearted students in the Department of Physic, Kasetsart University.

The last but not the least, my special thanks goes to my family and friends for their support and inspiration. Usefulness of this thesis, I dedicate to my family and all of my teachers.

Korsakul Punyavardhana
December 2005

TABLE OF CONTENTS

LIST OF TABLES

LIST OF FIGURES

LIST OF FIGURES (Cont'd)

LIST OF ABBREVIATIONS

FOC = Fiber Optic Gyroscope
IFOC = Interferometric Fiber Optic Gyroscope
RFOV = Resonant Fiber Optic Gyroscope
SLD = Super Luminescent Diode
PZT = Piezoelectric Transducer
CW = Clockwise
CCW = Counter Clockwise
UV = Ultra Violet
DC = Direct Current
NA = Numerical Aperture
BS = Beam Splitter
D.O.E. = Design of Experiment
LASER = Light Amplification by Stimulated Emission Radiation.
pcs. = Pieces
R.S.S. = Root Sum Square
S.D. = Standard Deviation
TC = Temperature Condition
VC = Vibration Condition
LC = Light Condition

MEASUREMENT OF ROTATION RATE BY USING FIBER OPTIC GYROSCOPE

INTRODUCTION

Sagnac effect was discovered in 1913 by Georges Sagnac. This effect occurs when two counter propagation beams, (one clockwise, CW, and another counter clockwise, CCW) arising from the same source, propagate inside an interferometer along the same closed path. At the output of the interferometer, the CW and CCW beams interfere to produce a fringe pattern. This pattern shift if a rotational rate is applied along an axis perpendicular to the plane of the path of the beam. Thus, the CW and CCW beams experience a relative phase different which is proportional to the rotational rate. Therefore, we can determine the rotational angle by the rotational rate and phase difference of CW and CCW beams. This effect became the most important basic theory for all optical gyroscopes.

After invention of a fiber optic in 1970, fiber optic gyroscope (FOG) had been created by combine the Sagnac effect and fiber optic technology. The fiber optic coil radius R is used in FOG instead of the interferometer. Because of this change the optical path and sensitivity was increase into multiple times. With the better quality, performance, resolution (0.001°/hr) and the lower manufacturing cost comparing with mechanical gyroscope. In the present, FOG was extensively used in many practical applications such as navigation guidance and control of aircraft missiles, automobiles, robots and spacecraft.

This field of technology does not attract many researchers in Thailand. The only way to acquire fiber optic gyroscope is to import from foreign country at high price. Consider from its capability and the reason above, it makes this research topic very interesting. The target of this research is the understanding of fiber optic gyroscope in theory and experiment to determine relation between angular displacement and output signal of fiber optic gyroscope. Result of this research will be the most important knowledge to create the fiber optic gyroscope at commercial scale.

Therefore, the objectives of the present study are:

1. To study Sagnac effect in fiber optic gyroscope,

2. To make a fiber optic gyroscope from a chosen design,

3. To analyze the relationship between angular displacement (rotational rate) and output signal from fiber optic gyroscope.

Scopes of this research are:

1. To design and make fiber optic gyroscope prototype and rotation table (controllable) using the proper design and equipment.

2. Experiment to determine the relation of an output signal from fiber optic gyroscope at different rotational rate.

LITERATURE REVIEW

Basic Physics of Light

Electromagnetic radiation visible to the human eye is generally referred to light, however, electromagnetic radiation that is not visible to the human eye is continuously being emitted and absorbed all around us at all times. The vast majority of the electromagnetic energy emitted by the sun is in the infrared region and is not visible. Our eyes are detectors that only respond to electromagnetic radiation within certain energy levels. The carriers of electromagnetic radiation are often referred to a "photons". The study of light as "groups of photons" or "waves" has been underway for hundreds of years. In this section, the basic fundamental principles of lights, useful for understanding fiber optic technology, are presented.

1. Photon

Eric U *et al.* (1998) Except in the limit of extremely low light levels, a study of individual photons is not needed to understand most of fiber optic technology. Certain facts regarding to photons are important, as they often are compared to electrons and electrical current, and are important for understanding how light interacts with matter such as glass or liquids. Further, large quantities of photons must be detected (and possibly measured) to determine their approximate number, and perhaps their distribution of wavelengths, or even their polarization properties. To that end, basic relationships between energy, velocity, wavelength, and frequency of light are introduced. In the following, SI units are used.

1.1 Energy, Velocity, Wavelength, and Frequency

Photons may be characterized by their energy-wavelength-frequency-velocity relationship. In its simplest form, the energy of a photon E (Joules), is equal to Planck's constant h (6.63×10^{-34} Joules·second) times the frequency f (cycles/second or "Hz") of the light:

$$E = hf \tag{1}$$

Frequency is related to velocity v (meters/sec) and wavelength λ (meters), as follows:

$$f = \frac{v}{\lambda} \tag{2}$$

Therefore, energy can be related to velocity, and wavelength or frequency:

$$E = \frac{hv}{\lambda} \tag{3}$$

Wavelength is usually measured in microns. With these simple relationships, it is easy to determine the energy of a photon, once the wavelength is known, or vice versa. Such determinations are common when analyzing the interaction of photons with various types of detectors, chemicals, or materials that may be utilized in fiber optic sensors. It is the energy of a photon that determines how a detector will respond to it. While optical fiber technologies utilize light throughout the electromagnetic spectrum, many applications do not use visible light. Figure 1 depicts the electromagnetic spectrum, the portion within which fiber technologies may operate, and the visible spectrum.

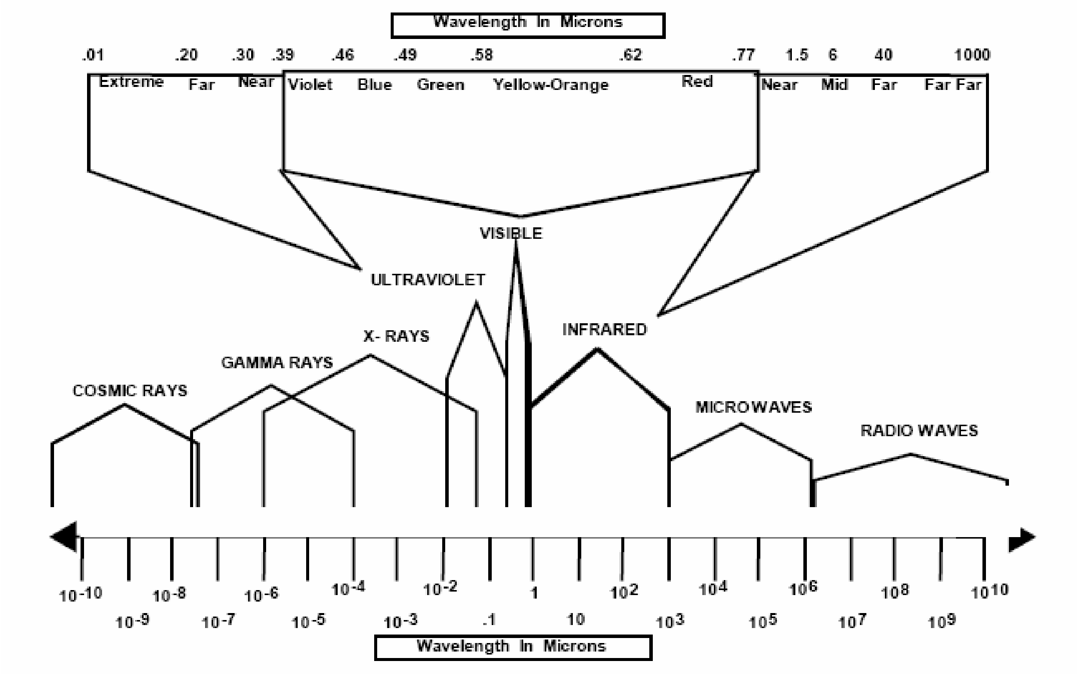

Figure 1 Electromagnetic spectrum.

2. **Light**

2.1 Ray Optics

Saleh and Teich (1994) Ray optics is the simplest theory of light. Light is described by rays that travel in different optical media in accordance with set of geometrical rules. Ray optics is concerned with the *location* and *direction* of light rays. It is therefore useful in studying image formation – the collection of rays from each point of an object and their redirection by an optical component onto a corresponding point of an image. Ray optics permits us to determine conditions under which light is guided within a given medium, such as a glass fiber.

2.1.1 Snell's Law

The index of refraction of an optical material (also called refractive index), denoted by n, plays a central role in geometric optics. It is the ratio of the speed of light c in vacuum to the speed v in the material.

$$n = \frac{c}{v} \tag{4}$$

Light always travels more slowly in a material than in a vacuum, so n for any material is always greater than unity. For vacuum $n = 1$.

For a monochromatic light and for a given pair of substances, a and b, on opposite sides of the interface, the ratio of the sine of the angle θ_a and θ_b, where both angles are measured from the normal to the surface, is equal to the inverse ratio of two indexes of refraction:

$$n_a \sin\theta_a = n_b \sin\theta_b, \tag{5}$$

where θ_a and θ_b are the incident and transmitted angles as shown in Fig. 2.

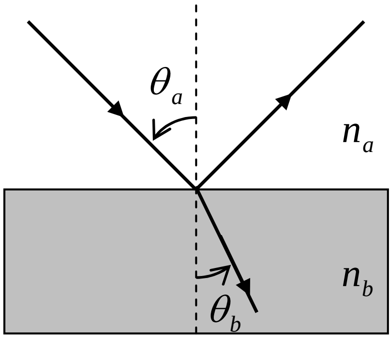

Figure 2 Reflection and refraction of light passing from first material to another.

2.1.2 Total Internal Reflections

For internal refraction ($n_1 > n_2$), the angle of refraction is greater than the angle of incidence, $\theta_2 > \theta_1$, so that as θ_1 increases, θ_2 reach 90° first. This occurs when $\theta_1 = \theta_c$ (The critical angle), with $n_1 \sin\theta_c = n_2$, so that

$$\theta_c = \sin^{-1}\frac{n_2}{n_1} \tag{6}$$

when $\theta_1 > \theta_c$, Snell's law cannot be satisfied and refraction does not occur. The incident ray is totally reflected as if the surface were a perfect mirror. The phenomenon of total internal reflection is the basic of many optical devices and optical fibers

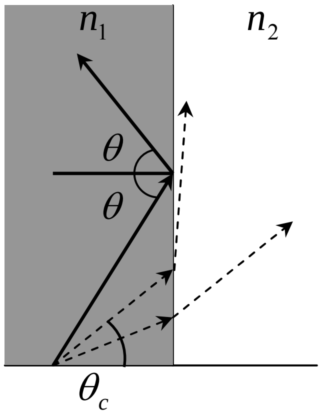

Figure 3 Total internal reflection at a planar boundary.

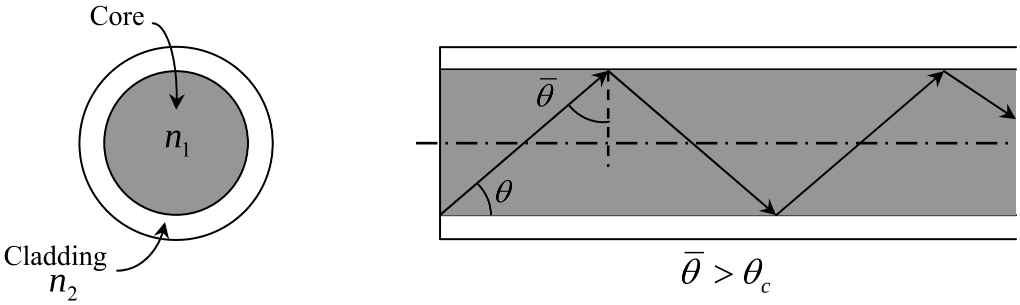

Figure 4 Total internal reflections in optical fiber.

2.2 Wave Optics

Light propagates in the form of wave. In free space, light wave travels with a constant speed $c_0 = 3.0 \times 10^8$ m/s (30 cm/ns or 0.3mm/ps). The range of optical wavelengths contains three band – ultraviolet (10 to 390 nm), visible (390 to 760 nm), and infrared (760 nm to 1 mm). The corresponding range of optical frequencies stretches from 3×10^{11} Hz to 3×10^{16} Hz, as illustrated in Fig. 5.

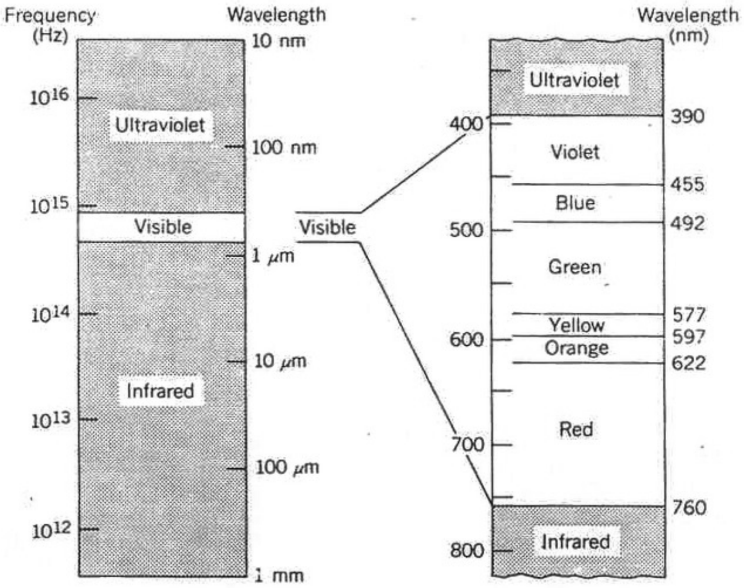

Figure 5 The Optical frequencies and wavelenghts.

Light is described by a scalar function, called the wave function, which obeys the wave equation. The precise physical meaning of the wave function is not specified; it suffices to say at this point that it may represent any components of the electric or magnetic fields. These, and a relation between the optical power density and the wave function, constitute the postulates of the scalar wave model of light, hereafter called wave optics.

2.2.1 Wave Equation

Light propagates in the form of wave. In free space, light wave travels with speed c_0. A homogeneous transparent medium such as glass is characterized by a single constant, its refractive index $n(\geq 1)$. In a medium of refractive index n, light wave travels with a reduced speed

$$c = \frac{c_0}{n} \tag{7}$$

An optical wave is described mathematically by a real function of position $r = (x, y, z)$ and time t, denoted $u(r, t)$ and known as the wave function**.** It satisfies the wave equation,

$$\nabla^2 u - \frac{1}{c^2}\frac{\partial^2 u}{\partial t^2} = 0 \tag{8}$$

Where ∇^2 is the Laplacian operator, $\nabla^2 = \partial^2/\partial x^2 + \partial^2/\partial y^2 + \partial^2/\partial z^2$. Any function satisfying (8) represents a possible optical wave.

Because the wave equation is linear, the principle of superposition is applicable. The statement of the principle is as follow if $u_1(r,t)$ and $u_2(r,t)$ represent optical waves then $u(r,t)=u_1(r,t)+u_2(r,t)$ also represents a possible optical wave.

At the boundary between two different media, the wave function changes in a way that depends on the refractive indices. However, the laws that govern this change depend on the physical significance assigned to the wave function The wave equation is approximately applicable to media with position-dependent refractive indices, provided that the variation is slow within distances of a wavelength. The medium is then said to be locally homogeneous. For such media, *n* in (7) and *c* in (8) are simply replaced by position-dependent functions *n*(*r*) and *c*(*r*), respectively.

2.2.2 Monochromatic wave

A monochromatic wave is represented by a wave function with harmonic time dependence

$$u(r,t)=a(r)\cos[2\pi\nu t+\varphi(r)] \tag{9}$$

as shown in Fig. 6 (a), where

$a(r)$ = amplitude
$\varphi(r)$ = phase
ν = frequency (cycles/s or Hz)
ω = $2\pi\nu$ = angular frequency (radians/s).

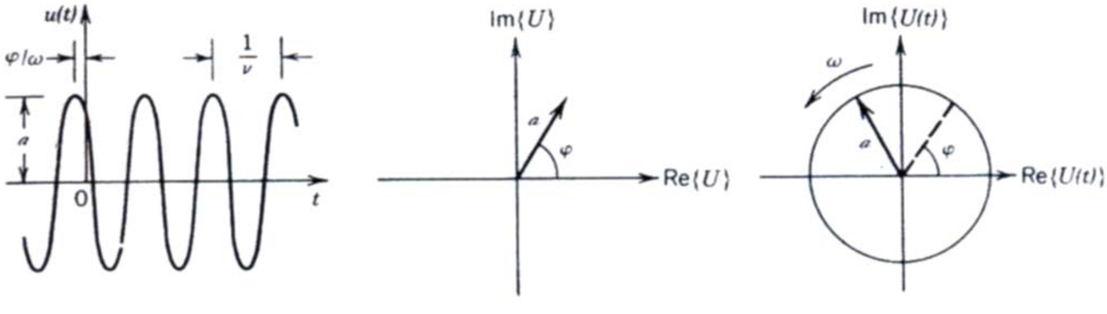

(a) (b) (c)

Figure 6 (a) The wave function *u*(*t*) is a harmonic function of time; (b) The complex amplitude $U=a\exp(j\varphi)$ is a fixed phasor; (c) The complex wave function $U=a\exp(j2\pi\nu t)$ is a phasor rotating with angular velocity $\omega=2\pi\nu$ radians/s.

Both the amplitude and the phase are generally position dependent, but the wave function is a harmonic function of time with frequency v at all positions. The frequency of optical waves lies in the range 3×10^{11} to 3×10^{16} Hz

2.2.3 Complex wave function

It is convenient to represent the real wave function *u*(*r*, *t*) in (9) in terms of a complex function

$$U(r,t) = a(r)\exp[j\varphi r]\exp(j2\pi vt), \tag{10}$$

so that

$$u(r,t) = \mathrm{Re}\{U(r,t)\} = \frac{1}{2}\left[U(r,t) + U^*(r,t)\right]. \tag{11}$$

The function *U*(*r, t*), known as the complex wave function, describes the wave completely; the wave function *u*(*r*, *t*) is simply its real part. Like the wave function *u*(*r*, *t*), the complex wave function *U*(*r, t*) must also satisfy the wave equation,

$$\nabla^2 U - \frac{1}{c^2}\frac{\partial^2 U}{\partial t^2} = 0 \tag{12}$$

Complex amplitude may be written in the form

$$U(r,t) = U(r)\exp(j2\pi\nu t), \tag{13}$$

where the time-independent factor $U(r) = U(r)\exp[j\varphi(r)]$ is referred to as the complex amplitude. The wave function *u*(*r*, *t*) is therefore related to the complex amplitude by

$$u(r,t) = \mathrm{Re}\{U(r)\exp(j2\pi\nu t)\} = \frac{1}{2}\left[U(r)\exp(j2\pi\nu t) + U^*(r)\exp(-j2\pi\nu t)\right]. \tag{14}$$

At a given position *r*, the complex amplitude *U*(*r*) is a complex variable [depicted in Fig. 6 (b)] whose magnitude $|U(r)| = a(r)$ is the amplitude of the wave and whose argument $\arg\{U(r)\} = \varphi(r)$ is the phase. The complex wave function *U*(*r, t*) is represented graphically by a phasor rotating with angular velocity $\varpi = 2\pi\nu$ radians/s [Fig. 6 (c)]. Its initial value at *t* = 0 is the complex amplitude *U*(*r*).

2.2.4 Optical intensity

The optical intensity is determined by use of $I(r,t) = 2\langle u^2(r,t)\rangle$. When

$$2u^2(r,t) = 2a^2(r)\cos^2[2\pi \nu t + \varphi(r)]$$

$$= |U(r)|^2 \{1 + \cos(2[2\pi \nu t + \varphi(r)])\} \tag{15}$$

is averaged over a time longer than an optical period, $1/\nu$, the second term of (15) vanishes, so that

$$I(r) = |U(r)|^2 . \tag{16}$$

Thus the optical intensity of a monochromatic wave is the absolute square of its complex amplitude. The intensity of a monochromatic wave does not vary with time.

2.2.5 Interference of two waves

When two monochromatic waves of complex amplitude U_1(r) and U_2(r) are superposed, the result is a monochromatic wave of the same frequency and complex amplitude

$$U(r) = U_1(r) + U_2(r) . \tag{17}$$

In accordance with $I = |U(r)|^2$, the intensities of the constituent waves are $I_1 = |U_1|^2$ and $I_2 = |U_2|^2$ and the intensity of total wave is

$$I = |U|^2 = |U_1 + U_2|^2 = |U_1|^2 + |U_2|^2 + U_1^* U_2 + U_1 U_2^* . \tag{18}$$

The explicit dependence on *r* has been omitted for convenience. Substituting

$$U_1 = I_1^{1/2} \exp(j\varphi_1) \quad \text{and} \quad U_2 = I_2^{1/2} \exp(j\varphi_2) \tag{19}$$

into (18), where φ_1 and φ_2 are the phases of the two waves, we obtain

$$I = I_1 + I_2 + 2(I_1 I_2)^{1/2} \cos\varphi , \tag{20}$$

with

$$\varphi = \varphi_2 - \varphi_1 . \tag{21}$$

This relation called the interference equation.

2.2.6 Interferometer

Consider the superposition of two plane wave, each of intensity I_0, propagating in the *z* direction, and assume that one wave is delayed by a distance *d* with respect to the other so that $U_1 = I_0^{1/2} \exp(-jkz)$ and $U_2 = I_0^{1/2} \exp[-jk(z-d)]$. The intensity *I* of the sum of those two waves can be determined by substituting $I_1 = I_2 = I_0$ and $\varphi = kd = 2\pi\, d/\lambda$ into the interference equation (20),

$$I = 2I_0 \left[1 + \cos\left(2\pi \frac{d}{\lambda} \right) \right] . \tag{22}$$

The dependence of *I* on the delay *d* is sketched in Fig 6. If the delay is an integer multiple of λ, complete constructive interference occurs and the total intensity $I = 4I_0$. On the other hand, if *d* is an odd integer multiple of $\lambda/2$, complete destructive interference occurs and *I* = 0. The average intensity is the sum of two intensities $2I_0$.

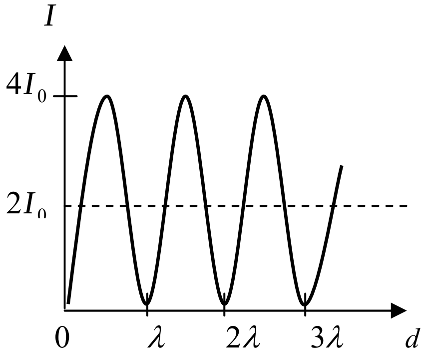

Figure 7 Dependence of the intensity *I* of the super position of two waves, each of intensity I_0, on delay distance *d*. When the delay distance is a multiple of λ, the interference is constructive; when it is an odd multiple of $\lambda/2$, the interference is destructive.

Optical Fibers

1. Fiber Structure

Eric U *et al*. (1998) The basic fiber structure needed to guide light consists of a core surrounded by a cladding (Figure 8). The index of refraction of the core, being greater than the index of refraction of the cladding, makes total-internal-reflection possible. Therefore, certain light 'rays' will remain inside the fiber, as long as they meet the critical angle criteria. Typical communications-grade optical fibers appear as long strands of glass material, usually less than 100 microns in core diameter. Plastic fibers with core diameters to 2mm have begun to be utilized for certain short distance applications (< 500 meters). More will be discussed about fiber types and specifications in following sections.

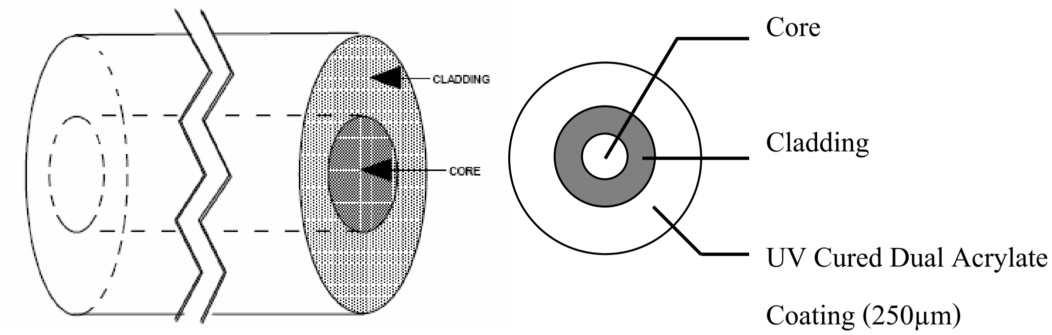

Figure 8 Basic fiber structures.

1.1 Core

Several different fiber configurations will be presented here, however the principle behind all fiber configurations is the same: a core material with an index of refraction greater than the cladding material. Common communications grade fibers usually have a core index of refraction of anywhere from 1.450 to 1.480, however this parameter can be varied enormously and, adjusted with great accuracy (1 part in 10,000) if necessary. The application for such control of this parameter is discussed in the Numerical Aperture Section.

1.2 Cladding

Without a cladding, the core would be "immersed in air", which has an index of refraction of about 1.0. Therefore, the critical angle of incidence would be close to the 41.8 degrees used in the example. In optical fibers however, it has been found that a much greater critical angle is desirable, (see Numerical Aperture section). In order to provide better insight into what happens in the fiber, look at a cladding index of 1.470 and a core index of 1.475 This results in a core-cladding difference of only 0.005, which yields a critical angle of about 85 degrees. Core and cladding diameters usually are specified together, for example, "100/140" refers to a fiber that has a core diameter of 100 microns and cladding diameter of 140 microns. Some fiber sizes manufactured in large quantities include; 10/125, 50/125, 62.5/125, 85/125, 100/140. Many other fibers with sizes different than these have been fabricated for many different applications, and, unique fibers can be acquired from a number of manufacturers.

1.3 Coatings, Jackets and Cabling

An optical fiber consisting only of core and cladding is extremely fragile and is subject to degradation from external transverse forces, as well as chemical attack. To protect the fiber, many types of coatings are available that may be applied over the cladding. Depending on the application, several coatings may be applied one on top of another. These coatings range from the consistency of hardened epoxy to soft rubber-like plastics or composite materials and even metals. Some are very hard and do not easily cut with a razor blade, while the softer materials may be almost peeled off, once a cut is made.

While coatings are extremely important for protecting fiber, nearly all working requirements with fiber necessitate removing the coating(s). This operation can be fairly challenging, and requires experience with fibers, knowledge of the coating materials, and the proper tools. Some hazard exists when working with glass fibers, since the fiber can be easily broken with improper handling, resulting in fiber fragments breaking off. These fiber fragments are dangerous, and should be treated as if they were glass ‘needles’. They can pierce the skin and break off like splinters, becoming extremely painful and difficult or impossible to remove. This hazard is greatest after the coating has been removed, and the fibers may be practically invisible, due to their small size. An untrained person should never attempt to work with fiber. Fiber coatings may be covered with “jackets”, that could consist of any type of material typically found on electrical wires, ranging from simple plastic sheathes to Kevlar fabric to gold and aluminum. (Occasionally, the terminology “coating” and “jacket” are used interchangeably and may refer to the same material.) The majority of optical fiber is designed and developed for communications applications; hence the fiber usually is in cable form. Cables must be pulled from one location to the other, so considerable forces are used during cable installation. For that reason, many optical fiber cables have additional “strength members” included. Such strength members may be steel strands or if weight reduction is important, continuous Kevlar thread may be used. Optical fiber cables with strength sufficient for resisting ocean environments are now common, as well as tactical-battlefield-specified cables, which must be able to withstand forces imparted from vehicles such as tanks. Cables for remotely controlled missiles also have been developed, which requires strength members that can survive enormous accelerations, stresses, and strains. From these examples, it is clear that cabling requirements vary enormously, yet in all situations, optical fiber cable has been successfully manufactured.

2. Step-Index Fibers

Saleh and Teich (1994) A step-index fiber is a cylindrical dielectric waveguide specified by its core and cladding refractive induces, n_1 and n_2, and radii a and b. Examples of standard core and cladding diameters $2a/2b$ are 8/125, 50/125, 62.5/125, 85/125, 100/140 (unit of μm). The refractive indices differ only slightly, so that the fractional refractive-index change

$$\Delta = \frac{n_1 - n_2}{n_1} \tag{23}$$

is small ($\Delta << 1$).

Almost all fibers currently used in optical communication systems are made of fused silica glass (SiO_2) of high chemical purity. Slight changes in the refractive index are made by addition of low concentrations of doping materials (titanium, germanium or boron, for example). The refractive index n_1 is in the range from 1.44 to 1.46, depending on the wavelength, and Δ typical lies between 0.001 and 0.02.

2.1 Numerical Aperture

Eric U *et al.* (1998) Once light has entered the fiber, it is guided by the critical angle relationships previously shown. Now, these relationships also can be used to determine how much light may be injected into the fiber from a source such as a laser or light emitting diode. The result also describes the "output-transmission cone", for light leaving the fiber. The "acceptance cone" defines how much light can enter the fiber (as well as exiting the fiber), and is referred to as the numerical aperture ("NA"). For step index fiber the NA is mathematically

$$NA = \sin\theta_{\max} = \left(n_{Core}^2 - n_{Clad}^2\right)^{\frac{1}{2}} \tag{24}$$

It now should be apparent that varying the core and cladding indices of refraction has a significant impact on the numerical aperture of the fiber. A typical communications grade fiber has a numerical aperture of about 0.2. Plastic fibers have been fabricated with NA's greater than 0.5. Light that enters the fiber within the NA will satisfy the critical angle requirement and remain in the fiber core.

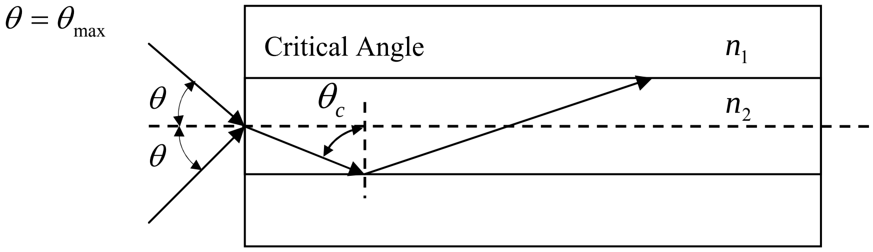

Figure 9 Numerical aperture.

Some light may enter the core at a higher angle than defined by the NA. A fraction of this light is transmitted to the cladding, however some also is reflected. At the next reflection more is transmitted into the cladding and again some is reflected; this all occurs even though the critical angle requirement is not met. Therefore, near the launch location, all of the light in the core may not be "bound" to the core, and eventually will "leak" out.

2.2 V Number

Newport Resource (2002) The normalized frequency parameter of a fiber, also called V number, is a useful specification. Many fiber parameters can be expressed in terms of *V*, such as: the number of mode at a given wavelength; mode cut off conditions; and propagation constants. For example, the number of guides modes in a step index fiber is given by $V^2/2$, and step index fiber becomes single-mode for a given wavelength when $V<2.405$. Mathematically,

$$V = \frac{2\pi \cdot NA \cdot a}{\lambda} \tag{25}$$

where "*a*" is the fiber core radius.

2.2.1 Core Modes

Eric U *et al.* (1998) In step index fiber, only light rays that are within the NA of the fiber will remain bound in the core of the fiber. Therefore, each light ray incident on the core that satisfies this requirement may be considered a unique "mode" injected into the fiber, Figure 10. (However, the waveguide model predicts mathematically, that only specific rays [angles] can be sustained within the fiber. Light rays at each of these specific angles are a true "mode". This results from the solutions of the electromagnetic waveguide equations.) Modes of light injected at the maximum NA angle are referred to as 'high-order modes", while light injected almost parallel to the axis of the fiber results in 'low-order modes'. High-order modes are more likely to scatter into the cladding and be lost, while low-order modes are more tightly bound to the core. Light that is perfectly parallel to the fiber axis sometimes is referred to as the 'zero-order mode'.

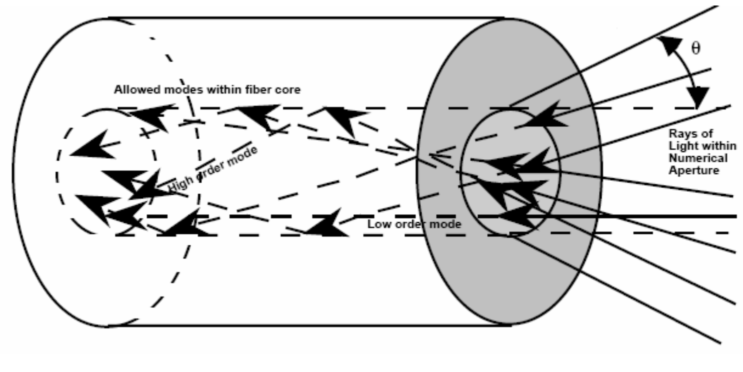

Figure 10 Rays representing modes in step index fiber.

When light is first injected into the fiber, it may "overfill" the NA, with rays at angles above the NA, Figure 11. A portion of this light may internally reflect while some of it may be lost into the cladding. Eventually however, any light that does not satisfy the critical angle requirement within the fiber, will be lost, mostly into the cladding. At some distance down the fiber, when this condition is met, it is referred to as having an "Equilibrium Mode Distribution". This means that light is essentially uniformly distributed among all the allowed modes in the fiber. Among other things, this condition allows for the most accurate measurement of power leaving the fiber. It also is important for enabling the optimum bandwidth utilization in communications applications.

2.2.2 Cladding Modes

It is possible that light will enter the fiber cladding from the end of the fiber, from the side of the fiber, or from the core (in which light does not meet the NA requirement). Since material outside the cladding will have a different index of refraction, some light will reflect at the cladding-edge boundary, as well as the cladding-core boundary, Figure 12. Such light has been known to propagate several meters in the cladding before being ejected, absorbed, or even launched back into the core. Most current fiber designs incorporate a coating with an index of refraction that is close to that of the cladding, thereby enhancing the loss of light from the cladding. Even with this design however, short-haul fiber links may carry some light in the cladding, which could negatively impact system performance.

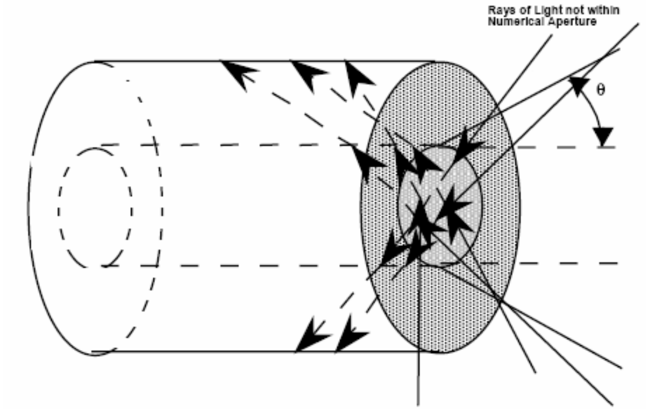

Figure 11 Overfill of numerical aperture.

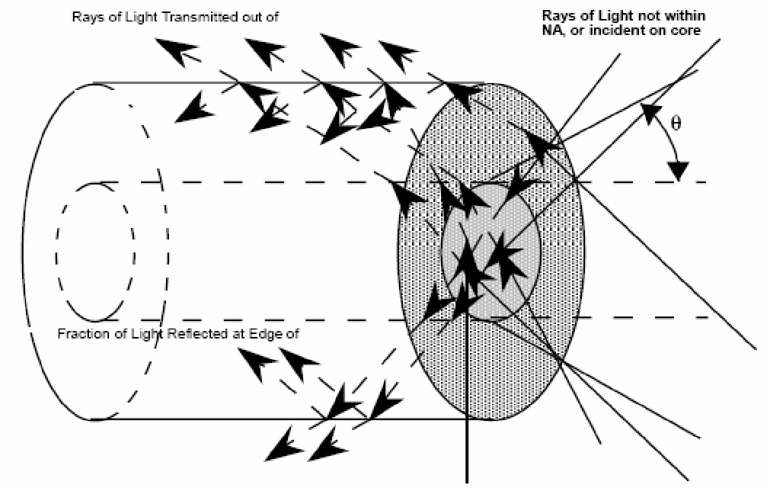

Figure 12 Cladding modes.

2.2.3 Modal Distortion

Understanding that there are different modes represented as rays at different angles in the fiber, leads to an important consideration for communications applications, or sensor applications that utilize high frequency modulation. This is the concept of modal distortion, which refers to the distortion of the temporal characteristics of an input pulse due to the different transit times of different modes through the fiber, Figure 13.

From this figure it is easy to see that higher order modes must travel a longer path than low order modes. If a fiber is very long, then the low order-mode from a given pulse will arrive at the exit before the high order mode arrives. Therefore, the pulse will spread out as it propagates through the fiber, Figure 14. For digital information, such spreading could lead to overlap of pulses, resulting in misinterpretation of bits, bytes, and words.

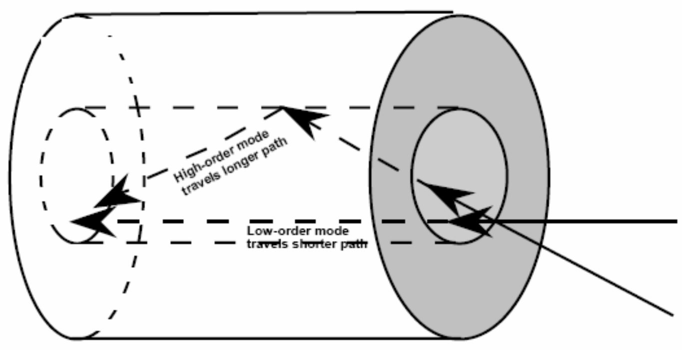

Figure 13 Mode paths through step-index fiber.

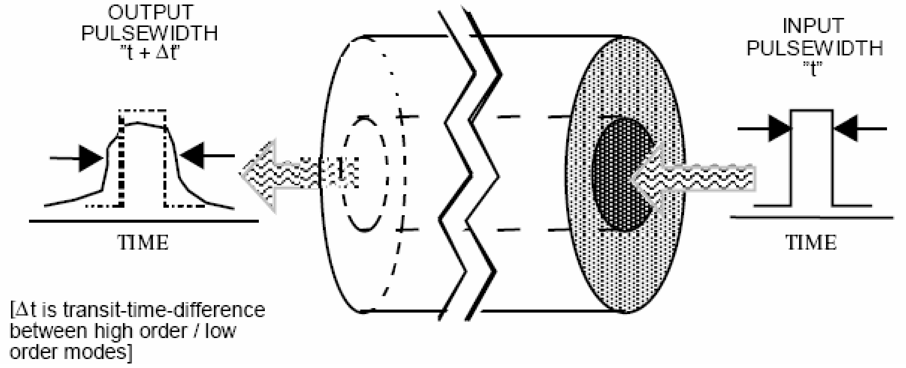

Figure 14 Pulse spreading from modes.

2.2.4 Single-mode Fiber

Single-mode fiber is extremely important for the highest bandwidth, longest length communications applications, as well as interferometric sensor applications. Single-mode fiber is typically step-index fiber, with a very small core diameter when compared to multimode fiber. In order to obtain single-mode propagation, it is necessary that the wavelength of light and the diameter of the fiber maintain a unique relationship. That relationship is determined when the normalized frequency is less than 2.405:

$$V = \frac{2\pi a}{\lambda}(n_{Core}^2 - n_{Clad}^2)^{\frac{1}{2}} < 2.405 \qquad (26)$$

In single-mode operation, the "single" mode may consist of two different polarizations. It is possible to obtain fiber that will only allow 1 polarization to propagate. Such polarization-preserving fiber is true single-mode, and very important in some sensor applications.

2.2.5 Cutoff Wavelength

Cutoff wavelength has not been discussed previously, but it is mentioned here since it may be of great importance for high bandwidth and/or certain wavelength multiplexed systems. Also, a special class of fiber sensors known as “few mode sensors” require knowledge of the cutoff wavelength. Simply put, the cutoff wavelength is the wavelength above which, single-mode operation is guaranteed. For example, if the cutoff wavelength is 1.305 microns, then operation above that wavelength will result in single-mode operation. Conversely, if a wavelength less than the cutoff is used, multimode operation will result. This enables possible modal distortion that would dramatically impact high bandwidth systems. From Equation 26, the cutoff wavelength is obtained by setting the normalized frequency equal to 2.405, and solving for wavelength:

$$\lambda_{Cutoff} = \frac{2.405 \quad 2\pi a}{\left(n_{core}^2 - n_{clad}^2\right)^{\frac{1}{2}}} \qquad (27)$$

Usually sufficient "engineering margin" exists with cutoff wavelength such that careful specification of source wavelength is not absolutely critical. A condition exists however with certain lasers that might result in a single-mode system switching to a "few-mode" system. Some diode lasers shift their wavelength due to temperature changes or reflected light coupled back into the laser. If the wavelength shift is to a longer wavelength, then no problem will occur as far as single-mode propagation is concerned. However, if the shift is to a shorter wavelength and the shorter wavelength is below cutoff, the system could shift to more than one mode. Such shifting typically degrades performance dramatically. Such occurrences are not common, consequently, it is important to match the source type and specifications to the fiber, to minimize the probability of such occurrences.

2.2.6 Dispersion

It was mentioned earlier that the temporal profile of an optical pulse launched into a multimode fiber would undergo modal distortion as it travels down the fiber. The longer the fiber is, the more the amount of modal distortion. By utilizing single-mode fiber, modal distortion is minimized, resulting in longer transmission distances. However, there is a phenomenon that both single-mode and multimode fibers are subject to; chromatic, or material, dispersion.

Chromatic dispersion refers to the wavelength dependence of the index of refraction. Since the index of refraction determines the velocity of light in a material, different wavelengths will have different velocities in the fiber. (This is the same principle by which a prism splits white light into its components.) As a result, if light that is truly one color, i.e., "monochromatic" is launched into fiber, no dispersion will occur. Contrarily, if light is polychromatic (has a continuum of wavelengths) then the different wavelengths will travel at different velocities, resulting in a temporal spreading of the optical pulse. This spreading is similar to the modal distortion of a pulse shown in Figure 15. A property known as waveguide dispersion also exists that is important in single-mode fibers. By combining the effects of material dispersion with waveguide dispersion, it is possible to fabricate fibers in which the total dispersion is theoretically zero at certain specified wavelengths, Figure 16. For communications applications this is an exceptional performance enhancer, it can be used with excellent practical benefits. The effects of dispersion are of greatest importance for very high frequency applications in communications, and/or very long distance applications of any kind. Currently, few sensor applications need be concerned about dispersion effects, unless broad-spectrum light sources are utilized.

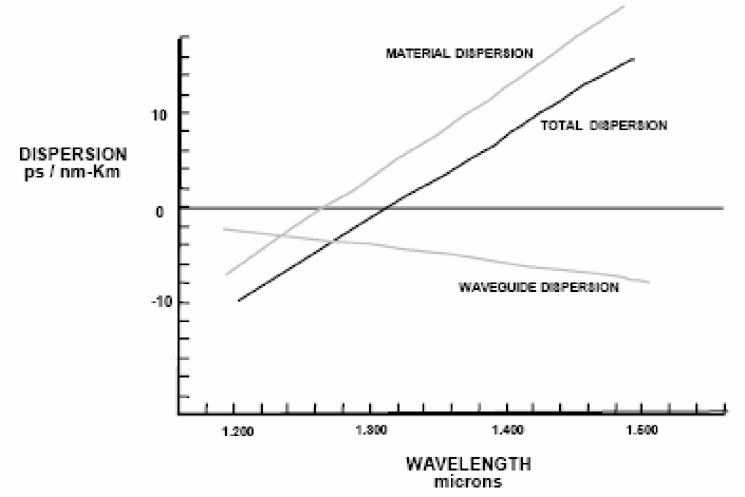

Figure 15 Material and waveguide dispersion for glass fiber.

3. Graded Index Fiber

Graded index optical fiber has been developed to reduce the amount of modal distortion inherent with step-index fiber. Whereas step index fiber has a uniform index of refraction across the core, the index of refraction for graded index fiber varies from the center of the core out to the cladding, Figure 16. One model for this design is to imagine several discrete layers of material, each with an index of refraction slightly less than the one closer to the core, Figure 17. As higher order modes encounter each of these layers, it is refracted according to Snell's law, and the transmitted light is "bent" slightly, Figure 18. Additionally, as the light approaches the core-cladding interface, where the index of refraction is lower than at the core, its velocity must increase.

Upon reflection at the core-cladding interface, the light is directed back towards the center of the fiber, where at each “layer” it is again refracted, and begins to slow down. When it reaches the axis of the fiber core, it will be traveling with the same velocity as the zero order mode, but in a “crossing” trajectory. The result of this design, is that the transit time through the fiber of higher order modes is much closer to the transit time of low order modes, thus reducing modal distortion.

Graded index fiber is extensively used in communications, with the dominant fiber being 62.5 micron core diameter with 125 micron cladding diameter.

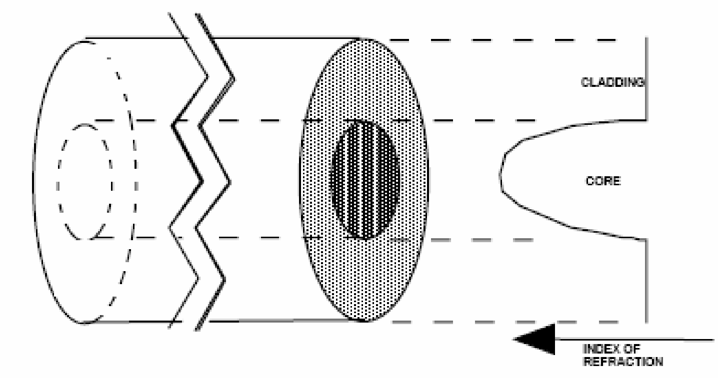

Figure 16 Profile of index of refraction for graded-index fiber.

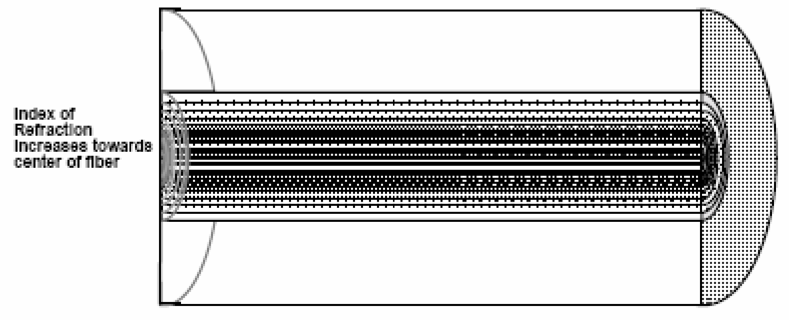

Figure 17 Model depicting layers of different indices of refraction for graded-index fiber.

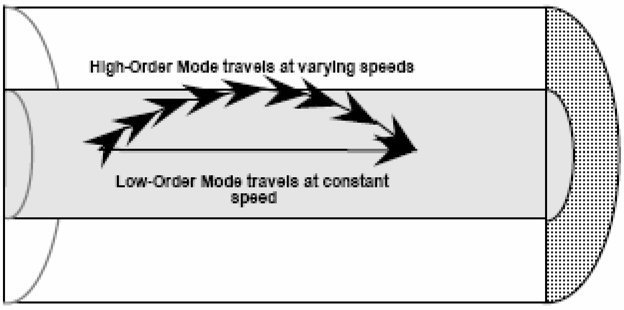

Figure 18 Modes propagating in graded-index fiber.

4. Losses in Fiber

An extremely important consideration for nearly all fiber applications is the loss, or “attenuation” of light within the fiber. While glass fiber losses are much less than losses in wire or metallic waveguides, they are not negligible, and must be considered for nearly every system, except those that are very short in length as well as those operating at highloss wavelengths. Plastic fiber losses may be significant, resulting in a limited range of application. Specialty fibers may have considerable losses, since they are optimized for performance in unique areas; and as a tradeoff, may end up being highly attenuating.

Fiber attenuation generally is measured in “decibels/kilometer”, and, optical power (P_o) usually is measured in dB_m. A level of 0 dBm is equal to 1 milliwatt, while 10 dB_m is 10 milliwatts, and 20 dB_m is 100 milliwatts. Formally:

$$P_0(dB_m) = 10\log\frac{P(milliwatts)}{1.0(milliwatt)} \tag{28}$$

As a result, one microwatt of energy would be -30 dBm and one nanowatt would be -60 dB_m. This scale is advantageous when dealing with optical power since power levels throughout fiber systems may vary by many orders of magnitude. For example, if fiber attenuation is 3 dB/km at the wavelength used, the fiber length is 10 km, and the light level launched into the fiber is 3 dB_m, the output light level would be -27 dB_m, or about

4.1 Wavelenght Dependence

Figure 19 provides a typical loss profile for silica glass fibers. It can be seen from this profile, that at 1.31 microns, a low level of attenuation is obtained. Beyond 1.31 microns, attenuation immediately increases until a wavelength of about 1.55 microns is reached, where the loss is less than at 1.31 microns. After about 1.6 microns, attenuation increases considerably. Due to this characteristic and the low dispersion near 1.31 microns, this wavelength currently is the most common for long distance communications.

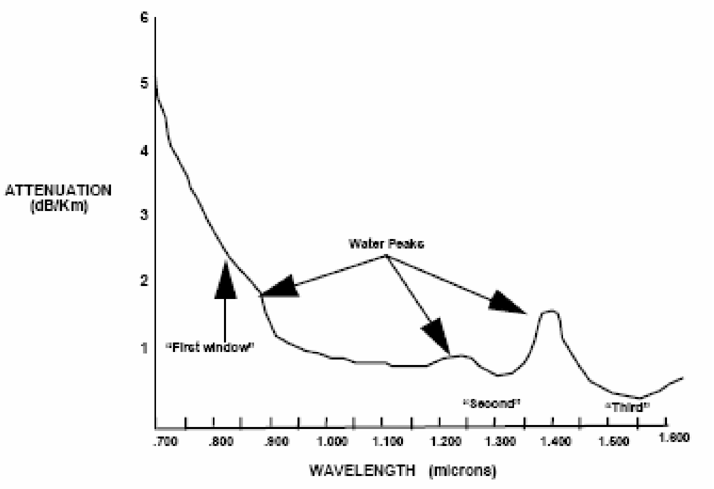

Figure 19 Attenuation vs. wavelength (single-mode, glass fiber).

4.2 Absorption and Scattering

Losses occur primarily from absorption and scattering of light. These losses are a result of imperfections in the fiber, contaminants, and inherent absorption properties of materials used to fabricate fiber. The dominant loss feature for silica glass fibers is known as Rayleigh scattering, which is a wavelength dependent phenomenon:

$$L_{Rayleigh} = \frac{A}{\lambda^4} \tag{29}$$

Here A is a constant that depends upon material composition. While other wavelength dependent losses exist, they typically are negligible compared to Rayleigh scattering in ordinary fibers. While Rayleigh scattering is from imperfections in the glass that are smaller than the wavelength of light, scattering also occurs from undesirable trace elements; molecules that entered the glass due to limitations of the technology to purify the fiber materials and the associated dopants. Absorption of light is inevitable: no perfect reflector exists. It is therefore not surprising that glass and the materials used in manufacturing will absorb some of the light. For silica-glass fiber, there are several absorption peaks that increase attenuation noticeably, as shown in Figure 19. These absorption bumps / peaks result from water trapped in the manufacturing process, resulting in formation of Si-OH (silicon-hydroxyl) in the fiber. When fiber is manufactured, the process strives for the greatest possible control over reducing contaminants, and introducing dopants that increase performance. Some manufacturing methods immerse the fiber in gases that bond and extract some contaminants. Fiber manufacturing technology still is advancing steadily, and improvements in performance are ongoing.

4.3 Bending Losses

Losses due to bending in fiber can result in drastic changes in system performance, almost always degrading desired results (*Miller*). Bending effects may result in more light lost in the fiber, since they can "extract" higher order modes from the core into the cladding, where they are more likely to be lost. Normally, the potential for the greatest bending impact on power transmission occurs when utilizing multimode fiber in short-length applications. (In interferometric sensors, bending may cause drastic changes to system performance, although the affect is due more to impacts on polarization and phase.)

A great deal of analysis has been performed on bending impacts from both "small" radius bends (< 1cm), and bends less than about 5 cm. Bends greater than about 10 cm seldom have much impact on light propagation Bends with less than a 5 cm radius should be avoided.

4.4 Temperature, Modal Exchange, and Transient Attenuation

While modern fibers and fiber cables for communications are designed to minimize environmental effects, it is important to assume that environmental factors *will* have any impact on light propagating through fiber. The mechanisms by which temperature may influence light in fiber are extremely complex, and in some sensing techniques, the effect is so overwhelming as to render the system dysfunctional. Single-mode interferometric sensors are very susceptible to temperature effects while multimode, intensity based sensors are much less sensitive. One reason for the sensitivity in single-mode sensors is that the index of refraction is temperature dependent (temperature causes materials to expand and contract, thus resultant stresses and strains occur in the material thereby influencing the index of refraction, with a subsequent impact on the phase of the light).

In multimode fibers, the effect of temperature on the index of refraction may cause light in some modes to be converted to other modes. If more light is in higher order modes, it is more susceptible to being lost, since higher order modes are more loosely bound in the core. This could be especially degrading if bending losses are occurring at the same time as temperature extremes are being experienced. Note that these potential susceptibilities may be exploited for sensor applications.

Another phenomena known as transient attenuation can lead to system performance problems in multimode fibers. As discussed in earlier sections, light from higher order modes or poor launching conditions may couple into the cladding and under certain circumstances may stay in the cladding a short distance. If the power level is measured at the end of this short distance, and light from the cladding is included in the power measurement, then the measurement is not an accurate measurement of the amount of light in the core. Therefore, more power is perceived to be in the system than actually will be available. This "transient power" results in a higher attenuation than would be expected if only the light in the core of the fiber is measured. This situation is seldom of concern if fiber lengths are longer than 50 meters, although the phenomenon could exist for up to 500 meters under certain circumstances.

Fiber Optic Gyroscope

1. Solid State Laser Light Source

According to Streetman B.G. (1990), the word “laser” is an acronym of “light amplification by stimulated emission radiation”. This sums up the operation of an important optical and electronics device. The laser is a source of highly directional, monochromatic, coherent light, and as such it has revolutionized some long standing the optical problems, and has created some new fields on basic and applied optics. The light from a laser, depending on the type, can be continuous beam of low or medium power, or it can be a shot burst of intense light delivering millions of watts. Light has always been a primary communication link between man and his environment. Before the inventions of the laser, the light sources available in transmitting information and performing experiments were generally neither monochromatic nor coherent, and were of relatively low intensity. Thus laser is of great interest in optics, and optoelectronics. The effort of creating the useful laser system involves the technique of solid state (or gaseous) electronics. The transmission and detection of a laser signal require a broad range of electronics.

The emission of radiations occurs when exited electron falls to lower energy states. The process can be classified as spontaneous emission. This means that the rate at which electrons fall from an upper level of energy E_2 to a lower level of energy E_1 is, at every instant, proportional to the number of electrons remaining in the state with energy E_2 (the population of electrons with energy E_2). Thus if an initial electron population in state with energy E_2 is allowed to decay, we would expect an exponentially empty lower energy level of the electrons. A mean decay time describes how much time average electron spends in the upper level. An electron in a higher or excited state need not wait for spontaneous emission to occur however; if conditions are right, it can be stimulated to fall to the lower level and emit its photon in a time much shorter than its mean spontaneous decay time. The stimulus is provided by the presence of photon of the proper wavelength. The electrons in state E_2 waiting to drop spontaneously to E_1, the emission is a photon of energy $h\nu_{12} = E_2 - E_1$ as illustrate in figure 20. The electron in the upper state is immersed in an intense field of photons, each having energy $h\nu_{12} = E_2 - E_1$, and in phase with each other. The electron is induced to drop in energy from E_2 to E_1, contributing a photon whose wave is in phase with the radiation field. If the process is continuous and other electrons are stimulated to emitted photons in the same fashion then a large radiation field can be build up. This radiation will be *monochromatic* since each photon will have an energy of precisely $h\nu_{12} = E_2 - E_1$ and will be *coherent*, because all the photons released will be in phase and reinforcing. This process of stimulated emission can be described quantum mechanically that the rate of the emission probability is proportional to the intensity of the radiation. Without quantum mechanics, we can make a few observations here about the relative rates at which the absorption and emission process occur. Assuming that the instantaneous populations of the E_1 and E_2 to be n_1 and n_2, respectively, at *thermal equilibrium*, the relative population will be.

$$\frac{n_1}{n_2} = e^{-(E_2 - E_1)/kT} = e^{-h\nu_{12}/kT} \tag{30}$$

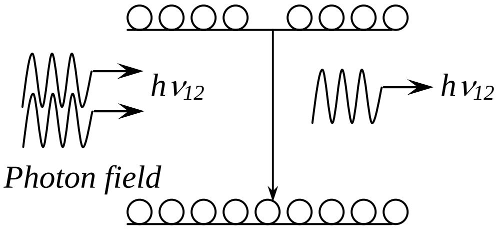

Figure 20 Stimulated transition of an electron from upper to lower state.

The negative exponent in this equation indicates that $n_2 << n_1$ at equilibrium; that is, most electrons are in the lower energy level as expected. If the atoms exist in a radiation field of photons with energy $h\nu_{12}$, such that the energy density of the field is $\rho(\nu_{12})$ (which indicates the total energy in the radiation field per unit volume and per unit frequency, due to photons with $h\nu_{12} = E_2 - E_1$), then stimulated emission can occur along with absorption and spontaneous emission. The rate of stimulated emission is proportional to the instantaneous number of electrons in the upper level n_2 and to the energy density of the stimulation field $\rho(\nu_{12})$. Thus we can write the stimulated emission rate as $B_{21}n_2\rho(\nu_{12})$, where B_{21} is a proportionality factor. The rate at which the electrons in E_1 absorb photons should also be proportional to $\rho(\nu_{12})$, and to the electron population in E_1. Therefore, the absorption rate is $B_{12}n_1\rho(\nu_{12})$, where B_{12} is a proportionality factor for absorption. Finally, the rate of spontaneous emission is proportional only to the population of the upper level. Introducing still another coefficient, we can write the rate of spontaneous emission as $A_{21}n_2$. For steady state the two emission rates must balance the rate of absorption to maintain constant populations of n_1 and n_2 (Figure 21).

$$B_{12}n_1\rho(\nu_{12}) = A_{21}n_2 + B_{21}n_2\rho(\nu_{12})$$

$$\text{(Absorption)} = \text{(Spontaneous)} + \text{(Stimulated)} \tag{31}$$

This relation was described by Einstein, and the coefficients B_{12}, A_{21}, B_{21} are called the *Einstein coefficients*. We notice from Equation (31) that no energy density ρ is required to cause a transition from an upper to a lower state; spontaneous emission occurs without an energy density to drive it. The reverse is not true, however; exciting an electron to a higher state (absorption) requires the application of energy, as we would expect thermodynamically.

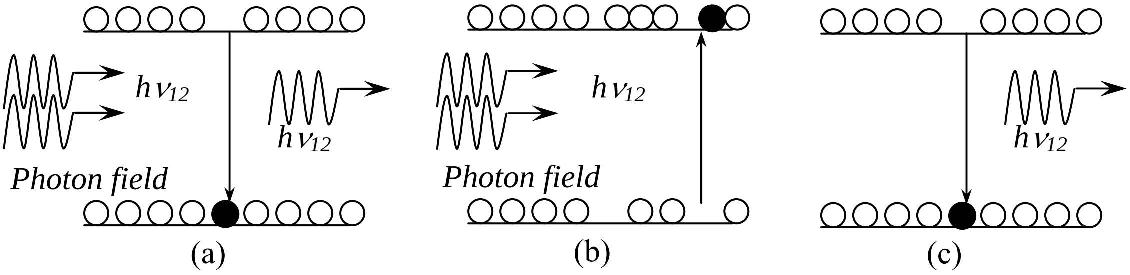

Figure 21 Balance of absorption and emission in steady state:
(a) Stimulated emission, (b) Absorption, (c) Spontaneous emission.

At thermal equilibrium, the ratio of the stimulated to spontaneous emission rates is generally very small, and the contribution of stimulated emission is negligible. With a photon field present,

$$\frac{\textit{Stimulated Emission Rate}}{\textit{Spontaneous Emission Rate}} = \frac{B_{21}n_2\rho(\nu_{12})}{A_{21}n_2} = \frac{B_{21}}{A_{21}}\rho(\nu_{12}). \tag{32}$$

As Equation (13) indicates, the way to enhance the stimulated emission over spontaneous emission is to have a very large photon field energy density $\rho(\nu_{12})$. In the laser, this is encouraged by providing an optical resonant cavity in which the photon density can build up to a large value through multiple internal reflections at certain frequencies (ν). To obtain more stimulated emission than absorption we must have $n_2 > n_1$:

$$\frac{\textit{Stimulated Emission Rate}}{\textit{Absorption Rate}} = \frac{B_{21}n_2\rho(\nu_{12})}{B_{12}n_1\rho(\nu_{12})} = \frac{B_{21}n_2}{B_{12}n_1}. \tag{33}$$

Thus if stimulated emission is to dominate over absorption of photons from the radiation field, we must have a way of maintaining more electrons in the upper level than in the lower level. This condition is quite unnatural, since Equation (30) indicates that n_2/n_1 is less than unity for any equilibrium case. Because of its unusual nature, the condition $n_2 > n_1$ is called *population inversion*. It is also referred to as a condition of *negative temperature*. This rather startling terminology emphasizes the nonequilibrium nature of population inversion, and refers to the fact that the ratio n_2/n_1 in Equation (30) could be larger than unity only if the temperature were negative. Of course, this manner of speaking does not imply anything about temperature in the usual sense of that word. The fact is that Equation (30) is a thermal equilibrium equation and cannot be applied to the situation of population inversion without invoking the concept of negative temperature.

In summary, Equations (32) and (33) indicate that if the photon density is to build up through a predominance of stimulated emission over both spontaneous emission and absorption, two requirements must be met. We must provide (1) an optical resonant cavity to encourage the photon field to build up and (2) a means of obtaining population inversion. A large part of our discussion in the following sections will be devoted to examining the second requirement for various energy level structures. There are many ways of obtaining population inversion in the atomic levels of many solids, liquids, and gases, and in the energy bands of semiconductors. Thus the possibilities for laser systems with various materials are quite extensive.

2.1 The Basic Semiconductor Laser

To build a p-n junction laser, we need to form a junction in a highly doped, direct semiconductor (GaAs, for example), construct a resonant cavity in the proper geometrical relationship to the junction, and make contact to the junction in a mounting which allows for efficient heat transfer. A simple fabrication technique is outlined in Figure 22. Beginning with a degenerate *n*-type sample, a *p* region is formed on one side, for example by diffusing Zn into the *n*-type GaAs. Since Zn is in column II of the periodic table and is introduced substitution on Ga sites, it serves as an acceptor in GaAs; therefore, the heavily doped Zn diffused Zn diffused layer forms a *p*+ region (Figure 22b). At this point we have a large-area planar *p*-*n* junction. Next, grooves are cut or etched along the length of the sample as in Figure 22c, leaving a series of long p regions isolated from each other. These *p*-*n* junctions can be cut or broken apart (Figure 22d) and then cleaved into devices of the desired length.

At this point in the fabrication process, the very important requirement of a resonant cavity must be considered. It is necessary that the front and back faces (Figure 16e) be flat and parallel. This can be accomplished by cleaving. If the sample has been oriented so that the long junctions of Figure 22d are perpendicular to a crystal plane of the material, it is possible to cleave the sample along this plane into laser devices, letting the crystal structure itself provides the parallel faces. The device is then mounted on a suitable header, and contact is made to the *p* region. Various techniques are used to provide adequate heat sinking of the device for large forward current levels.

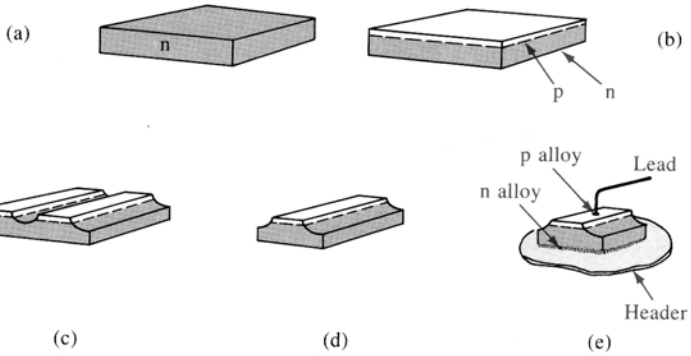

<u>Figure 22</u> Fabrication of a simple junction laser: (a) Degenerate *n*-type sample; (b) Diffused *p* layer; (c) Isolation of junctions by cutting or etching; (d) Individual junction to be cut or cleaved into devices; (e) Mounted laser structure.

2.2 Heterojunction Lasers

The device described above was the first type used in the early development of semiconductor lasers. Since the device contains only one junction in a single type of material, it is referred to as a *homojunction* laser. To obtain more efficient lasers, and particularly to build lasers that operate at room temperature, it is necessary to use multiple layers in the laser structure. Such devices, called *heterojunction* lasers, can be made to operate continuously at room temperature to satisfy the requirements of optical communications. An example of a heterojunction laser is shown in Figure 23. In this structure the injected carriers are confined to a narrow region so that population inversion can be built up at lower current levels. The result is a lowering of the *threshold* current at which laser action begins. Carrier confinement is obtained in this single-heterojunction laser by the layer of AlGaAs grown epitaxially on the GaAs.

In GaAs the laser action occurs primarily on the *p* side of the junction due to a higher efficiency for electron injection than for holes injection. In a normal *p-n* junction the injected electrons diffuse into the *p* material such that population inversion occurs for only part of the electron distribution near the junction. However, if the *p* material is narrow and terminated in a barrier, the injected electrons can be confined near the junction. In Figure 23a, an epitaxially layer of *p*-type AlGaAs ($E_g \cong$ 2 eV) is grown on top of the thin *p*-type GaAs region. The wider band gap of AlGaAs effectively terminates the *p*-type GaAs layer, since injected electrons do not surmount the barrier at the GaAs-AlGaAs heterojunction (Figure 23b). As a result of the confinement of injected electrons, laser action begins at a substantially lower current than for simple *p-n* junction. In addition to the effects of carrier confinement, the change of refractive index at the heterojunction provides a waveguide effect for optical confinement of the photons.

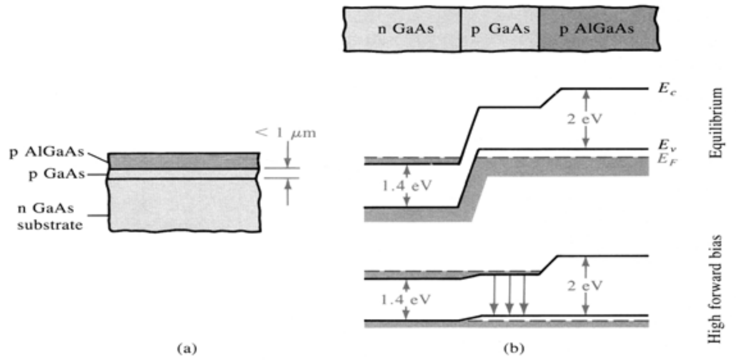

Figure 23 Use of a single heterojunction for carrier confinement in laser diodes:
(a) AlGaAs heterojunction grown on the thin *p*-type GaAs layer;
(b) Band diagrams for the structure of (a), showing confinement of electrons to the thin *p* region under bias.

A further improvement can be obtained by sandwiching the active GaAs layer between two AlGaAs layers (Figure 24). This *double-heterojunction* structure further confines injected carriers to the active region, and the change in refractive index at the GaAs-AlGaAs boundaries helps to confine the generated light waves. In the double-heterojunction laser shown in Figure 24b the injected current is restricted to a narrow stripe along the lasing direction, to reduce the total current required driving the device. This type of laser was a major step forward in the development of lasers for fiber-optic communications.

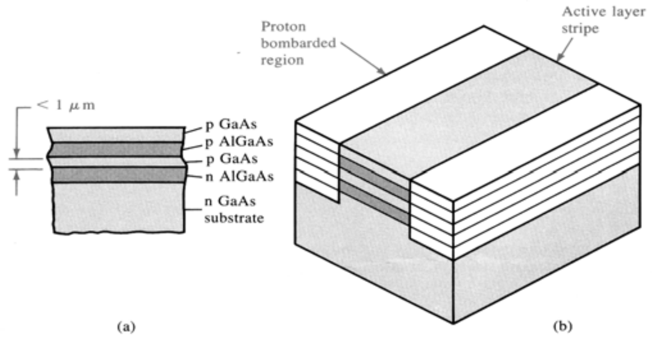

Figure 24 Double-heterojunction laser structures

(a) Multiple layers used to confine injected carriers and provide wave guiding for the light.

(b) A stripe geometry designed to restrict the current injection to a narrow stripe along the lasing direction.

2. Beam Splitter

Saleh and Teich (1994), the beam splitter is an optical instrument that splits the incident light beam into a reflected beam and transmitted beam, as illustrated in figure 13. Beam splitters are also frequently used to combine the two light beams into one [as shown in figure 25(c)]. Beam splitters are often constructed by depositing a thin semitransparent metallic or dielectric film on a glass substrate. A thin glass plate or cube prism can also serve as a beam splitter.

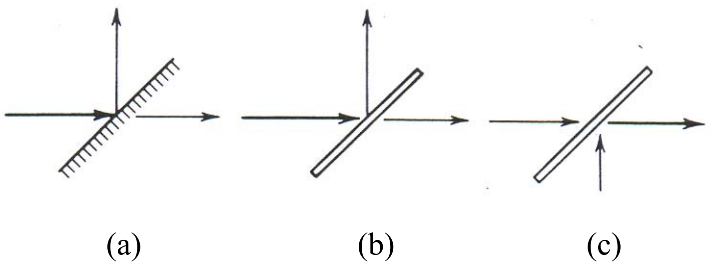

Figure 25 Beam Splitters:

(a) The metallic film on glass substrate type beam splitter.

(b) The prism type beam splitter.

(c) Beam splitter used as a beam combiner.

3. Couplers

In addition to the transmitter, the fiber link, and the receiver, a communication system uses couplers and switches which direct the light beams that represent the various signals to their appropriate destinations. *Couplers* always operate on the incoming signals in the same manner. *Switches* are controllable couplers that can be modified by an external command. Photonic switches are described in Chap. 21. Examples of couplers are shown schematically in Fig. 26. In the T-coupler, a signal at input point 1 reaches both output points 2 and 3; a signal at either point 2 or point 3 reaches point 1. In the star coupler, the signal at any of the input points reaches all output points. In the four-port directional coupler, a signal at any of the input points 1 or 2 reaches both output points 3 and 4; and a signal coming from any of the output points 3 or 4 in the opposite direction reaches both points 1 and 2. When operated as a switch, the four-port directional coupler is switched between the parallel state (1-3 and 2-4 connections) and the cross state (1-4 and 2-3 connections).

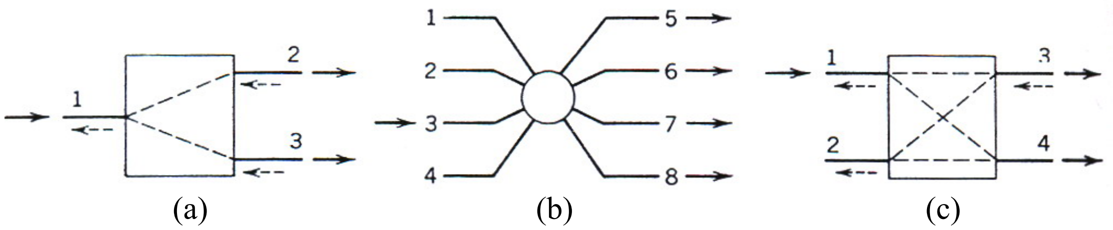

Figure 26 Examples of coupler: (a) T coupler; (b) star coupler; (c) directional coupler.

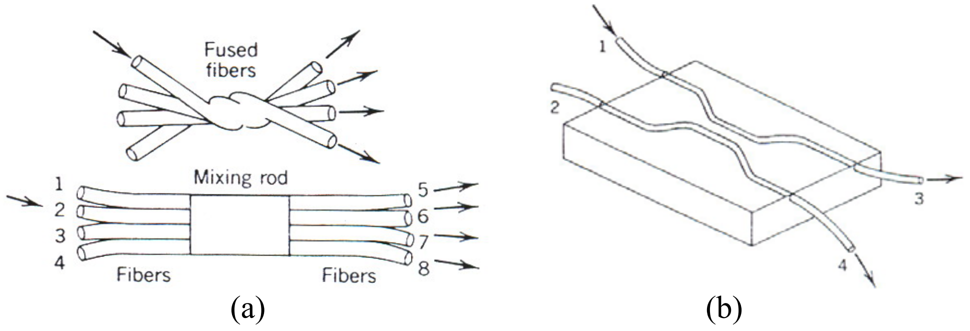

Figure 27 (a) A star coupler using fused fibers and another using mixing rod, a slab of glass through which light from fiber dispersed to reach all other fibers.
(b) An integrated-optic four-port directional coupler.

Optical couplers can be constructed by use of miniature beamsplitters, lenses, graded-index rods, prisms, filters, and gratings compatible with the small size of the optical beams transmitted by fibers. This new technology is called micro-optics. Integrated-optic devices may also be used as couplers; these are more suitable for single-mode guided light. Figure 27 shows some examples of optical couplers.

4. Electro Optic Modulator

The refractive index of an electro-optic medium is a function *n*(*E*) of the electric field *E*. This function varies only slightly with *E* so that it can be expanded in a Taylor's series about *E* = 0,

$$n(E) = n + a_1 E + \frac{1}{2} a_2 E^2 + ..., \tag{34}$$

where the coefficients of expansion are $n = n(0)$, $a_1 = (dn/dE)|_{E=0}$, and $a_2 = (d^2 n/d^2 E)|_{E=o}$. For reasons that will become apparent subsequently, it is convention' to write (1) in terms of two new coefficients $r = -2a_1/n^3$ and $\varsigma = -a_2/n^3$ known as the electro-optic coefficients, so that

$$n(E) = n - \frac{1}{2} rn^3 E - \frac{1}{2} \varsigma n^3 E^2 + ... \tag{35}$$

The second- and higher-order terms of this series are typically many orders of magnitude smaller than *n.* Terms higher than the third can safely be neglected.

4.1 Pockels Effect

In many materials the third term of (2) is negligible in comparison with the second, where upon

$$n(E) \approx n - \frac{1}{2} rn^3 E \,. \tag{36}$$

The medium is then known as a Pockels medium (or a Pockels cell). The coefficient *r* is called the Pockels coefficient or the linear electro-optic coefficient. Typical values of *r* lie in the range 10^{-12} to 10^{-10} rn/V (Ito 100 pm/V). For *E* = 106 V/m (10 kV applied across a cell of thickness 1 cm), for example, the term $\frac{1}{2} rn^3 E$ in (36) is on the order of 10^{-6} to 10^{-4}. Changes in the refractive index induced by electric fields are indeed very small. The most common crystals used as Pockels cells include $NH_4H_2PO_4$ (ADP), KH_2PO_4 (KDP), $LiNbO_3$, $LiTaO_3$, and CdTe.

4.2 Electro-Optic Modulators

When a beam of light traverses a Pockels cell of length *L* to which an electric field *E* is applied, it undergoes a phase shift $\varphi = n(E) k_0 L = 2\pi n(E) L/\lambda_0$, where λ_0 is the free-space wavelength. Using (36), we have

$$\varphi = \varphi_0 - \pi \frac{rn^3 EL}{\lambda_0}, \tag{37}$$

where $\varphi = 2\pi nL/\lambda_0$. If the electric field is obtained by applying a voltage *V* across two faces of the cell separated by distance *d*, then *E* = *V/d*, and (37) gives

$$\varphi = \varphi_0 - \pi \frac{V}{V_\pi}, \tag{38}$$

where

$$V_\pi = \frac{d}{L} \frac{\lambda_0}{rn^3}. \tag{39}$$

The parameter V_π known as the half-wave voltage, is the applied voltage at which the phase shift changes by π. Equation (38) expresses a linear relation between the optical phase shift and the voltage. One can therefore modulate the phase of an optical wave by varying the voltage *V* that is applied across a material through which the light passes. The parameter V_π is an important characteristic of the modulator. It depends on the material properties (*n* and *r*), on the wavelength λ_0 and on the aspect ratio d/L.

The electric field may be applied in a direction perpendicular to the direction of light propagation (transverse modulators) or parallel to that direction (longitudinal modulators), in which case *d* = *L* (Fig.28). The value of the electro-optic coefficient *r* depends on the directions of propagation and the applied field since the crystal is anisotropic. Typical values of the half-wave voltage are in the vicinity of 1 to a few kilovolts for longitudinal modulators, and hundreds of volts for transverse modulators.

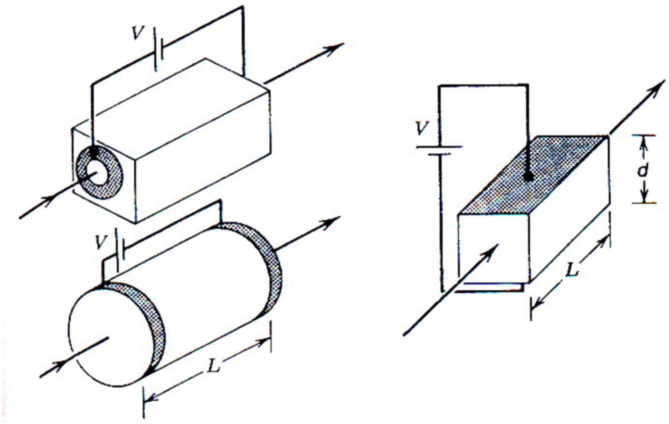

(a) (b)

Figure 28 (a) Longitudinal modulator. (b) Transverse modulator

5 Sagnac Effect

Yu, Francis T. S. (2002) The physical phenomenon that explains the operation of an optical gyroscope is known as the *Sagnac effect,* named after French physicist Georges Sagnac. A simple representation of the Sagnac effect is shown in Fig. 29. The Sagnac interferometer acts as a nonreciprocal device where the light waves propagating in one direction of a loop under rotation is not equivalent to the light waves propagating in the opposite direction. Consider two light waves propagating in opposite directions around the ring interferometer shown in Fig. 29, which is rotating at a rate Ω in the clockwise direction. The two light waves travel a different fiber length and take a different time to traverse the total length of fiber. The effective path lengths are $L_{cw} = 2\pi R + R\Omega t_{ccw} = ct_{cw}$ and $L_{ccw} = 2\pi R - R\Omega t_{ccw} = ct_{ccw}$ where the transit times t_{cw} and t_{ccw} are

$$t_{cw} = \frac{2\pi R}{c - R\Omega} \tag{40}$$

and

$$t_{ccw} = \frac{2\pi R}{c + R\Omega} \tag{41}$$

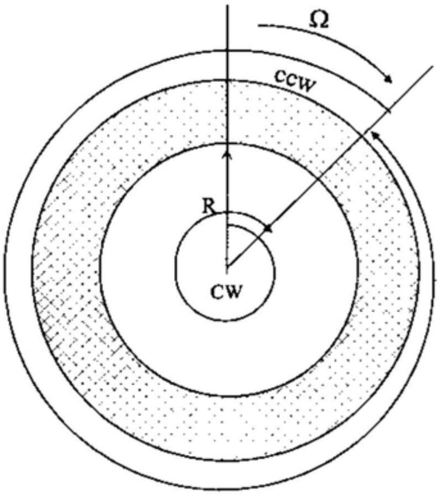

Figure 29 Illustration of Sagnac effect.

for light waves traveling in the clockwise and counterclockwise directions, respectively. The free-space speed of light is denoted by *c,* and *R* is the radius of the ring. The transit time difference δt between the counter-propagation waves, in the case of *N* loops that enclose an area $A = \pi R^2$ can be expressed as

$$\delta t = t_{cw} - t_{ccw}$$

$$= \left(\frac{4NA}{c^2} \right) * \Omega \tag{42}$$

The assumption is made that $c^2 >> R^2\Omega^2$. The resultant optical path length difference, δL, is $c * \delta t$, or

$$\delta L = \left(\frac{4NA}{c} \right) * \Omega \tag{43}$$

In the case of the analog or interferometric fiber optic gyroscope (IFOG), the Sagnac phase shift caused by a rotation can be expressed in terms of *L* as

$$\begin{aligned} \delta\phi_s &= \left(\frac{2\pi}{\lambda} \right) * \delta L \\ &= \left(\frac{8\pi NA}{\lambda c} \right) * \Omega \end{aligned} \tag{44}$$

where λ is the wavelength of the free-space optical energy. Multiple wraps of fiber can be wound to significantly increase thus improving the sensitivity. However, the optical attenuation tends to limit the length of fiber to several kilometers.

In the case of the digital or resonant fiber optic gyroscope (RFOG), the energy in the counterpropagating beams is coupled into the fiber loop at two different frequencies in the presence of a rotation. The relative frequency difference δf between the counterpropagating waves can be written in terms of δL as

$$\frac{\delta f}{f} = \frac{\delta L}{L} \tag{45}$$

where $f = c/\lambda$ and $L = 2\pi RN$ is the total distance traversed. The fundamental RFOG equation that relates δf to Ω is given by

$$\delta f = \left(\frac{2R}{\lambda} \right) * \Omega \tag{46}$$

Sagnac interferometers are highly sensitive measurement devices. The magnitude of the Sagnac effect can be realized from the following example. Consider a fiber optic ring interferometer of area *A* = 100 cm^2, which experiences maximum earth rotational rate Ω = 15/hr. Equation (43) suggests that $\delta L \approx 10^{-15}$ cm, which is very small. This requires phase detection with a resolution in the region of 10^{-8} rad for a 1μm light source.

6. FOG Basic Configuration

The IFOG is the object of discussion from this point. A basic IFOG configuration is shown in Fig. 30. Light from a broadband source, such as a superluminescent diode (SLD), is projected into a 3-dB fiber optic coupler that splits the light into two waves. After traversing the coupler, the two light waves propagate equally in opposite directions around the fiber optic coil. The light waves interfere upon return to the coupler and project a fringe pattern onto a photodetector.

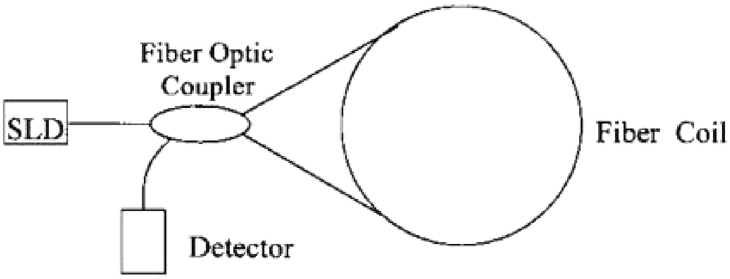

Figure 30 Basic IFOG configuration.

The basic IFOG configuration is not reciprocal in the absence of rotation, that is, both light waves do not traverse identical paths upon recombination at the fiber optic coupler. The clockwise (CW) light wave experiences two reflections through the fiber optic coupler, whereas the counterclockwise (CCW) light wave experiences two transmissions through the coupler, which introduces a degree of nonreciprocity.

7. FOG Minimum Configuration

The Stanford group proposed a minimum configuration IFOG, as shown in Fig. 23. A second coupler has been added after the polarizer to ensure identical paths by equalizing the intensity in CW and CCW waves. The polarizer, which also functions as a single-mode filter, ensures that the two light waves return to the first coupler in a single polarization, thus forming a fringe pattern on the photodetector. The fringe shift ΔZ is written in terms of the Sagnac phase shift $\delta\phi_s$ expressed in Eq. (47) as $= \delta\phi_s / 2\pi$ or

$$\Delta Z = \left(\frac{2RL}{\lambda c} \right) * \Omega = SF_0 \Omega \tag{47}$$

where $SF_0 = 2RL/\lambda c = \Delta S_0 / \Delta S_i$ (ratio of change in output signal and change in input signal) is the open-loop optical scale factor. The characteristics of the scale factor depend on the stability of the light source.

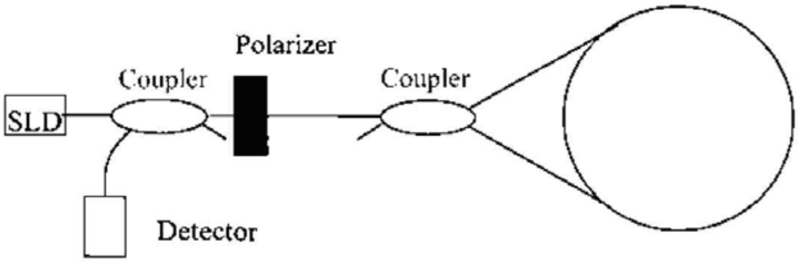

Figure 31 Schematic of minimum-configuration IFOG.

In accordance with any two-wave interferometer, the intensity on the photodetector, which represents a mixture of the two light waves, varies as the cosine of Sagnac phase with its maximum value at zero as shown in Fig. 32. This intensity is expressed as

$$I = I_0\left[1+\cos\left(\delta\phi_s\right)\right] \tag{48}$$

where I_0 is the mean value of the intensity. The detected intensity is used to calculate the rotational rate. In the case of no rotation, $\delta\phi_s = 0$, the light waves will combine in phase, which results in maximum intensity.

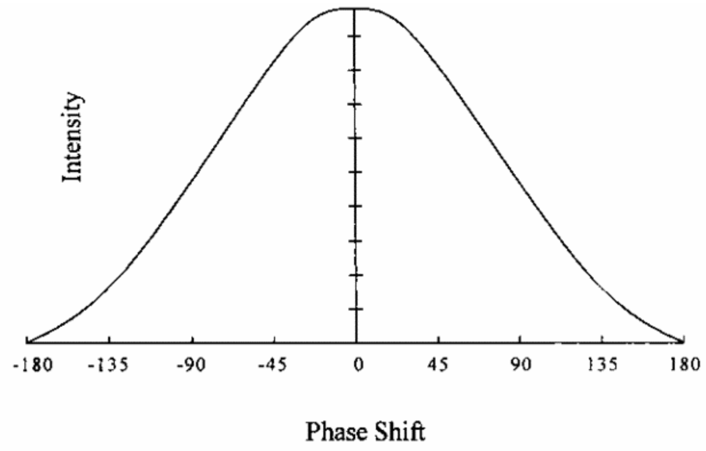

Figure 32 Optical intensity versus phase differences between interfering waves.

8. FOG Open Loop Biasing Scheme

In the presence of a rotation, the light waves travel different path lengths and mix slightly out of phase. The intensity is reduced due to the degree of destructive interference. The cosine function, which is symmetrical about zero, has its minimum slope there. For small rotational rates, it is impossible to determine the direction of rotation (CW or CCW) from the symmetrical aspect of Fig. 32, where the slope is near zero. Furthermore, the gyroscope operating in this mode has minimum sensitivity near zero. Incorporating a dithering phase modulator with drive modulation capability asymmetrically in the loop (near one end of the coil) provides a means to introduce a non- reciprocal phase shift to bias the gyroscope to its maximum sensitivity point [16, 17]. This corrective measure solves both the low-sensitivity problem and the issue of ambiguous direction of rotation at low rotational rates. The piezoelectric transducer (PZT) phase modulator shown in Fig. 33 stretches the fiber at controlled rates via the application of a voltage. The phase modulator produces an optical shift as a result of the applied voltage. After exiting the coupler, the CCW wave or pulse encounters the phase modulator, which is fully stretched. After traversing the coil loop in a time $\tau = n_f\ L/c$ (n_f is the refractive index of the fiber), the waves return to the coupler. The phase modulator is timed such that when the light wave propagating in the CW direction reaches the phase modulator the stretch has been relieved. Therefore, the light wave propagating in the CCW direction travels a longer distance. The two light waves experience a net nonreciprocal phase shift due to this path length difference. A schematic of the output of a gyroscope that is biased to operate at its maximum sensitivity point is shown in Fig. 34 for zero input. When a phase modulator is used, the expression for the intensity on the photodetector is

$$I = I_0\left[1+\cos(\delta\phi_s + \delta\phi_m)\right] \tag{49}$$

or with no rotation, $\delta\phi_s = 0$

$$I = I_0\left[1+\cos(\delta\phi_m)\right] \tag{50}$$

where the alternating bias phase shift is

$$\delta\phi_m = 2\phi_m \sin(\omega_m\ \tau/2)\cos[\omega_m(t-\tau/2)].$$

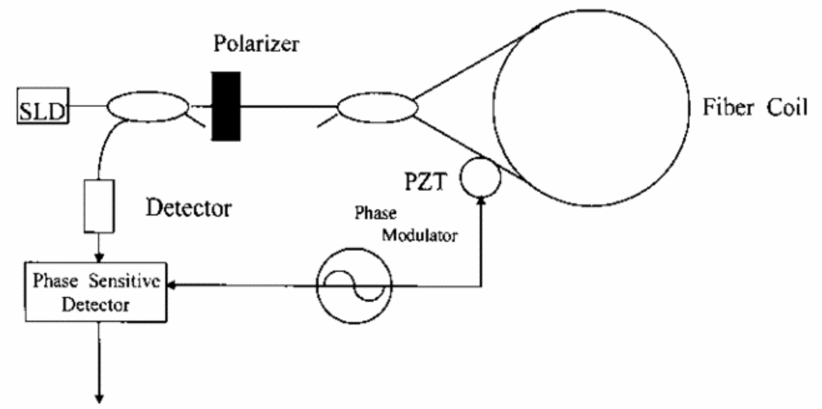

Figure 33 Schematic of IFOG with biasing phase modulator.

The modulation frequency is $\omega_m = 2\pi f_m$ and the amplitude of phase modulation is ϕ_m. The detector is synchronized to this alternating bias signal to permit detection of any variations in the output due to rotations. The phase is maximized at

$$f_m = \frac{1}{2\tau} = \frac{c}{2nL} \tag{51}$$

An expression for the sensitivity is devised from Eq. (50) as

$$\left|\frac{dI}{d\phi_m}\right| = I_0 \sin(\delta\phi_m) \tag{52}$$

It is obvious from Eq. (52) that a phase bias of 90° maximizes the sensitivity, that is, the gyroscope operates off its proper frequency when $\delta\phi_m = \pi/2$. For a 1-km length of fiber, the modulation frequency is 100 KHz. Shorter lengths of fiber require increased modulation frequencies for maximum sensitivity.

The intensity increases for a CCW rotation and decreases for a CW rotation, as illustrated in Fig. 34. An expression for the intensity at the photodetector of an IFOG biased to operate at maximum sensitivity $\delta\phi_m = \pi/2$, in the presence of a rotation is derived from Eq. (49) as

$$I = I_0[1 + \sin(\delta\phi_s)] \approx I_0[1 - \delta\phi_s] \tag{53}$$

Open-loop IFOGs, which have moderate scale factor stability, have good bias stability and are basically immune to random noise, the open-loop IFOG, however, has limited dynamic range. The FOG becomes nonlinear for large rotational rates when operating in the open-loop configuration. It is obvious from Eq. (53) that the rotational rates are limited between $\delta\phi_s = \pi/2$. The maximum rate in an open-loop IFOG operating at a wavelength of 1 μm with A = 100 cm^2 and N = 1000 is approximately 200°/s.

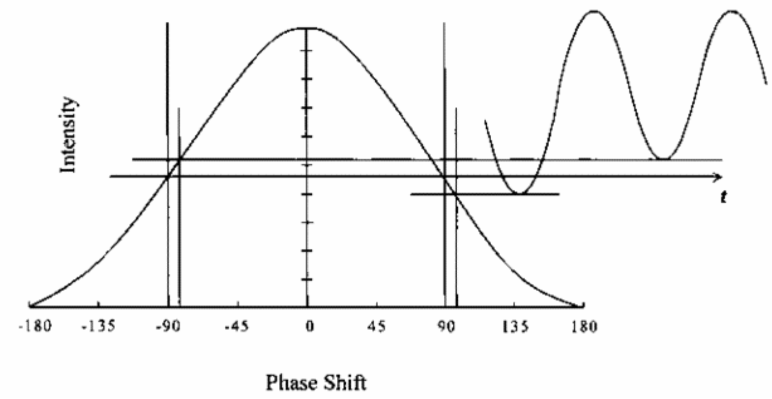

Figure 34 Optical intensity versus phase differences between interfering waves.

Designing of Experiment

Experiment is designed to give a process of powerful approach. To attain this approach, it is necessary that everyone involved in the experiment has a clear idea, in advance of the experiment, exactly what factors are to be studied, how the experiment is to be conducted, and at least a qualitative understanding of how the data will be analyzed. Montgomery (1997) gave an outline of the recommended procedure, reproduced in Figure 19. We now briefly amplify each point in this checklist.

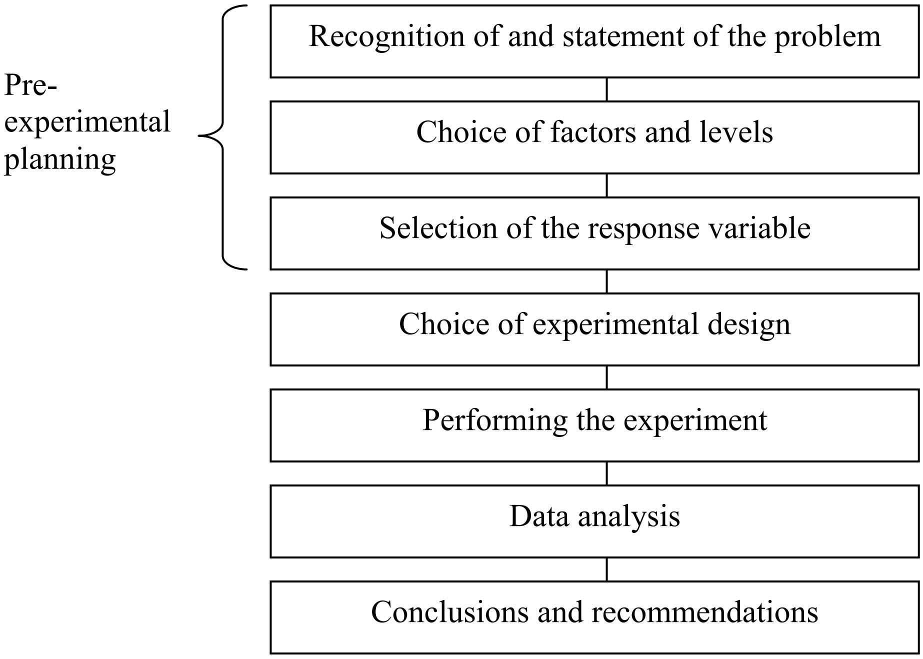

Figure 35 Procedure for designing an experiment.

1. Recognition of and statement of the problem. In practice, it is often difficult to realize that a problem requiring formal designed experiments exists, so it may not be easy to develop a clear and generally accepted statement of the problem. However, it is absolutely essential to fully develop all ideas about the problem and about the specific objectives of the experiment. Usually, it is important to solicit input from all concerned parties in the aspects of engineering, quality, marketing, the customer, management, and the operators (who usually have much insight that is all too often ignored). A clear statement of the problem and the objectives of the experiment often contribute substantially to better process understanding and eventual solution of the problem.

2. Choice of factors and levels. The experimenter must choose the factors to be varied in the experiment, the ranges over which these factors will be varied, and the specific levels at which runs will be made. Process knowledge is required to do this. This process knowledge is usually a combination of practical experience and theoretical understanding. It is important to investigate all factors that may be of importance and to avoid being overly influenced by past experience, particularly when we are in the early stages of experimentation or when the process is not very mature. When the objective is factor screening or process characterization, it is usually best to keep the number of factor levels low. (Most often two levels are used.) As noted in Fig. 12-4, steps 2 and 3 are often carried out simultaneously, or step 3 may be done first in some applications.

3. Selection of the response variable. In selecting the response variable, the experimenter should be certain that the variable really provides useful information about the process under study. Most often the average of standard deviation (or both) of the measured characteristics will be the response variable. Multiple responses are not unusual. Gage capability is also an important factor. If gage capability is poor, then only relatively large factor effects will be detected by the experiment, or additional replication will be required.

4. Choice of experimental design. If the first three steps are done correctly, this step is relatively easy. Choice of design involves consideration of sample size (number of replicates), selection of a suitable run order for the experimental trials, and whether or not blocking or other randomization restrictions are involved. The next chapter illustrates some of the more important types of experimental designs.

5. Performing the experiment. When running the experiment, it is vital to carefully monitor the process to ensure that everything is being done according to plan. Errors in experimental procedure at this stage will usually destroy experimental validity. Up-front planning is crucial to success. It is easy to underestimate the logistical and planning aspects of running a designed experiment in a complex manufacturing environment.

6. Data analysis. Statistical methods should be used to analyze the data so that results and conclusions are objective rather than judgmental. If the experiment has been designed correctly and if it has been performed according to the design, then the type of statistical methods required is not elaborate. Many excellent software packages are available to assist in the data analysis, and simple graphical methods play an important role in data interpretation. Residual analysis and model validity checking are also important.

7. Conclusions and recommendations. Once the data have been analyzed, the experiment must draw *practical* conclusions about the results and recommend a course of action. Graphical methods are often useful in this stage, particularly in presenting the results to others. Follow-up runs and confirmation testing should also be performed to validate the conclusions from the experiment.

Steps 1 to 3 are usually called pre-experimental planning. It is vital that these steps be performed as well as possible if the experiment is to be successful, Coleman and Montgomery (1993) discussed this in detail and offered more guidance in pre-experimental planning, including worksheets to assist the experimenter in obtaining and documenting the required information.

Throughout this entire process, it is important to keep in mind that experimentation is important parts of the learning process, where we tentatively formulate hypotheses about a system, perform experiments to investigate these hypotheses, and on the basis of the results formulate new hypotheses, and so on. This suggests that experimentation is iterative**.** It is usually a major mistake to design a single, large comprehensive experiment at the start of a study. A successful experiment requires knowledge of the important factors, the ranges over which these factors should be varied, the appropriate number of levels to use, and the proper units of measurement for these variables. Generally, we do not know perfectly the answers to these questions, but we learn about them as we go along. As an experimental program progresses, we often drop some variables, add others, change the region of exploration for some factors, or add new response variables. Consequently, we usually experiment sequentially**,** and as a general rule, no more than about 25% of the available resources should be invested in the first experiment. This will ensure that sufficient resources are available to accomplish the final objective of the experiment.

MATERIALS AND METHODS

The Equipment Designation

This designed equipment was composed of two parts which were rotation table (controllable) and fiber optic gyroscope (laboratory scale) as shown in Figure 36.

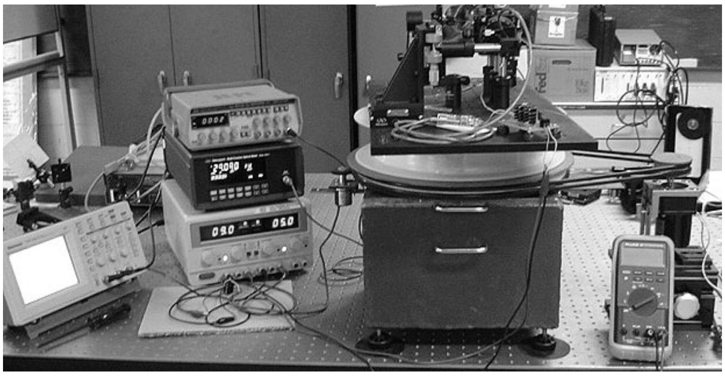

Figure 36 Experimental setup

1. Rotation Table

Rotation table consist of four parts that is rotation stand, rotation plate, reversible motor, and encoder (Figure 37)

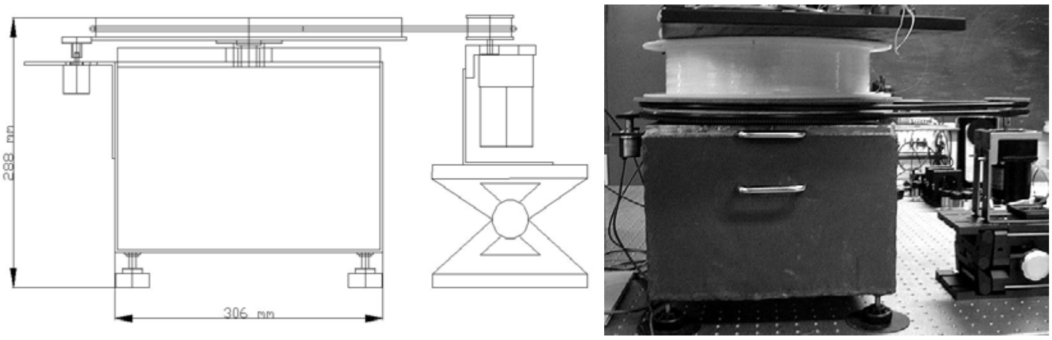

(a) (b)

Figure 37 a) Design of rotation table b) Rotation table

1.1 Rotation Stand Make from four iron plates, combine in to a box (300×300×200 mm) using gas wielding machine. The stand can correct a level of rotation table by using four level adjustable legs at the bottom.

1.2 Rotation Plate With two parts, lower part as a base with the roller bearing at the center and upper part is a gear wheel radius 180×4.5 mm connected with axle with cylindrical wood radius 175×20 mm on the top.

1.3 Reversible Motor model 2RJ4GA-A2 with resolution 1200 rpm/min manufactured by Oriental Motor (Figure 37 a).

1.4 Rotary Encoder model OSS-01-2 manufactured by Nemicon Corporation. As shown in Figure 37 b, this encoder can generate square pulse signal (5V), 100 pulses per round.

(a) (b)

Figure 38 a) Reversible motor b) Rotary encoder

Rotation plate will connect with reversible motor wheel by 2 rubber belts, so rotation rate is depend on how fast motor can drive.

2. Fiber Optic Gyroscope

Use open-loop configuration, the whole setup illustrates in Figure 39

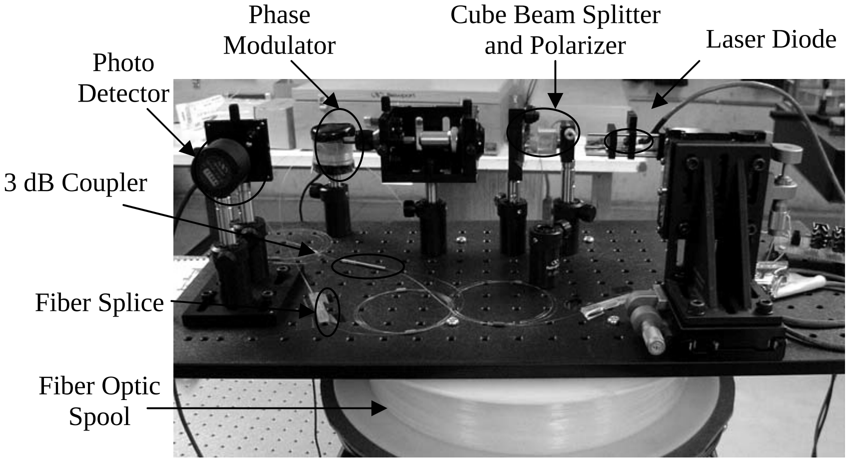

Figure 39 Fiber optic gyroscopes

List of equipment

- Sharp laser diode (type 022MCO, 3mW, 780 nm)

- Single-mode fiber optic spool (180 meters)
- Cube beam splitter
- Fiber splice
- Phase modulator (piezoelectric transducer)
- Function generator
- Laboratory DC power supply
- Multi-function optical meter and photo detector
- Oscilloscope (Tektronix TDS220)
- Laser diode power supply circuit: using voltage regulator LM317L as a current limiter to adjust current (at threshold current of laser diode) from power supply or battery and send it to laser diode.

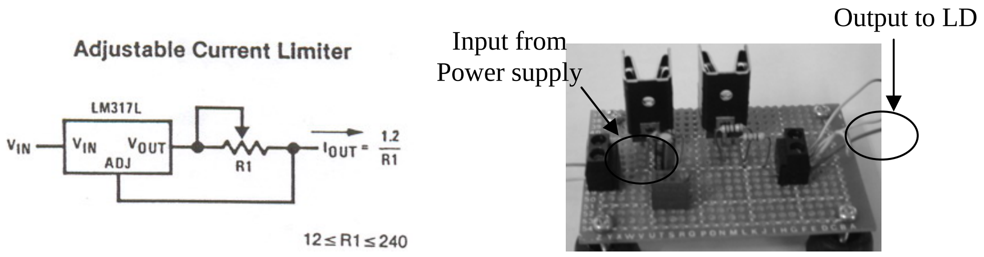

(a) (b)

Figure 40 a) Current limiter circuit diagram b) Current limiter circuit

We can measure output signal of fiber optic gyroscope by using a photo detector of multi-function optical meter as a sensor and display output pattern via oscilloscope.

3. Control and Measure Rotation Rate

Rotation rate can be controlled by adjust speed of reversible motor. As in Figure 42, reversible motor control circuit and variable transformer had been implemented. Using triac's number Q4004LT, this circuit can control input waveshapes of voltage from variable transformer by adjust variable resistance. With this ability to control waveshape, it can control motor's speed as well.

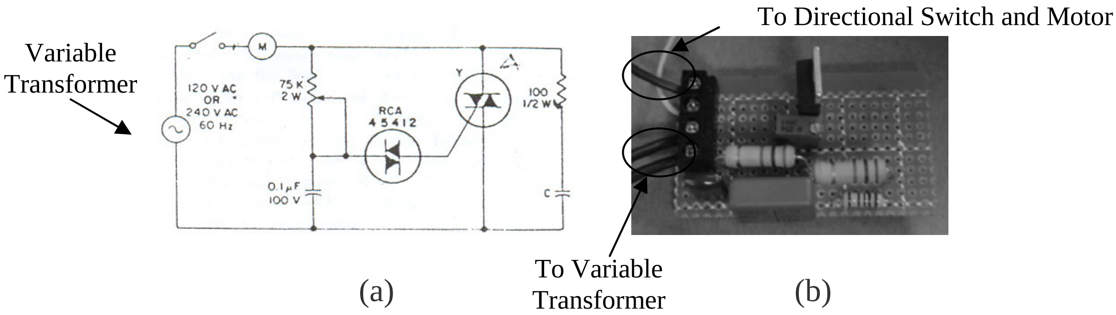

(a) (b)

Figure 41 a) Reversible motor control circuit diagram b) Reversible motor control circuit

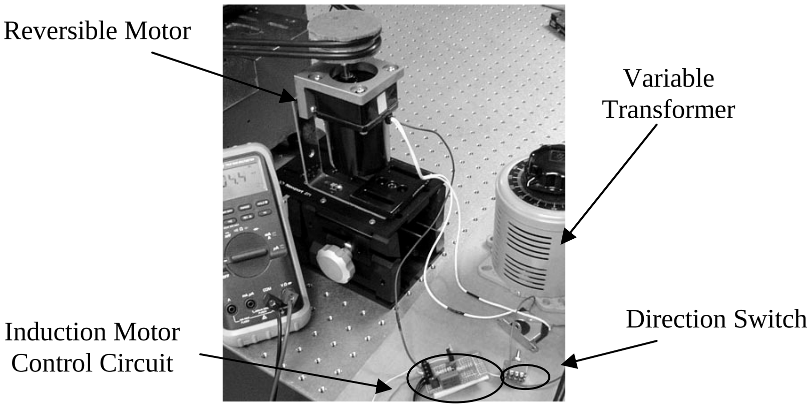

Figure 42 Reversible Motor's speed control set

We can determine rotation rate by count the pulse per round and measure period time of square wave that was generated from rotary encoder.

The experiment to measure pulse per round will perform as in Figure 43 (b), a counter circuit MT101 manufactured by Multihitech company had been used. MT101 will count output signal from rotary encoder while reversible motor is running. Until the main gear rotate 360 degrees, screw that attached to surface plate over main gear will touch the stopper switch. MT101 will stop. Result of this experiment will show as a 1 radian per pulse.

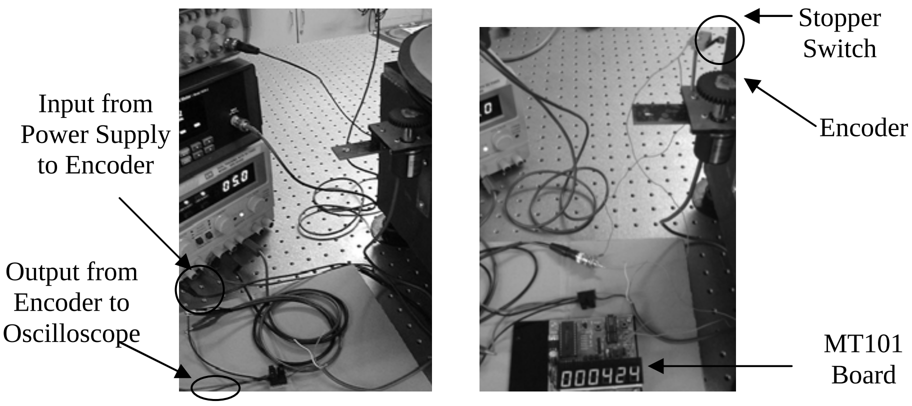

(a) (b)

Figure 43 a) Encoder set b) Pulse counter set

As in Figure 43 (a), Pulse width from encoder can be measure with oscilloscope. By divine radian per pulse with period time, rotation rate at the moment can calculate. (See appendix C for rotation rate calculate method and measurement information)

Design of Experiment

The experimental design follows the "Guidelines for Designing Experiments" described above. The guidelines provide seven steps to carry out the experimental design. There are several methods to handling the experimental plan such as "factorial method" or "Tagushi's method". Each method is provided by several supporting software such as the "Minitab" program. Following the seven step guideline of the "Minitab" software, the experiments run step by step with Tagushi's method as follows.

1. Recognition of and statement of the problem.

An objective of this experiment is to determine output signal of fiber optic gyroscope from photo detector. Therefore, the main factors that have effect on the accuracy of measurement are environment light, vibration and temperature.

2. Choice of factors and levels.

The 3 factors selected in the experiment are environment light, vibration and temperature. The control condition (level) for each factor is described below. Each factor is defined by 2 levels as illustrated in table 3.

The temperature factor can be controlled by adjusting air conditioner. This parameter is divided into 2 levels, i.e. 20°C (TC-1), 28°C (TC-2)

The fiber optic gyroscope was set on optical table. Therefore, the vibration factor can be controlled by turn optical table on (VC-1) and off (VC-2)

The experiment was performed in a close room. Each level of environment light factor is light on (LC-1) and light off (LC-2)

3. Selection of the response variables.

Table 1 Factors and levels of experimentation.

Number	Parameter	Level-1	Level-2
1	Temperature	TC-1	TC-2
2	Vibration	VC-1	VC-2
3	Environment light	LC-1	LC-2

4. Choice of experimental design.

At 3 factors and 2 levels, the Tagushi's method (Design of Experiment (DOE) from the "Minitab" software) designs the experiment as illustrate in table 4.

Table 2 Design of experimentation.

Experiment No.	Factor-1 (Temperature)	Factor-2 (Vibration)	Factor-3 (Environment light)
1	TC-1	VC-1	LC-1
2	TC-1	VC-2	LC-2
3	TC-2	VC-1	LC-2
4	TC-2	VC-2	LC-1

Note: Tagushi's experimental design provides a great benefit on making decision of experiment. As shown in table 4, the operator can perform only 4 experiments to retrieve the correlation of parameters those may cause effect with the calibration result. (Compare to 3^2 experiments).

5. Performing the experiment.

After designing the experiment, the real experiment will perform at rotation rate 0.0002 rad/s in counter clockwise direction. Output signal is collected ten times as a voltage from oscilloscope via multi-function optical meter.

Table 3 Experimental data

Exp No.	Output Voltage from oscilloscope (V)									
	Run1	Run2	Run3	Run4	Run5	Run6	Run7	Run8	Run9	Run10
1	3.62	3.61	3.54	3.55	3.63	3.56	3.54	3.58	3.61	3.61
2	3.29	3.27	3.31	3.28	3.28	3.26	3.32	3.28	3.26	3.26
3	3.57	3.51	3.52	3.57	3.54	3.56	3.52	3.56	3.51	3.57
4	3.72	3.77	3.64	3.60	3.72	3.69	3.60	3.60	3.75	3.70

6. Data analysis.

Using analyze tagushi design function of "Minitab" software to analyze data from the experimental results, the "main effect plot for mean values" illustrate in Figure 44, the "main effect plot for standard deviation" in Figure 45. The 3 columns of line graph showed the effect of data cause by varying the controllable factor and level (3 factors @ 2 levels). These analyzed data provide information of the system performance.

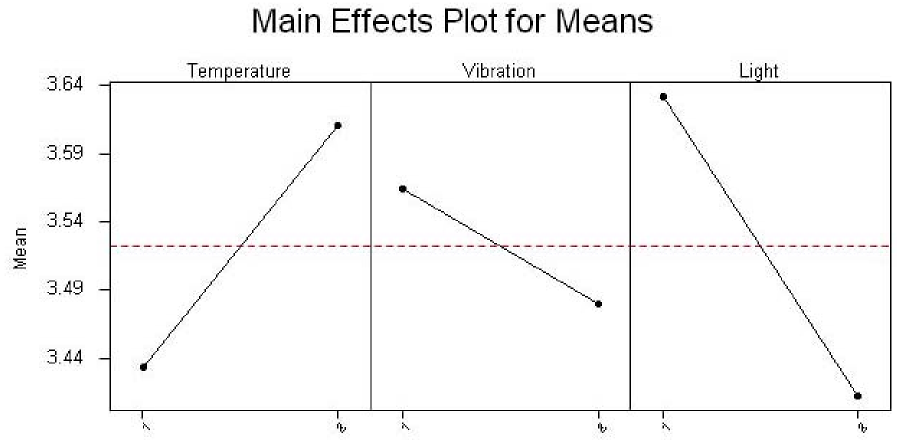

Figure 44 Main effect plot for the experimental mean value.

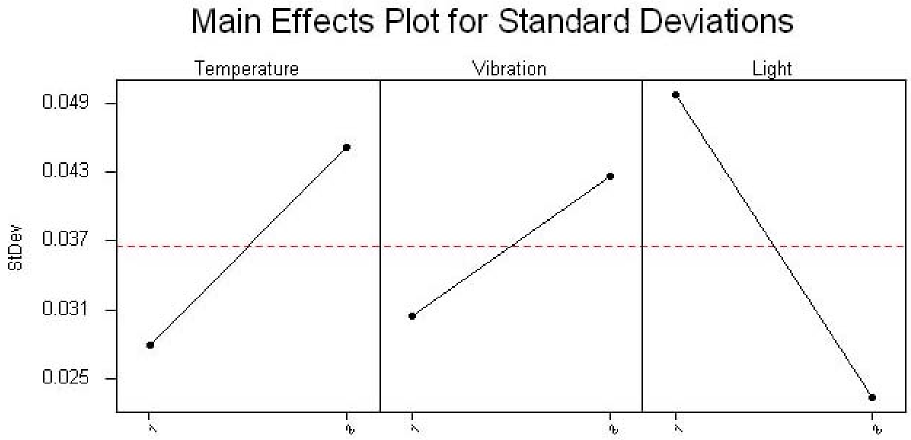

Figure 45 Main effect plot for the experimental standard deviation.

Main effect plot for mean (Figure 44) shown that the most effected factor is environment light then temperature and vibration. The best experiment condition consider from smallest standard deviations. From Figure 45, there have not many different between standard deviations of 2 conditions but it still have slightly different. The best condition is temperature at 20°C (TC-1), optical table on (VC-1) and turn off light (LC-2).

Statistical Analysis

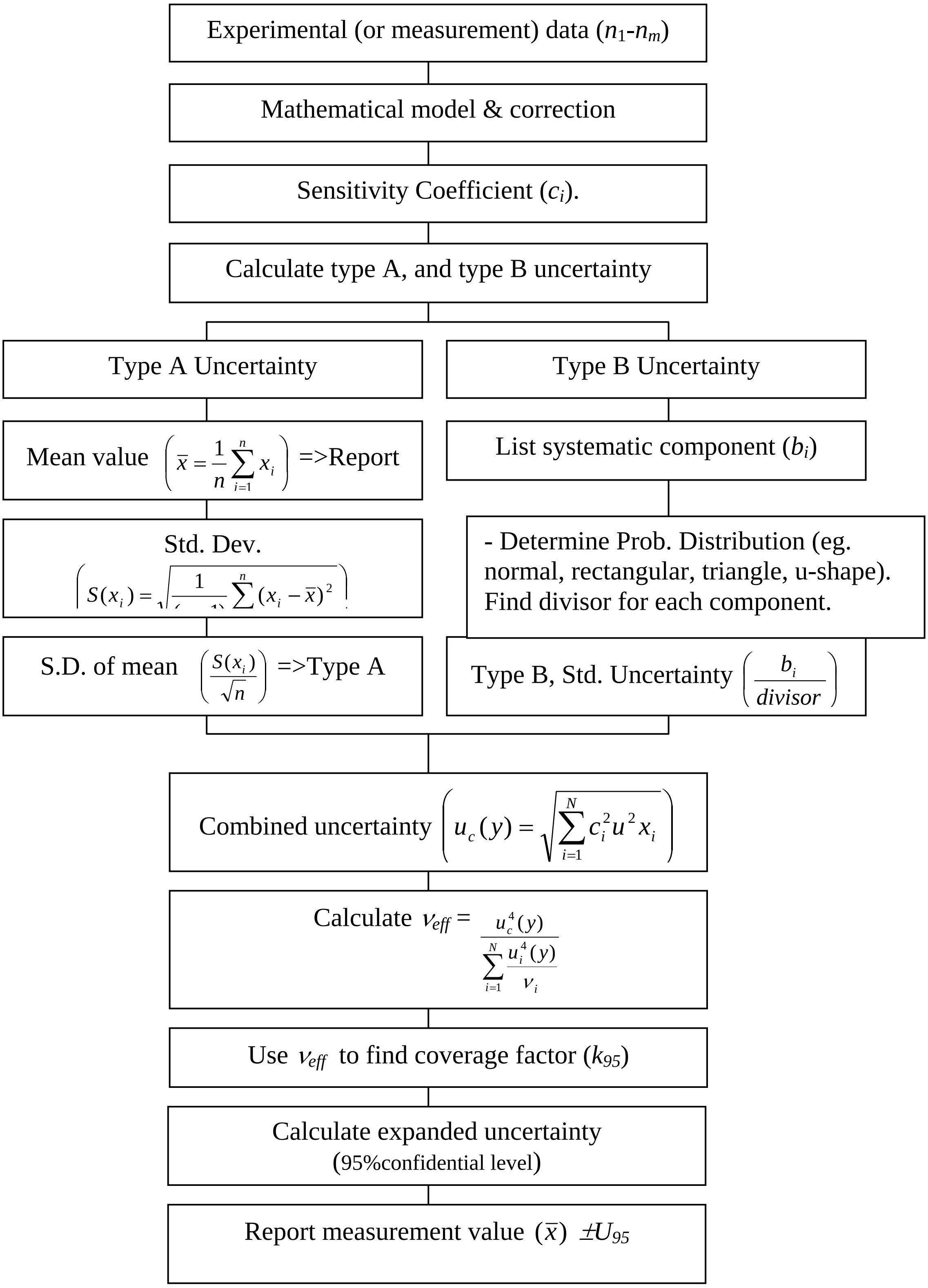

Figure 46 Flowchart for the determination of measurement uncertainty.

Place and Duration

Place: Photonic Metrology Laboratory, Department of Physics, Faculty of Science, Kasetsart University

Duration: April, 2004 – December, 2005

RESULT

At selected environment condition from design of experiment above (temperature at 20°C, turn on optical table and light off). The experiment is preformed at 5 different rotational rates (0, 0.13, 0.16, 0.24, 0.38 radian/s) in counter clockwise and clockwise direction. Multi-function optical meter detect output signal from fiber optic gyroscope and display its pattern on oscilloscope. To collect data, use "Wave Star" software to act as a data acquisition program to collect data log from oscilloscope via RS232 port. (Ratio of output from multi-function optical meter and oscilloscope is 10 µW per 1 volt.)

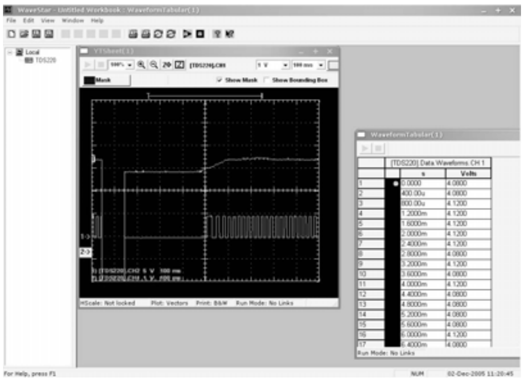

HScale: Not locked Plot: Vectors Print: B&W Run Mode: No Links

	[TDS220] Data.Waveforms.CH 1	
	s	Volts
1	0.0000	4.0800
2	400.00u	4.0800
3	800.00u	4.1200
4	1.2000m	4.1200
5	1.6000m	4.1200
6	2.0000m	4.1200
7	2.4000m	4.1200
8	2.8000m	4.0800
9	3.2000m	4.1200
10	3.6000m	4.0800
11	4.0000m	4.1200
12	4.4000m	4.0800
13	4.8000m	4.0800
14	5.2000m	4.0800
15	5.6000m	4.0800
16	6.0000m	4.1200
17	6.4000m	4.0800

Run Mode: No Links

02-Dec-2005 11:20:45

Figure 47 Wave star software

With wave form tabular functions, collect data log ten times at every rotational rate and direction. Each data log contains 2500 points of data of waveform. Find the mean of all data logs then calculate the uncertainty. (See appendix D for method to calculate an uncertainty.)

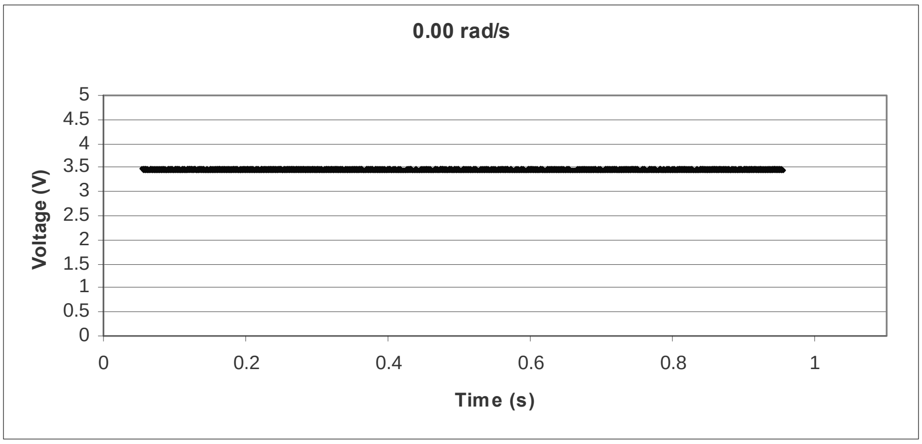

Figure 48 Graph of data log at rotational rate equal zero.

Note: As in Figure 48, some part of data log is including sweep part of oscilloscope. We can ignore it and consider only signal part.

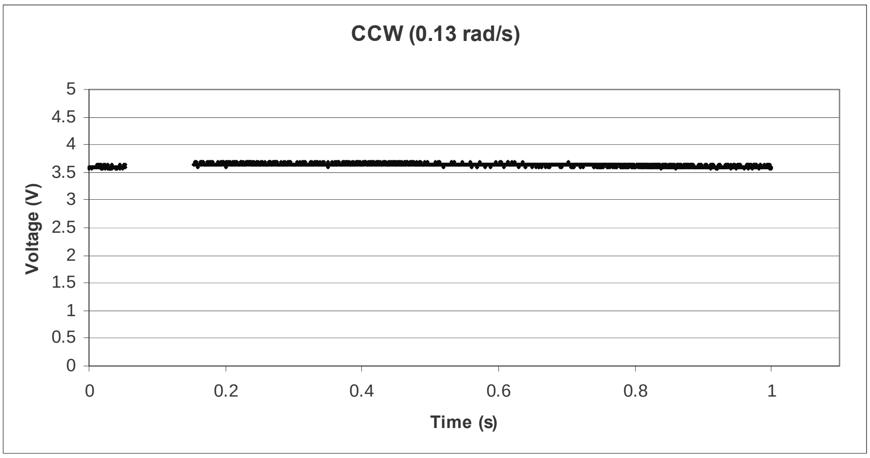

Figure 49 Graph of data log at rotational rate 0.13 radian/s. (CCW direction)

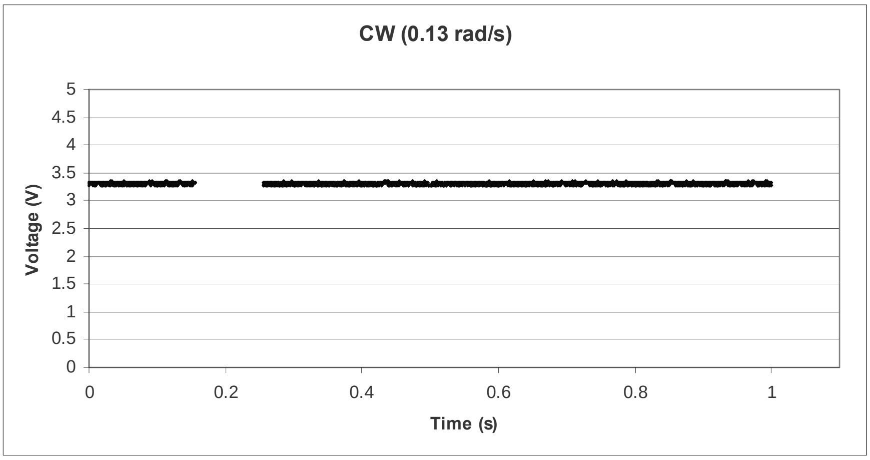

Figure 50 Graph of data log at rotational rate 0.13 radian/s. (CW direction)

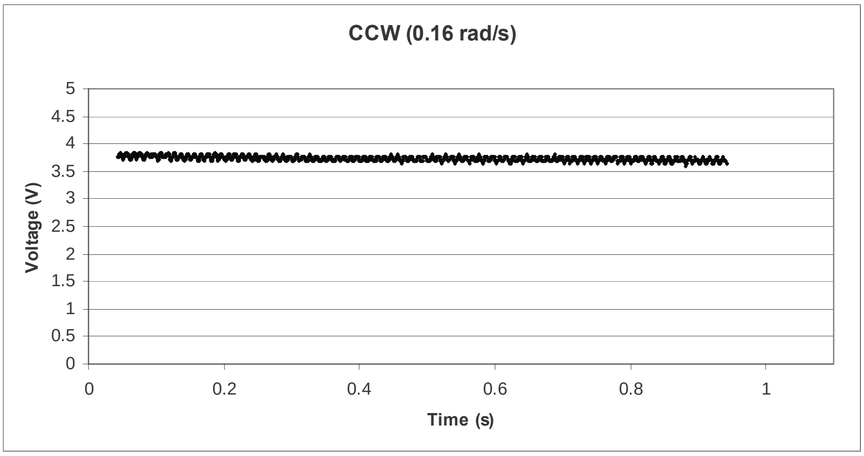

Figure 51 Graph of data log at rotational rate 0.16 radian/s. (CCW direction)

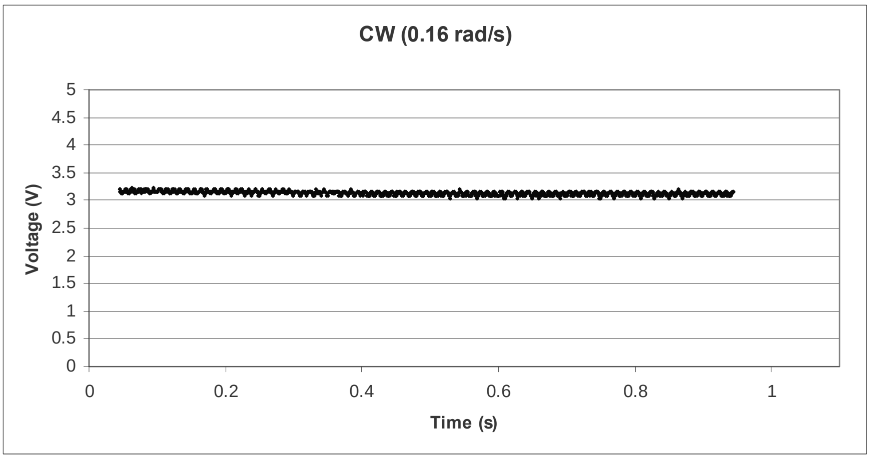

Figure 52 Graph of data log at rotational rate 0.16 radian/s. (CW direction)

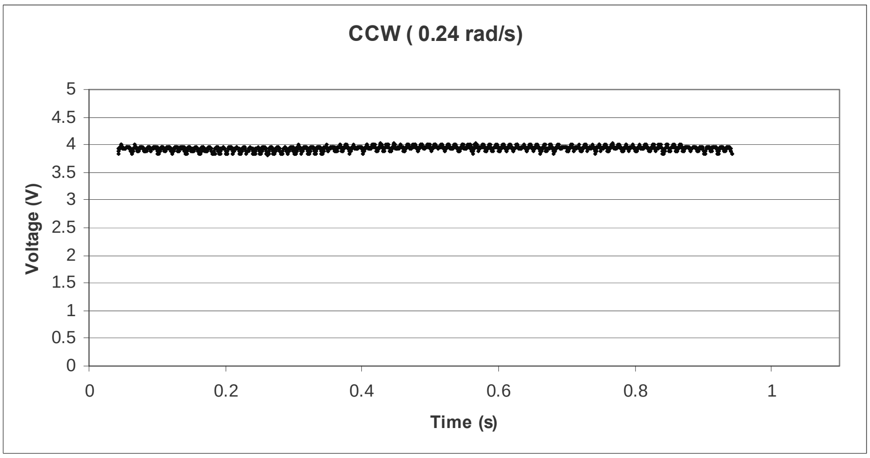

Figure 53 Graph of data log at rotational rate 0.24 radian/s. (CCW direction)

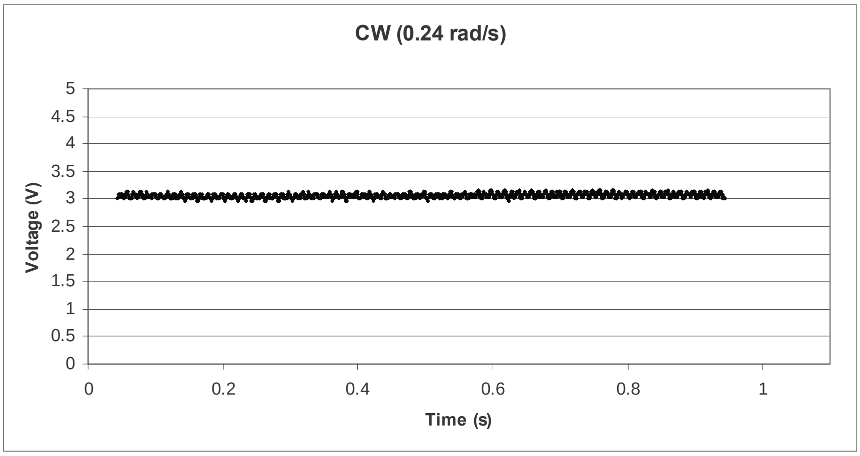

Figure 54 Graph of data log at rotational rate 0.24 radian/s. (CW direction)

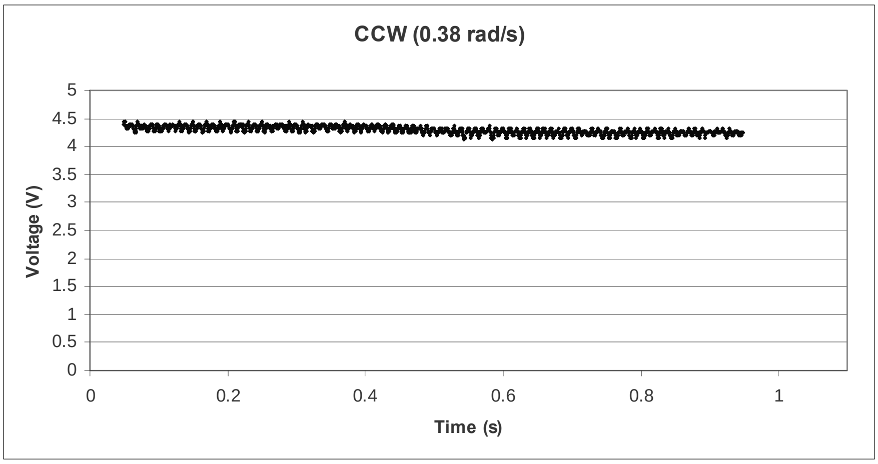

Figure 55 Graph of data log at rotational rate 0.38 radian/s. (CCW direction)

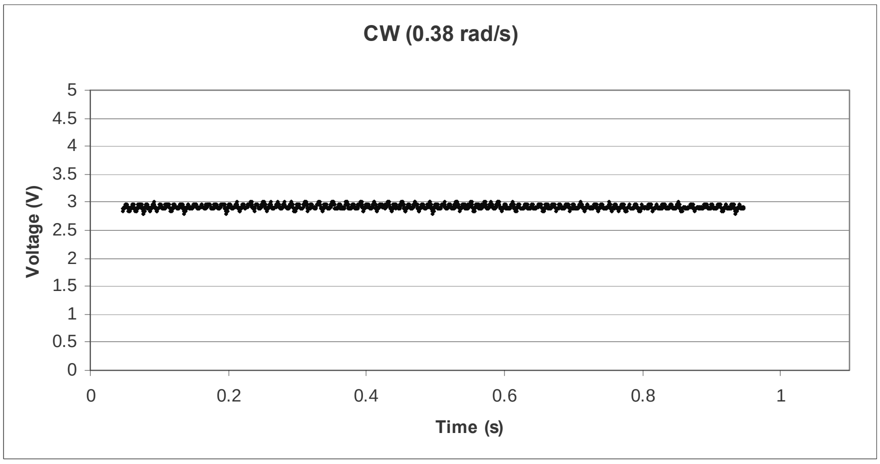

Figure 56 Graph of data log at rotational rate 0.38 radian/s. (CW direction)

Figure 48 to 56 showed the plot of data log of output voltage versus rotational rate at the moment. The plotting data were taken from oscilloscope by wave star software via RS232 port at 5 different rotational rates.

Table 4 Mean of data logs of output voltage at counter clockwise direction.

ω (rad/s)	Voltage (V) at counter clockwise direction									
	Run 1	Run 2	Run 3	Run 4	Run 5	Run 6	Run 7	Run 8	Run 9	Run 10
0.00	3.45	3.45	3.44	3.44	3.45	3.44	3.44	3.46	3.45	3.44
0.13	3.53	3.64	3.63	3.61	3.67	3.63	3.66	3.66	3.68	3.60
0.16	3.69	3.66	3.69	3.73	3.77	3.79	3.73	3.78	3.80	3.82
0.24	3.86	3.84	3.93	3.94	3.97	3.91	3.94	3.95	3.95	3.96
0.38	4.12	4.33	4.22	4.21	4.29	4.30	4.31	4.25	4.24	4.22

Table 5 Mean of data logs of output voltage at clockwise direction.

ω (rad/s)	Voltage (V) at clockwise direction									
	Run 1	Run 2	Run 3	Run 4	Run 5	Run 6	Run 7	Run 8	Run 9	Run 10
0.00	3.45	3.45	3.44	3.44	3.45	3.44	3.44	3.46	3.45	3.44
0.13	3.29	3.29	3.27	3.31	3.31	3.33	3.33	3.34	3.34	3.29
0.16	3.13	3.00	3.10	3.17	3.16	3.16	3.17	3.19	3.11	3.17
0.24	2.99	3.05	3.07	3.08	3.07	3.06	3.05	3.08	3.07	3.06
0.38	2.92	2.87	2.80	2.91	2.92	2.91	2.92	2.91	2.90	2.90

In Table 4 and 5, output voltage from fiber optic gyroscope at counter clockwise direction increase when rotational rate is faster. In the other hand, output voltage at clockwise direction decrease.

Table 6 Result of measurement and uncertainty

Rotational rate (radian/s)	Output from FOG (V)	
	CCW	CW
0.00 ± 0.000	3.44 ± 0.287	3.44 ± 0.287
0.13 ± 0.005	3.63 ± 0.298	3.31 ± 0.281
0.16 ± 0.005	3.75 ± 0.304	3.14 ± 0.274
0.24 ± 0.008	3.93 ± 0.313	3.06 ± 0.268
0.38 ± 0.011	4.25 ± 0.330	2.90 ± 0.260

Table 6 show the analyzed uncertainty of rotational rate and output voltage from fiber optic gyroscope. From appendix D, the highest uncertainty came from digital oscilloscope due to the specification of oscilloscope itself. That is because manufacturers always limit the uncertainty of instrument at the maximum. The uncertainty of output voltage can be reduce by finding the real uncertainty of oscilloscope by calibration or change the oscilloscope to another one with more accuracy.

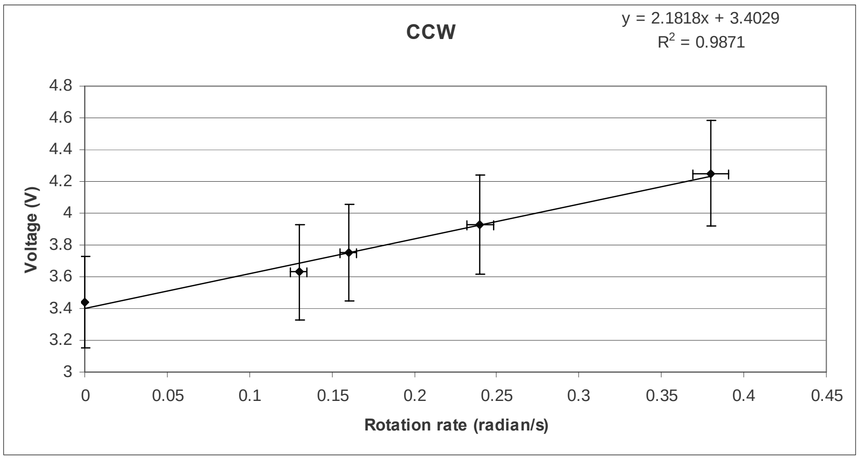

Figure 57 Graph of rotational rate 0.00-0.38 radian/s. (CCW direction)

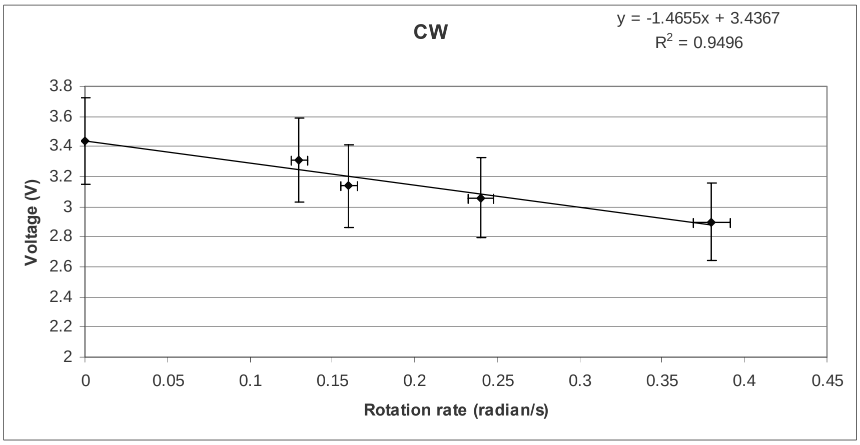

Figure 58 Graph of rotational rate 0.00-0.38 radian/s. (CW direction)

Figure 57 and 58 showed the trend line, voltage and uncertainty at every rotational rate and direction. In counter clockwise direction, the output voltage increase when rotational rate increase and decrease in clockwise direction. R-square value of both figures showed that actual data is close to 1 that means estimated values of trend line is reliable.

DISCUSSION

1. Difference of Output Signal in CW and CW Direction

Consider from the trend line of figure 57 and 58, output voltage in counter clockwise direction increases 0.05 mV per 0.1 radian/s and in clockwise direction decreases 0.07 mV per 0.1 radian/s. Normally, it should change equally. This difference happens because the rotational rate of reversible motor in CW and CCW direction, at the same input voltage, is not equal. And the motor itself is not stable. Rotational rate of motor in CCW direction is slightly faster than CW direction. This problem can be solved by increasing input voltage in CW direction but it is almost impossible to make it equal to CCW direction. The best way is to change this motor to the one with higher accuracy and more stable.

Another reason that causes a drift in output signal is fiber splice and the polarization of two lights (CCW and CW). Fiber splice that used to connect 3 dB coupler and fiber optic coil is temporally type. Light can easily leak from this type. The output signal will maximize if the input intensity from 3 dB coupler to both fibers is equal. It is true that it has never been done but we can minimize it by changing fiber splice to fiber connector (ST-type or etc...). Another reason is that the fiber optic single mode is not a polarization preserve type. It causes some difference in polarization of light when it travels in fiber optic coil and affect the ratio of output signal. By changing fiber splice and fiber optic to connector type and polarization preserve, this can minimize this problem.

2. Fiber Optic Gyroscope

Result of measurement from this prototype is satisfactory. Due to the low budget and fund this is the best configuration we can make. Many parts needed to be improved are the size of the fiber optic gyroscope, piezoelectric transducer and the fiber optic itself. The size of this prototype is too big and heavy. Piezoelectric transducer is not effective and stable. It works by wrap a fiber optic around it and hold it with adhesive tape. It increases output signal sensitivity but it does not have much affect to result due to the rotational rate is already high enough. It can be used around 1 week or more but the adhesive tape will deteriorate with time. All of this can be solved by using integrated optic circuit that contains coupling guide, modulate crystal and polarizer in it. This optical circuit combines 3 different instruments into one small device. This will totally decrease size of FOG. With a smaller size, we can measure the output on the controllable rotational plate at higher accuracy.

3. Laser Source Alignment

One of the most difficult parts of this research is to coupling light from light source into fiber optic single mode. Due to the single mode fiber core is really small (around 5.7μm), light can not enter fiber without alignment. To do that, using target screen with a center reference point to check the angle of light at 3 ranges (close, middle and longest). It has to be sure that its angle is parallel to surface plate and not incline from center point. The light will easily propagate into optical fiber after adjust x-y knob of fiber coupler assembly.

4. Fiber Optic

Normally, fiber optic is really flexible material. It can resist amount of stress, and blending but it still can be broken easily too. When it is broken, it can pierce in to your skin and it is really hard to take it out because of its size. To connect fiber optic with another instrument, cladding needs to be removed. Plastic solvent as a chloroform had been used. It is a dangerous solution. Breathing chloroform can cause dizziness, fatigue, and headaches. With all reasons above, great care is needed when you work with fiber optic.

Environmental effects, such as temperature, stress, light, etc., have impact on light propagating through fiber. The mechanisms by which temperature may influence light in fiber are extremely complex. Especially in single mode fiber interferometric sensors are very susceptible to temperature. And each optical fiber had it own property. Only one range of light can effectively travel in it. So, to understand more of optical fiber and environment effect to make a better fiber optic gyroscope, further study and research in this topic is needed.

5. Rotation Table

In first design, the reversible motor is connected with rotation stand. But after turning on the motor, vibration from it causes a lot of noise. It happens because fiber optic gyroscope is very sensitive even with the small vibration. Then the design changed into present one by separate motor from rotation stand and using rubber belt to drive to main gear. The result makes the noise gone and the signal from fiber optic gyroscope can be detected.

CONCLUSION

The objective of this thesis is to measure the output from fiber optic gyroscope (prototype) comparing with rotational rate. With reversible motor, 4 different rotational rates can be generated (0.00, 0.13, 0.16, 0.24 and 0.38 radian/s). After analyzing the result from design and the experiment result, it is found that the most important factor that affects the measurement system is environmental light. The other factors are temperature and vibration. The experiment was performed at temperature 20°C, on optical table and light off in both directions (clockwise and counter clockwise).

Results of the above experiment showed that the higher rotational rates, the greater change of output voltage were obtained. From figure 57 and 58, the output voltage increases in the ratio 0.1 V per 0.05 radian/s in counter clockwise direction and decreases 0.1 V per 0.07 radian/s in clockwise direction (regarding to the output voltage at zero rotational rate is 3.44 V).

The study of measurement results revealed that the output signal obtained from fiber optic gyroscope is consistent with rotational rate. It increases and decreases proportionally to rotational rate in CCW and CW directions. Therefore, angular displacement and rotational rate can be determined. And fiber optic gyroscope itself had really high sensitivity. It can detect even a small rotational rate. On the other hand, it can easily detect the noise from environment too. With improvement discussed above, this fiber optic gyroscope will be the best low cost instrument to measure rotational rate.

LITERATURE CITED

Anonymous 2000. **MINITAB Statistical Software, Release 13.20.** Minitab Inc. Available Source: http://www.minitab.com, June 15, 2005

Beckwith, T.G. 1993. **Mechanical Measurements.** 5th ed 1993. Addison-Wesley Publishing Company, Inc.

Levfevre, H.C. 1996. **Fundamental of the Interferometric Optic Gyroscope.** Photonetics, n.p.

Montgomery, D.C. 2001. **Introduction to Statistical Quality Control.** 4th ed. John Wiley & Sons, Inc., New York.

Newport. 1993. **The project in single mode fiber optics.** Newport Corporation. n.p.

Newport. 2002. **The Newport Resource.** Newport Corporation. n.p.

Pedrotti, F.L. and L.S. Pedrotti. 1987. **Introduction to Optics**. 2nd ed. Prentice Hall. Englewood Cliffs, New Jersey.

Ruffin, P.B. 2002. Fiber Gyroscope Sensors, pp.383-415. *In* F.T.S. Yu, ed. **Fiber Optic Sensors.** Marcel Dekker Incorporated, New York.

Saleh, B.E.A. and M.C. Teich. 1991. **Fundamental of Photonics.** John Wiley & Sons, Inc., New York.

Singapore Institute of Standards and Industrial Research. 1995. **Guidelines on The Evaluation and Expression of The Measurement Uncertainty.** 1st ed. n.p.

Taylor, B. N. 1995. **Guide for the Use of the International System of Units (SI).** National Institute of Standard and Technology (NIST). Gaithersburg, MD.

Tektronix, Inc, **TDS 200-Series Digital Real-time Oscilloscope (User Manual).** n.p.

Udd, E., W. Schulz, J. Seim, J. Corones and H.M. Laylor. 1998. **Fiber Optic Sensors for Infrastructure Applications.** n.p.

United Kingdom Accreditation Service. 1997. **The Expression of Uncertainty and Confidence in Measurement, M-3003.** 1st ed. Teddington, Middlesex.

APPENDIX

Appendix A

M-3003

The Expression of Uncertainty and Confidence in Measurement

0 Introduction

0.1 The *NAMAS Accreditation Standard*, M10, requires accredited laboratories to produce estimates of uncertainty of its measurements for all calibrations using accepted methods of analysis. This requirement may be met by following the procedures described in this publication which supersedes NIS 3003 Edition 8: 1995 and is intended for application to all fields of measurement.

0.2 The requirements for estimation of measurement uncertainty apply to all results provided by calibration laboratories. They also apply to results produced by testing laboratories under the following circumstances:

(a) Where it is required by the client.

(b) Where it is required by the specification to which the test is carried out.

(c) Where the uncertainty is relevant to the application or validity of the result; eg. where the uncertainty affects compliance to a specification or stated limit.

0.3 It is also a requirement that any laboratory, testing or calibration, which carries out international calibrations in support of its accredited activities, produces estimates of uncertainty for those internal calibrations. Further details can be found in Section 3 of the M10 Supplement, *Measurement and Calibration Systems.*

0.4 The need for an internationally accepted procedure for expressing measurement uncertainty led, in 1981, to the international authority in metrology, the Committee International des Poids et Measures (CIPM), approving brief outline recommendations (1) submitted by a working group of representatives from the major national standards laboratories. The International Organization for Standardization (ISO) was then given the task of developing a detailed guide applicable to all levels of accuracy from fundamental research to shop floor operations. The responsibility for the preparation of such a comprehensive document for this broad spectrum of measurements was assigned to a working group of the ISO Technical Advisory Group on Metrology (ISO/TAG4/WG3) and led to publication of the ISO *Guide to the Expression of Uncertainty in Measurement* [2] (hereafter referred to as the *Guide*) in 1993. The *Guide* is now available as a BSI publication.

0.5 The uncertainty calculations given in this publication are consistent with the recommendations made in the *Guide* and with the European Accreditation of Laboratories (EAL) document R2 [3]. There are some areas where EAL R2 uses different terminology to that of the Guide. For example, EAL R2 uses the term “standard uncertainty of the output estimate” in place of “combined standard uncertainty” which is used in the *Guide*. Where such differences occur, this edition of M 3003 has been kept consistent with the *Guide* (see, however, the Note to Section 10). At the same time other changes have been made in this edition, as follows:

(a) To correct transcription errors that occurred in Edition 8 of NIS 3003.

(b) To improve the presentation and to broaden the document to include aspects of testing activities.

(c) Some of the uncertainty examples in Appendix H have been updated as a result of welcomed comments from the users of the document.

(d) Sections describing *Best Measurement Capability* and the use of calculators or spreadsheets have been added.

(e) The situation where uncertainty has to be expressed for a range of values has been addressed.

0.6 Appendices D, E, F and G in this publication provide details of common sources of error and uncertainty for a number of different fields of calibration and Appendix H provides examples of the application of M 3003 to the expression of uncertainty in these fields. Appendix I address the situation where an expression of uncertainty is required for a range of values; Appendix J deals with reporting “compliance with specification”. An overview of the expression of uncertainties for testing activities is given in Appendix K. The use of calculators and spreadsheets for calculation of uncertainty is discussed in Appendix L.

0.7 As far as possible the terms and symbols used in this publication have been aligned with the *Guide*. A full list of symbols and their definitions is given is Section 10. Definitions of some of the general metrological terms are given in the *Guide*.

1. Overview

1.1 It has long been recognized that most measurements in calibration and testing work are subject to errors which are not perfectly quantifiable and that, therefore, there is uncertainty associated with the results of such measurements. A measurement result is therefore in complete without a statement of the corresponding measurement uncertainty.

1.2 This section of M 3003 briefly examines methods of combining and expressing uncertainties and gives an overview of the approach taken herein, in the *Guide* (2) and in its derivatives such as EAL-R2 [3]. The detail of the methodology involved is presented in Sections 2 to 8 and Appendices B and C of this document.

1.3 It should be stated at this point that there is no fundamentally correct way of combining uncertainties. The *Guide* describes the accepted methods used by most laboratories and required by most accreditation bodies, but it should be remembered that it is a guide – a set of conventions, designed to produce a reasonably quantifiable uncertainty statement, mainly based on statistical techniques. We are trying to express the concept of impreciseness as consistently as possible!

1.4 By using a predetermined set of conventions, such as is presented in the *Guide*, accreditation bodies, laboratories and their clients are able to compare results from different sources in a meaningful manner. This approach also means that uncertainties, passed down from National Standards to the end user (often through a chain of several laboratories), are treated in a consistent and meaningful manner at each step of this process.

1.5 An easy and obvious way of combining uncertainty contributions would be simply to sum their limit values and quote the total as the overall uncertainty. This has certainly been the tradition in a number of fields of measurement but is no longer acceptable. Arithmetic summation has the advantages that it is quick, easy and generally yields a high level of confidence. In fact, at first sight, the use of arithmetic summation would appear to imply 100% confidence in the extent of the uncertainty associated with the measurement result.

1.6 Arithmetic summation does, however, have disadvantages. First, it is unlikely that, when errors from a number of different sources are combined, the sign and magnitude of the errors are such that they will all add up to the limit value produced by arithmetic summation. Arithmetic summation means, therefore, that an unduly pessimistic estimate of uncertainty would often be quoted.

1.7 Secondly, every experienced metrologist knows that if a measurement is repeated a number of times under the same conditions, a spread of values will be obtained. Furthermore, there will occasionally be a result that is so inconsistent with the others that the metrologist might ignore it, regarding it as an outlier or spurious result. But how far away does this outlier have to be from the mean value before it is ignored? This is where the experience of the metrologist comes in – he or she will, through knowledge and experience, have developed an almost intuitive "feel" for results that should be discounted. So, almost without thinking about it, the metrologist might impose statistical limits on the spread of values that are included in the overall uncertainty – and without any quantifiable justification for the extent of these limits.

1.8 It follows that if this intuitively truncated spread of values is added in with other sources of error, there is a small but finite possibility that the "true value" actually lies outside the stated uncertainties – in other words, the 100% confidence implied by arithmetic summation is not attainable. Using this approach, a statement of the confidence with which it is assumed that the "true value" does lie within the stated limits is not possible.

1.9 For these reasons, the *Guide* approaches the subject of measurement uncertainty using statistical methods as with all methods of addressing this subject it is not perfect – it sometime depends, for example, on imperfectly known probability distribution being assumed to have particular characteristics – but it enable reasonable values to assign to overall uncertainty. Complete with information regarding the confidence probability with which the uncertainty statement is associated.

1.10 It is now apparent that the subject of measurement uncertainty is complex. The *Guide* takes a logical approach to the subject and it is worth, at this point, summarizing this approach:

(a) There is an input quantity to the measurement process, for example the imported calibration uncertainty, effects of ambient temperature or the repeatability of the process. This input quantity is represented by the symbol x. There will usually be more than one input quantity so the i_{th} quantity can be represented by the symbol x_i.

(b) The standard uncertainty associated with the i_{th} input quantity is represented by $u(x_i)$. The standard uncertainty is defined as one standard deviation and is derived from the uncertainty of the input quantity by dividing by a number associated with the assumed probability distribution. The divisors for the distributions most likely to be encountered are as follows:

Normal	1
Normal (k = 2)	2
Rectangular	$\sqrt{3}$
Triangular	$\sqrt{6}$
U-shaped	$\sqrt{2}$

(c) There is an output quantity for the measurement process – the estimated value of the measurand – and this is given the symbol y.

(d) In some cases the input quantity to the process may not be in the same units as the output quantity. For example, one contribution to a measurement of, say, a gauge block or a Weston cell, may be the effect of temperature. In these cases the input quantity is temperature, but the output quantity is dimensional or electrical. It is therefore necessary to introduce a sensitivity coefficient so that the output quantity (y), can be related to the input quantity (x_i). This sensitivity coefficient is referred to as c_i. The sensitivity coefficient is effectively a conversion factor from one unit to another.

(e) The relationship between the input quantity and the output quantity may not be linear. The partial derivative $\partial f / \partial x_i$ can be used to obtain the sensitivity coefficient and this is one of the reasons that mathematical modeling is used to describe measurement systems. In practice the derivation of the partial derivatives can be difficult and the effort involved is not always justified by the results obtained. A linear approximation such as the quotient $\Delta f / \Delta x_i$, where Δf is the change in f resulting from a change Δx_i in x_i, is often sufficient.

(f) Once the output quantities associated with each input quantity x_i have been obtained in the form of a standard uncertainty (one standard deviation) they are combined by taking the square root of the sum of the squares. This yields the combined standard uncertainty $u_c(y)$.

(g) The combined standard uncertainty, $u_c(y)$, is also in the form of one standard deviation. This does not give sufficient confidence, for most purposes, that the “true value” lies within the stated limits. For this reason $u_c(y)$ is then multiplied by a coverage factor, k, to provide an expanded uncertainty, U. For most purposes a value of 2 is used for k, yielding a confidence level of approximately 95%.

(h) The result of the measurement is then reported, normally in form of $y \pm U$. This statement is not complete without mention of the coverage factor used to obtain the expanded uncertainty. An indication of the confidence level obtained should also be included. Appropriate statements are described later in this document.

1.11 There are some exceptions to the general approach for the method of combining uncertainties described above. These are dealt with later in the document but can be summarized as follows:

(a) Where there are unreliable input quantities – for example, poor repeatability.

(b) Where there is a dominant systematic uncertainty contribution.

(c) Where there is correlation between two or more of the input quantities.

(d) Where the uncertainties are not bilateral, ie the positive uncertainty limit differs from the negative one.

2. Concepts

2.1 An expression of the result of a measurement is incomplete unless it includes a statement of the associated uncertainty. The uncertainty of a measurement result is a parameter that characterizes the spread of the values that could reasonably be attributed to the measurand. It states the range of values within which the value of the measurand is estimated to lie within a stated level of confidence.

2.2 It is essential to distinguish the term ‘error’ (in a measurement result) from the term ‘uncertainty’. Error is the measurement result minus the *true* value of the measurand. Whenever possible a correction equal and of opposite sign to an error is applied to the result. Because true values are never known exactly (else there is no need to make a measurement), corrections are always approximate and a residual error remains. The uncertainty in this residual error will contribute to the uncertainty of the reported result.

2.3 Given the meaning of ‘error’ it follows that uncertainty can also be defined as the range about zero in which the error is thought to lie. It can be characterized in terms of the spread of the probability distribution for the error. This error distribution may be derived from the observed random variation in results, from theoretical knowledge of the error mechanism, or in some other way. The CIPM recommends a standard deviation as a measure of the spread of the distribution (one 'standard deviation'), but this is not sufficient in most fields of measurement where a confidence interval needs to be defined. It can be said that the true value of the measurand (or the error) lies within the stated range with a certain level of confidence. (eg 95% or 99%).

2.4 The basis for the treatment of uncertainty in this publication is the assumption that all uncertainty components can be treated in the same way irrespective of the nature of their associated errors. In particular, it is assumed that their associated error distributions can be combined using ordinary statistical procedures, whether they are fixed during a measurement process (systematic error) or vary randomly (random error).

2.5 Sometimes a normal (ie Gaussian) distribution will adequately describe an error. At other times, when information is lacking, it may be appropriate to model it with a rectangular distribution, assigning equal probabilities to values between extreme limit. It must be noted that there will sometimes be circumstances when this assumption would give rise to optimistically small uncertainty estimates, eg, when the distribution is 'U' –shaped; Appendix D9 gives an example. It may be pessimistic, such as when the distribution is trapezoidal. In cases of doubt the rectangular distribution can be assumed; this assumption should, however, always be recorded. Further information on the treatment of various distributions is given in the *Guide*. When a number of distributions of whatever form are combined it can be shown that, apart from in one exceptional case, the resulting probability distribution tends to the normal form in accordance with the Central Limit Theorem (6). The importance of this is that it makes it possible to assign at least a minimum level of confidence in terms of probability to the total uncertainty. The exceptional case arises when one contribution to the total uncertainty dominates; in this circumstance the resulting distribution departs little from that of the dominant contribution.

2.6 Faced with the task of identifying and evaluating uncertainties in any specific measurement process it is convenient to classify them in terms of their effect on that process. When a measurement is repeated a number of times under substantially the same conditions, then, provided the measurement process has sufficient sensitivity to resolve small differences, the results will not all be the same due to the cumulative effect of small independent random variables. It is because of the observable random effects that this indeterminacy is referred to as the random component of uncertainty.

2.7 Corrections for errors in a measurement process may have to be made to ensure the traceability of the mean value of a sample of results to the national standard. The residual errors in these corrections are systematic in their effect on the measurement process at the time of its use, and therefore the corresponding uncertainty components are sometimes classified as systematic by association.

2.8 In mentioning the traditional classification of describing components of uncertainty as 'random' or 'systematic', it has to be appreciated that this is only meant to apply to the specific measurement process under consideration. In a hierarchical national measurement system, as uncertainties are propagated down through the calibration laboratories in the system, the classification of an influence quantity as a random component of uncertainty at one echelon will change to being a systematic component of uncertainty at the next lower level. For example, a calibration laboratory undertaking a calibration of a reference standard for another laboratory in a lower echelon will report a single value of total measurement uncertainty that combines the calibration laboratory's random and systematic components of uncertainty for the measurand. When the lower echelon laboratory uses the calibrated standard, the total uncertainty of its value will then be a systematic component in its effect within the uncertainty budget of that laboratory's further measurements.

2.9 Because the nature of the effect of an uncertainty component can change the CIPM has advocated the grouping of uncertainty components accordance to the method used to estimate their numerical values:

Type A: those that are evaluated by statistical methods.
Type B: those that are evaluated by other means.

2.10 In paragraph 3.3.4 of the *Guide* it is said that the purpose of the type A , and type B classification is to indicate the two difference ways of evaluating uncertainty component and it for convenient in discussion only. Whether components of uncertainty are classify as "random" or "systematic" in relation to specific measurement process, or describe as "Type A" or "Type B" depending on the method of evaluation, all component regardless of classification are modeled by probability distributions quantify by variances or standard deviations. Therefore any convention as to how they are classified does not affect the estimation of total uncertainty. But it should always be remembered that, in the present publication, when the term "random" and "systematic" are used they refer to the effects of uncertainty on specific measurement process. It is the usual case that random components require Type A evaluation, and the systematic component require the Type B evaluations, but there are some exception.

2.11 In general a measurement process can be regarded as having estimated input quantities, given the symbol x, which contribute to the estimated value of the measurand or output quantity, given the symbol y. Where, as in most cases, there are several input quantities these are represented by x_i and the standard uncertainty associated with the estimated value of each input quantity is represented by $u(x_i)$. Standard uncertainty and its evaluation are discussed in Sections 3 and 4.

2.12 The measurement process can usually be modeled by a functional relationship between the estimated input quantities and the output estimate in the form

$$y = f(x_1, x_2, x_3\ldots\ldots x_n) \qquad (1)$$

For example, if electrical resistance R is measured in terms of voltage V and current I then the relationship is $R = f(V,I) = V / I$. The mathematical model of the measurement process is used to identify the input quantities that need to be considered in the uncertainty budget and their relationship to the total uncertainty for the measurement. In some cases the input quantities are not in the same units as the output quantity, as in the above example, and each input uncertainty will need to be multiplied by an appropriate factor (see section 5) before it is combined with the other uncertainties.

3. Type A evaluation of standard uncertainty.

3.1 A Type A evaluation will normally be used to obtain a value for the repeatability or randomness of a measurement process exhibited on one particular occasion. For some measurements, the random component of uncertainty may not be significant in relation to other contributions to uncertainty. It is nevertheless desirable for any measurement process that the relative importance of random effects be established. When there is a significant spread in a sample of measurement results, the arithmetic mean or average of the results should be calculated. If there are *n* independent repeated values for a quantity *q* then the mean value $\overline{q}$ is given by

$$\overline{q} = \frac{1}{n}\sum_{j=1}^{n} qj = \frac{q_1 + q_2 + ... + q_n}{n} \qquad (2)$$

3.2 The spread in the results, ie the range, indicates the merit or repeatability of the measurement process and depends on the apparatus used, the method, and sometimes on the person making the measurement. A useful statistic is the standard deviation σ of the *n* values that comprise the sample, which is given by

$$\sigma = \sqrt{\frac{1}{n}\sum_{i=1}^{n}\left(q_j - \overline{q}\right)^2} \qquad (3)$$

3.3 If further measurements are made, using the same experimental conditions as specified in paragraph 3.2, then, for each sample of results considered, different values for the arithmetic mean and standard deviation will be obtained. For large values of *n*, these mean values approach a central limit value of a distribution of all possible values. This probability density distribution can often be assumed to have the normal form. In practice the measurement process may have limitations in response for large deviations from the mean value and this will cause the actual form of the distribution curve to be truncated to some extent.

3.4 From the results of a single sample of measurements, an estimate, $s(q_i)$, can be made of the standard deviation σ of the whole population of possible values of the measurand from the relation

$$s(q_j) = \sqrt{\frac{1}{(n-1)} \sum_{j=1}^{n} \left(q_j - \overline{q}\right)^2} \qquad (4)$$

It will be noted that this result differs from the standard deviation of the sample itself by the factor 1/(*n*-1) in place of 1/*n* under the square root sign, the difference becoming smaller as the number of measurements *n* is increased.

3.5 The estimated standard deviation of the uncorrected mean value of the measurand is given by

$$s(\overline{q}) = \frac{s(q_j)}{\sqrt{n}} \qquad (5)$$

It may not always be practical to repeat the measurement many times during a calibration. In these cases a more reliable estimate of the standard deviation of a measurement system can be obtained from an earlier Type A evaluation, based on a larger number of readings. If a prior assessment of $s(q_j)$ is used then the value of *n* used in equation (5) to calculate the standard deviation of the mean is the number of repeat readings made for the calibration itself and not that used in equation (4) to obtain the estimated standard deviation.

3.6 Whenever possible at least two measurements should be made as part of the calibration procedure; however, it is acceptable for a single measurement to be made when it is known that the random contributions in the measurement, including those for the device being calibrated, are negligible. For some calibrations it may be desirable to make only one measurement on the device being calibrated, even though it is known to have imperfect repeatability, and to rely on a previous assessment of the repeatability of like devices. This procedure must be treated with caution because the reliability of a previous assessment will depend on the number of devices sampled and how well this sample represents all devices. It is also recommended that data obtained from prior assessment should be regularly reviewed. Of course, when only on measurement is made on the device being calibrated a value of $s(q_j)$ must have been obtained from prior measurements, if only to establish that its effect can be ignored, and *n* in equation (5) is than 1.

NOTE: The degrees of freedom under these circumstances are related to the number of measurements used for the previous assessment and not to that for the calibration itself. Degrees of freedom are discussed in Appendix B.

3.7 A previous estimate of standard deviation can only be used if there has been no subsequent change in the measurement system or procedure that could have an effect on the repeatability. If an apparently excessive spread in measurement values is found the cause should be investigated before proceeding further.

3.8 Although no correction can be made for a random component of uncertainty, equation 5 shows the benefit of increasing the number of measurements even when using a previous good estimate for the standard deviation of the whole population of possible value. However, the benefit becomes progressively less as the number is increased, and it is usually not necessary to make more than about ten measurements and often 4 measurements are sufficient, provided the guidelines mentioned in paragraph 7.3 for the required level of confidence are followed.

3.9 The above statistical analysis of measurement values is a Type A evaluation for a random component of uncertainty. However, a random effect can produce a fluctuation in an instrument's indication, which is both noise-like in character and significant in terms of uncertainty. It may then only be possible to estimate limits to the range of indicated values. This is not a common situation but when it occur a Type B evaluation of the uncertainty component will be required. This is done as described in paragraph 4.5 for the case of a Type B uncertainty when only upper and lower bounds can be assessed.

3.10 The term *standard uncertainty*, $u(x)$, is used for the uncertainty of the result of a measurement expressed as a standard deviation. As mentioned in 2.11, there well usually is more than one input quantity so any individual contribution is identified by a subscript or a unique symbol. Thus the standard uncertainty, $u(x_i)$, of an input quantity, x_i, evaluated by means of repeated measurements is obtained from

$$u(x_i) = s(\overline{q}) \qquad (6)$$

Where $s(\overline{q})$ is calculated in accordance with equation (5).

4. Type B evaluation of standard uncertainty

4.1 It is probable that systematic components of uncertainty, ie those that account for errors that remain constant while the measurement is made, will be obtained from Type B evaluation: the most important of these systematic components, for an instrument, will often be the uncertainties associated with the corrections to indicated values on a calibration certificate issued by a calibration laboratory in a higher echelon in the national calibration system. However, there can be, and usually are, other important contributions to systematic errors in measurement that arise in the instrument user's own laboratory. The successful identification and evaluation of these contributions depends on a detailed knowledge of the measurement process and the experience of the person making the measurements. The need for the utmost vigilance in preventing mistakes cannot be overemphasized. Common examples are errors in the corrections applied to values, transcription errors, and faults in software designed to control or report on a measurement process. The effects of such mistakes cannot readily be included in the evaluation of uncertainty.

4.2 In evaluating the components of uncertainty it is necessary to consider and include at least the following possible sources:

(a) The reported uncertainty for the reference standard and any drift of instability in its value or reading;

(b) the calibration or measuring equipment, including ancillaries such as connecting leads etc., and any drift or instability in values or readings;

(c) The equipment being calibrated or measured, for example its resolution and any instability during calibration;

(d) The operational procedure;

(e) The effects of environmental conditions on any or all of the above.

More detailed guidance concerning sources of error and uncertainty is given in appendices D, E, F and G for electrical calibrations, mass calibrations, temperature calibrations and dimensional calibrations, respectively.

4.3 Whenever possible, corrections should be made for errors revealed by calibration or other sources; the convention is that an error is given a positive sign if the measured value is greater than the conventional true value. The correction for error involves *subtracting* the error from the measured value. On occasion, to simplify the measurement process it may be preferable to treat such an error, when it is small compared with other uncertainties, as if it were a systematic uncertainty equal to (±) the uncorrected error magnitude.

4.4 Having identified all the possible systematic components of uncertainty based as far as possible on experimental data or on theoretical grounds, they should be characterized in terms of standard deviations based on the assessed probability distributions. The probability distribution of an uncertainty obtained from a Type B evaluation can take a variety of forms but it is generally acceptable to assign well defined geometric shapes for which the standard deviation can be obtained from a simple calculation. The distributions discussed below will be applicable in the majority of cases.

4.5 When it is possible to assess only the upper and lower bounds of an error a rectangular probability distribution should be assumed for the uncertainty associated with this error, (See, however, Section 2.5.). Then, if a_i is the semi-range of variation the standard deviation, again referred to as the standard uncertainty, $u(x_i)$, is given by

$$u(x_i) = \frac{a_i}{\sqrt{3}} \tag{7}$$

The *Guide* gives some information on the derivation of this expression.

4.6 An uncertainty obtained from a calibration certificate where the level of confidence or a coverage factor (k) has been reported may, unless otherwise indicated, be treated as having a normal probability distribution and the standard uncertainty will be given by

$$u(x_i) = \frac{Expanded\ Uncertainty}{k} \qquad (8)$$

See paragraph 7.2 for a definition of expanded uncertainty. For example a calibration certificate issued by an accredited laboratory for an instrument will normally report an expanded uncertainty based on $k = 2$ and include a statement that relates this to a confidence level of approximately 95% (see Section 8.1). However, if only a level of confidence is given, for example "confidence probability not less than 95%", then a normal distribution can be assumed with a coverage factor $k = 2$. The following relationships apply, in the case of a normal distribution, to other levels of confidence:

k = 2.58 for 99% confidence
k = 3 for 99.7% confidence

If a value of k greater than 2 is given but the level of confidence is quoted as 95% (see Appendix B for details of when this will occur) then the value given for k must be used in equation (8). In this situation the effective degrees of freedom υ_{eff} will also need to be considered.

4.7 When an instrument has been certified as conforming to specification then the uncertainty in the calibration should have been taken into account. Since it is not the normal practice of most instrument manufacturers to declare confidence levels for tolerances, rectangular probability distributions can be assumed (see, however, paragraph 2.5), ie

$$u(x_i) = \frac{Tolerance\ Limit}{\sqrt{3}}$$

Note: If tolerance limits had, for example, been quoted with a level of confidence corresponding to 3 standard deviations of the manufacturer's production probability distribution then one would have taken the instrument's uncertainty contribution as

$$u(x_i) = \frac{Tolerance\ Limit}{3}$$

4.8 In some cases an uncertainty may already be expressed as a standard uncertainty, eg. when it is derived from a calibration performed on one of the component parts of a measurement system. Clearly, in this case, no further calculation is required.

5. Combined standard uncertainty

5.1 Once the standard uncertainties $u(x_i)$of the input quantities x_i have been derived from both Type A and Type B evaluations, the standard uncertainty of the output quantity $y = f(x_1, x_2, \ldots.., x_N)$, can be calculated as follows

$$U_c(y) = \sqrt{\sum_{i=1}^{n} c_i^2 u^2(x_i)} \equiv \sqrt{\sum_{i=1}^{n} u_i^2(y)} \qquad (9)$$

where c_i , a sensitivity coefficient, is the partial derivative $\partial f / \partial x_i$, or in some cases a known coefficient, such as the temperature coefficient of expansion and $u_i(y) \equiv | c_i | ux_i$ An example of the combined standard uncertainty is as follows

$$U_c(y) = \sqrt{\left(\frac{c_1 U_1}{k}\right)^2 + \frac{c_2^2 a_2^2 + c_3^2 a_3^2}{3} + c_4^2 u^2(x_4)}$$

Where the error associated with U_1 has a normal probability distribution, a_2 and a_3 are limits with rectangular probability distributions, all obtained from Type B evaluation, and $u(x_4)$ is obtained from Type A evaluation.

5.2 The calculations required to obtain sensitivity coefficients by partial differentiation can be a lengthy process, particularly when there are many individual contributions and uncertainty estimates are needed for a range of values. If the functional relationship is not known for a particular measurement system the sensitivity coefficients can sometimes be obtained by the practical approach of changing one of the input variables by a known amount, while keeping all other inputs constant, and noting the change in the output quantity. This approach can also be used if f is known, but if f is not a straightforward function the determination of partial derivatives required is likely to be error prone. In this approach the partial derivative $\partial f/\partial x_i$ can be replaced by the quotient $\Delta f/\Delta x_i$ where Δf is the change in f resulting from a change Δx_i in x_i It is important to choose the magnitude of the change Δx_i carefully. It should be balanced between being sufficiently large to obtain adequate numerical accuracy (number of numerically significant figures) in Δf and sufficiently small to provide a mathematically sound approximation to the partial derivative.

5.3 If the functional relationship is an addition or subtraction of the input quantities, for example

$$Wx = f(W_s, D_s, \delta I_d, \delta C, Ab) = W_s + D_s + \delta I_d + \delta C + Ab$$

Then all the input quantities will be in the same units as the output quantity and the partial derivatives will all be unity.

5.4 If the functional relationship is product or quotient, ie the output quantity is obtained from only the multiplication or division of the input quantities, this can be transform to a linear addition by the use of relative uncertainties, eg expressed in % or part per million. The general form is $y = cx_1^{p_1} \cdot x_2^{p_2} .....x_m^{p_m}$ where the exponent p_i are known positive or negative numbers. The standard uncertainty will then be given by

$$\frac{u_c(y)}{y} = \sqrt{\sum_{i=1}^{n}\left[\frac{p_i u(x_i)}{|x_i|}\right]^2} \qquad (10)$$

This of the same form as equation (9) but with the standard uncertainties expressed as relative values.

Some examples of the use of the relative uncertainty are

$P = f(V,I) = V{\cdot}I$ and $\frac{u(P)}{P} = \sqrt{\left[\frac{u(V)}{V}\right]^2 + \left[\frac{u(I)}{I}\right]^2}$

$P = f(V,R) = V^2/R$ and $\frac{u(P)}{P} = \sqrt{\left[\frac{2u(V)}{V}\right]^2 + \left[\frac{u(R)}{R}\right]^2}$

$V = f(P,Z) = (P{\cdot}Z)^{1/2}$ and $\frac{u(V)}{V} = \sqrt{\left[\frac{u(P)}{2P}\right]^2 + \left[\frac{u(Z)}{2Z}\right]^2}$

The use of relative uncertainties can often simplify the calculations and is particular helpful when the input quantities and the uncertainties are already given in relative terms. However, sensitivity coefficients may still be required to account for known relationship, such as temperature coefficient. Relative uncertainties should not be used when the functional relationship is already an addition or subtraction.

6. Correlated input quantities

6.1 The expressions given for the standard uncertainty of the output estimate, equations (9) and (10), will only apply when there is no correlation between any of the input estimates, that is, the input quantities are independent of each other. It may be the case that some input quantities are affected by the same influence quantity, eg temperature, or by the errors in a particular instrument that is used for separate measurements in the same process. In such cases the input quantities are not independent of each other and the equation for obtaining the standard uncertainty of the output estimate must be modified.

6.2 The effects of correlated input quantities may serve to reduce the combined standard uncertainty, such as when an instrument is used as a comparator between a standard and an unknown, and this is referred to as negative correlation. In other cases measurement errors will always combine in one direction and this has to be accounted for by an increase in the combined standard uncertainty. This is referred to as positive correlation. Knowledge concerning the possibility of correlation can often be obtained from the functional relationship between the input quantities and the output quantity but it may also be necessary to investigate the effects of correlation by making a planned series of measurements.

6.3 If positive correlation between input quantities is suspected but the degree of correlation cannot easily be determined then the most straightforward solution is to add arithmetically the standard uncertainties for these quantities to give a new standard uncertainty that is then dealt with in the usual manner in equation (9) or (10). The Guide should be consulted for a more detailed approach to dealing with correlation based on the calculation of correlation coefficients.

7. Expanded uncertainty and level of confidence

7.1 In most fields of measurement there is a need for some statement of confidence that can be associated with a calculated total uncertainty. It is helpful in making valid comparisons of measurement results and in giving proper meaning to an uncertainty reported on a certificate in terms of probability that the reported value of a measurand with its associated (±) uncertainty provides a range of values that includes the true value. A further consideration is the choice of level of confidence, also referred to as coverage probability. Although the utmost confidence in a statement of total uncertainty for a measurement will always seem desirable, in a hierarchical national system of laboratories involving the propagation of uncertainties from one echelon to the next, this level of confidence is not possible for many measurements.

7.2 The *Guide* recognizes the need for providing a level of confidence associated with an uncertainty and uses the term expanded uncertainty, U, which is obtained by multiplying the combined standard uncertainty by a coverage factor, k, thus

$$U = k \cdot u_c(y) \qquad (11)$$

7.3 UKAS, in line with EAL and generally accepted international practice, recommends that a coverage factor of $k = 2$ is used to calculate the expanded uncertainty. This value of k will give a level of confidence of approximately 95% (95.45%), assuming a normal distribution. However, if the random contribution to uncertainty is relatively large compared with other contributions and the number of repeat readings is small there is a possibility that the probability distribution will not be normal in form and a value of $k = 2$ will give a level of confidence of less than 95%. In these circumstances the procedure given in

Appendix B should be used to obtain a value for the coverage factor that maintains the level of confidence at approximately 95%. A criterion that can be used to determine whether or not to use the procedure in Appendix B is as follows:

Generally, if an uncertainty assessment involves only one Type A evaluation and the number of readings, n, is greater than 2 and the combined standard uncertainty is more than twice the Type A uncertainty then k = 2 will provide a coverage probability of approximately 95% and there is no need to use Appendix B to obtain a different value for the coverage factor.

Further detail on the justification for this criterion is given in paragraph B7.

This may be of particular relevance to testing laboratories where it may not be practical, or even possible, to carry out many repeat measurements. It might be noted that it was not considered necessary to use Appendix B for any of the calibration examples included in Appendix H.

7.4 It has been mentioned that the ideal level of confidence for all measurements would be the utmost level of confidence, which is approaching 100% probability. If each uncertainty contribution were based on a rectangular distribution, arithmetic summation of their ranges would yield such a level of confidence. However, this procedure leads to considerably increased values of total uncertainty with very small probabilities that the true values are actually near the range limits, when the input quantities are uncorrelated.

7.5 If a level of confidence of 95% is considered to be too low for a particular calibration then a higher coverage factor, eg k = 3, giving a level of confidence of approximately 99.7%, can be used.

7.6 A statement of confidence cannot in practice report a specific level of probability, such as 95%, as this requires knowledge of the actual probability distribution for each quantity upon which the value of a measurand depends. Nevertheless the ability to report an approximate level of confidence does give a very valuable meaning to a measurement result.

7.7 In some circumstances the value of U calculated for a level of confidence of 95% using the procedure given in this document will be greater than the total uncertainty obtained by arithmetic summation and there fore represents an unrealistic result. This situation could occur where there is a dominant type B contribution with a theoretical U shape or assumed rectangular distribution, in which case the procedure given in appendix C should be followed to obtain the value of U.

8. Reporting of results

8.1 After the expanded uncertainty has been calculated for a level of confidence of 95% the value of the measurand and expanded uncertainty should be reported as $y \pm U$ and accompanied by the following statement of confidence:

"The reported expanded uncertainty is based on a standard uncertainty multiplied by a coverage factor k = 2, providing a level of confidence of approximately 95%. The uncertainty evaluation has been carried out in accordance with UKAS requirements".

8.2 In cases where the procedure of Appendix B has been followed the actual value of the coverage factor should be substituted for k = 2 and the following statement used:

"The reported expanded uncertainty is based on a standard uncertainty multiplied by a coverage factor k = XX, which for a t-distribution with ν_{eff} = YY effective degrees of freedom corresponds to a coverage probability of approximately 95%. The uncertainty evaluation has been carried out in accordance with UKAS requirements".

8.3 The common use of the word "approximately" in this context has generated a considerable amount of debate about its specific meaning. For the purposes of this document "approximately" is interpreted as meaning "effectively" or "for most practical purposes".

8.4 In the special circumstances where a dominant Type B contribution occurs refer to Appendix C. If a two-part uncertainty is being reported, refer to Appendix I.

8.5 Uncertainties are usually expressed in bilateral terms (±) either in units of the measurand or as relative values, for example as a percentage (%), parts per million (ppm), 1 in 10^x, etc. However there may be situations where the upper and lower uncertainty values are different; for example if cosine errors are involved. If such differences are small then the most practical approach is to report the expanded uncertainty as ± the large of the two. However if there is a significant difference between the upper and lower values then they should be evaluated and reported separately.

8.6 The number of figures in a reported uncertainty should always reflect practical measurement capability. In view of the process for estimating uncertainties it is seldom justified to report more than two significant figures. Uncertainties should normally be rounded up to the appropriate number of figures but may be rounded down when this does not significantly reduce confidence in a measurement result.

8.7 The numerical value of the measurement result should normally be rounded to the least significant figure in the value of the expanded uncertainty quoted unless there are justifiable reasons for quoting more figures. The normal rules of rounding apply however if the rounding decreases the value of the uncertainty by more than 5% the rounded-up value should be used. Rounding of results and uncertainties should be carried out only at the final stages of the calculation in order to prevent cumulative rounding errors having a significant effect.

9. Step by step procedure for the determination of measurement uncertainty

The following is a guide to the use of this code of practice for the treatment of uncertainties. The left hand column gives the general case while the right hand column indicates how this relates to example H4 in Appendix H. Although this example relates to a calibration activity, the process for testing activities is unchanged.

9.1 If possible determine the mathematical relationship between the input quantities and the output quantity:

$$y = f\,(x_1, x_2, x_3, \ldots\ldots\ldots\ldots x_n) \qquad (1)$$

9.2 Identify all corrections that have to be applied to the results of measurements of a quantity (measurand) for the conditions of measurement.

9.3 List systematic components of uncertainty associated with corrections and uncorrected systematic errors treated as uncertainties.

Seek prior experimental work or theory as a basis for assigning uncertainties and probability distributions to the systematic components of uncertainty.

Calculate the standard uncertainty for each component of uncertainty, obtained from Type B evaluation, using equation (7) for assumed rectangular distributions:

$$u(x_i) = \frac{a_i}{\sqrt{3}} \qquad (7)$$

Or equation (8) for assumed normal distributions:

$$u(x_i) = \frac{Expanded\ Uncertainty}{k} \qquad (8)$$

Or refer to other references if the assumed probability distribution is not covered in this publication.

9.4 Use prior knowledge of make trial measurements and calculations to determine if there is going to be a random component of uncertainty that is significant compared with the effect of the listed systematic components of uncertainty:

9.5 If a random component of uncertainty is significant make repeated measurements to obtain the mean from equation (2):

$$\overline{q} = \frac{1}{n}\sum_{j=1}^{n} q_j \qquad (2)$$

9.6 Either calculates the standard deviation of the mean value from equations (4) and (5):

$$s(q_j) = \sqrt{\frac{1}{(n-1)}\sum_{j=1}^{n}\left(q_j - \bar{q}\right)^2} \tag{4}$$

$$s(\bar{q}) = \frac{s(q_j)}{\sqrt{n}} \tag{5}$$

Or refer to the results of previous repeatability measurements for a good estimate of $s(q_j)$ based on a larger number of readings.

9.7 Even when a random component of uncertainty is not significant, where possible always check the instrument indication at least once to minimize operator recording mistakes.

9.8 Derive the standard uncertainty for the above Type A evaluation from equation (6):

$$u(x_i) = s(\bar{q}) \tag{6}$$

9.9 Calculate the combined standard uncertainty for uncorrelated input quantities using equation (9) if absolute values are used:

$$U_c(y) = \sqrt{\sum_{i=1}^{n} c_i^2 u^2(x_i)} \equiv \sqrt{\sum_{i=1}^{n} u_i^2(y)} \tag{9}$$

Where c_i is the partial derivative $\partial f/\partial x_i$, or a known sensitivity coefficient.

Alternatively use equation (10) if the standard uncertainties are relative values:

$$\frac{u_c(y)}{y} = \sqrt{\sum_{i=1}^{n}\left[\frac{p_i\ u(x_i)}{|x_i|}\right]^2} \tag{10}$$

Where p_i are the known positive or negative exponent in the functional relationship.

9.10 If correlation is suspected use the guidance in paragraph 6.3 or refer to other referenced documents.

9.11 Either calculates an expanded uncertainty from equation (11):

$$U = k \cdot u_c(y) \tag{11}$$

Or, if there is a significant random contribution evaluated from a small number of readings (see section 7.3), use Appendix B to calculate a value for k_p and use this value to calculate the expanded uncertainty.

9.12 Report the expanded uncertainty in the value of the measurand in accordance with Section 8.

Appendix B

Sharp Laser Diode, Rotary Encoder,
MT101 Counter Circuit Board,
Multi-Function Optical Meter and
Digital Real-time Oscilloscope (TDS220)

Sharp Laser Diode LT022MC

LT022MC/MD/MF

Features

- Low noise
  S/N: 60 dB (according to measurement method Fig. 29-2)
- Wavelength: 780nm
- Single transverse mode

Applications

- CD-ROMs
- CD players
- Information processing equipment

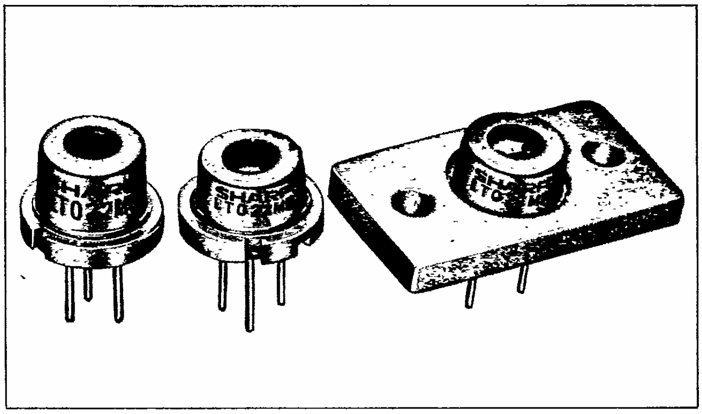

Absolute Maximum Ratings

(Tc=25°C)

Parameter		Symbol	Ratings	Units
Optical power output		Po	5	mW
Reverse voltage	Laser	V_R	2	V
	PIN		30	
Operating temperature*1		Topr	−10~+60	°C
Storage temperature*1		Tstg	−40~+85	°C
Soldering temperature*2		Tsol	260 (less than 5 seconds)	°C

*1 Case temperature *2 At point 1.6 mm from lead base

Electro-optical Characteristics*1

(Tc=25°C)

Parameter			Symbol	Condition	Ratings			Units
					MIN	TYP	MAX	
Threshold current			Ith	—	—	50	80	mA
Operating current			Iop	Po=3mW	—	65	100	mA
Operating voltage			Vop	Po=3mW	—	1.75	2.2	V
Wavelength*2			λp	Po=3mW	770	780	790	nm
Monitor current			Im	Po=3mW V_R=15V	0.3	0.9	1.6	mA
Radiation characteristics	Angle*3	Parallel to junction	θ //	Po=3mW	8.5	11	16	deg
		Perpendicular to junction	θ⊥	Po=3mW	20	33	45	deg
	Ripple			Po=3mW	—	—	±20	%
Emission point accuracy	Angle		Δϕ //	Po=3mW	—	—	±2	deg
			Δϕ⊥	Po=3mW	—	—	±3	deg
	Position*4		Δx, Δy, Δz	—	—	—	±80	μm
Differential efficiency			η	$\frac{2mW}{I_F(3mW)-I_F(1mW)}$	0.1	0.25	0.6	mW/mA

*1 Initial value *3 Angle at 50% peak intensity (full width at half-maximum)
*2 Single transverse mode *4 Not specified for LT022MF

Electrical Characteristics of Photodiode

(Tc=25°C)

Parameter	Symbol	Condition	Ratings			Units
			MIN	TYP	MAX	
Sensitivity	S	V_R=15V	—	0.3	—	mA/mW
Dark current	I_D	V_R=15V	—	—	150	nA
Terminal capacitance	Ct	V_R=15V	—	8	20	pF

Rotary Encoder

Nemicon : Rotary Encoder
Model OSS-1-2 Resolution 100 P/R

Electronic Feature

- Supply Voltage 4.5-5.5 V
- Output Voltage 5 V
- Maximum Output Current 20 mA
- Rise Time and Fall Time 2 µS
- Maximum Frequency Response 150 kHz

Wave From

$$P = \frac{1}{\text{Resolution}}\ ,\ a, b, c, d = \frac{P}{4} \pm \frac{P}{8}$$

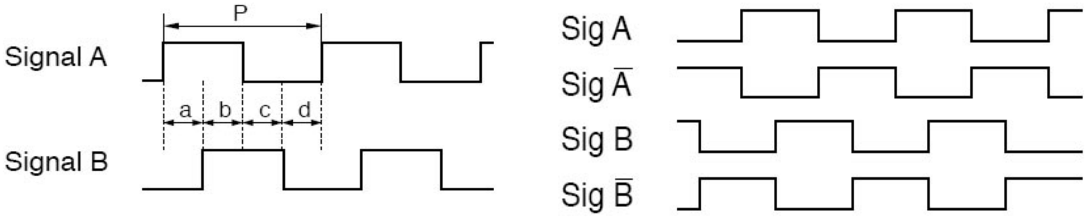

Appendix Figure B1 Output signal A and B

External Dimension

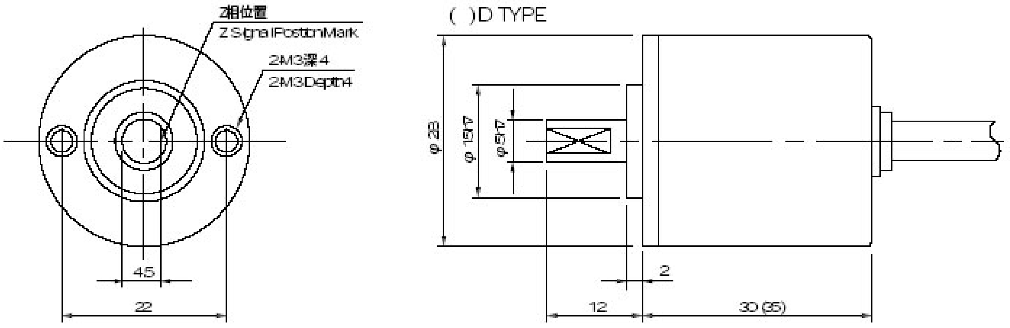

Appendix Figure B2 External dimension

Electrical Connection

Appendix Table B1 Rotary Encoder Electrical connection

Color of Lead Wire	Description
Red	Power Source
Black	0V Common
Green or Blue	Signal A
White	Signal B
Shielding Braid	NC

MT101 Counter Circuit Board

1. Circuit Block Diagram

The even counter circuit is designed on the printed circuit board (pcb.) size 90 × 90 mm. The circuit consists of blocks diagram as illustrated in appendix figure D1.

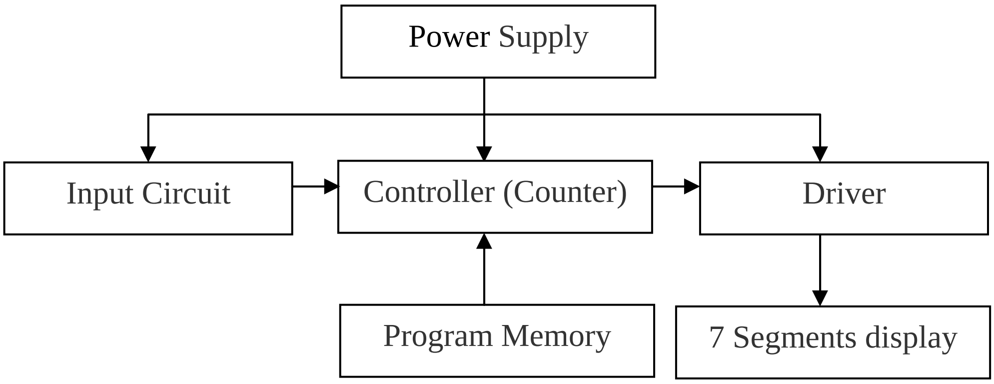

Appendix Figure B3 Block Diagram

The power supply block diagram consists of C6, C5 IC4, D1 and D2. The IC4 is the voltage regulator circuit using IC number 7805 to regulate a stable 5 volts (VCC), supply to the whole circuit. Diode D1 acts as the rectifier circuit, while the D2 also acts as rectifier, but after filter by C5, R1 the current feed to RB0 of IC1 to enable the IC1 to perform the power down nonvolatile operation, and protect the whole circuit from accidental reverse polarity voltage.

This circuit provides 2 channels of counting input (input 1, and input 2). Those 2 channels have benefit of performing several input signal types such as photo transistor, infrared sensor, external contact switch, and also provide internal switch for failure testing. The block diagram of input circuit consists of IC3, R6, R7, JP2, D3 and C7. IC3 is a CMOS number 4093 that contain 2 AND gates which could perform Schmidt trigger ability. Resistor R6 and R7 is a pull up resistor those perform a noise reduction, and signal condition. In this thesis, the interference fringes deviation which comes while the optical path difference change could be detected by semiconductor sensor such as photo diode or photo transistor. Detection signal from semiconductor sensor provide 2 modes of operation, the photo conductive and photo voltaic mode. The jumper JP2 of input channel 2 is designed for the purpose of photo detector operation in photo conductive mode. For normal operation, JP2 is closed, and the circuit could detect the pulse voltage, or contact switch. When JP2 is open, the circuit performs counting signal pulse from semiconductor sensor.

The main counter circuit is operated with microcontroller IC1 (PIC 16C57) (software compatible with micro controller MCS51). The controller received input signal from IC3 through resistors RA0, RA1 of port A. The resistors RA2, RA3 are the CPU enable signal such as reset, or up/down mode selector (open or shot JP1), this operation must be together with resistors RC6 and RC7. The group of components such as T7, R22 to R25, and C1 is the clock circuit which supplying the e-clock pulse, and also acts as power on reset.

At port C, resistors RC0 to RC5 generate sequence of negative pulse applied to the PNP transistor T1 to T6 (C9012) as driving signal. When each transistor receives driving signal, it allows the current from power supply to feed each of LED 7 segment. The display is a six digit display. Each of the six digit is turn on one at a time. It means that each digit scans the switching display at different time. The 7 segment circuit is designed to use common cathode to fit this operation. The numeric signals codes (of 7 segments LED) are form resistors RB1 to RB7. Each code synchronizes with the digit scanning signal.

2. Circuit Schematic Diagram

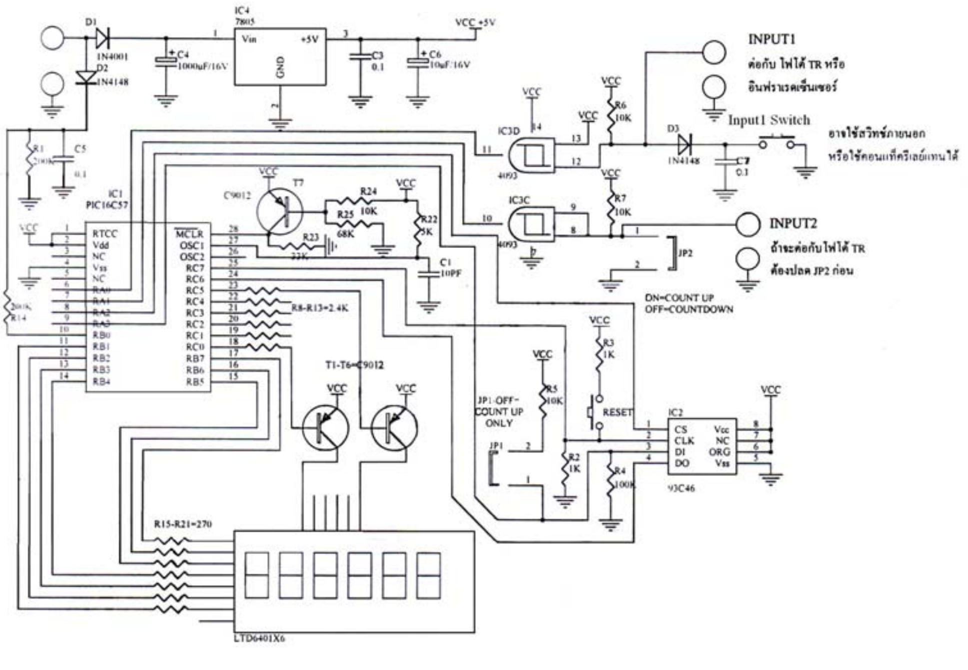

Appendix Figure B4 Circuit schematic diagram

3. Part List

Appendix Table B2 MT101 counter board parts list

Number	Symbol	Description	Amount (pcs.)	Note
1	R1, R14	200 KΩ	2	
2	R2, R3	1 KΩ	2	
3	R4	100 KΩ	1	
4	R5-R7, R24	10 KΩ	4	
5	R8-R13	204 KΩ	6	
6	R15-R21	270 Ω	7	
7	R22	5 KΩ	1	
8	R23	33 KΩ	1	
9	R25	68 KΩ	1	
10	C1	10 pF	1	
11	C3, C5, C7	0.1 μF	1	
12	C4	1000 μF/16V	1	
13	T1-T7	C9012	7	
14	JP1-JP2	-	2	
15	IC Socket	8 pin	1	
16	IC Socket	14 pin	1	
17	IC Socket	28 pin	1	
18	LED 7 segment	LTD4601P	3	
19	D1	1N4004	1	
20	D2-D3	1N4148	2	
21	IC1	PIC16C57	1	
22	IC2	93C46	1	
23	IC3	4093B	1	
24	IC4	7805	1	
25	PCB	MT101	1	

Multi-Function Optical Meter

Appendix Figure B5 Multifunction optical meter

Appendix Table B3 Specifications

Display Type	Info
Sampling Resolution	20,000 count £25 Hz, 4096 count £1 kHz
Gain Ranges	7 decades
Current Sensitivity (full-scale)	2.5 nA–2.5 mA
Voltage Sensitivity (full-scale)	790 µV–25 V
Resolution	100 fA, 125 nV
Sampling Rate	Up to 1 kHz single-channel, Up to 500 Hz dual-channel
Bandwidth (-3 dB)	DC to 1 MHz(1)
Analog Output	0–2.5 V into 50W
DC Accuracy	<±0.1% typical
Peak-to-Peak Accuracy	±1% typical
Pulse-to-Pulse Accuracy	±1% typical
Integration Accuracy	±1% typical
Power Requirements	90–240 VAC
Weight [lb (kg)]	2.5 (1.1)
Dimensions (W x H x D) [in. (mm)]	8.5 (216) x 4 (102) x 14 (356)
Operating Temperature	10°C to 40°C, <80% RH
Storage Temperature	-25°C to 60°C, <90% RH

Appendix Table B4 System specifications (with Low-Power 818-Series Detectors)

Model	**818-UV/CM**	**818-SL/CM**	**818-F-SL**	**818-ST/CM**	**818-IR/CM** **818-F-IR**	**818-IG/CM**	**818-IS-1**
Material	Silicon	Silicon	Silicon	Silicon	Germanium	Indium Gallium Arsenide	InGaAs/Si
Diameter (cm)	1.13	1.13	0.3	1 x 1	0.3	0.3	N/A
Wavelength (nm)	190–1100	400–1100	400–1100	400–1100	780–1800	800–1650	400–1650
Power Range (dBm)	-83 to +23	-90 to +33	-90 to +3	-70 to +33	-70 to +21.5(2)	-90 to +21.5	-70 to +23
Accuracy (%)(1)	±2	±2	±2	±2	±3	±2	±2.5
Applicable wavelength range (nm)	200–1100	400–1100	400–1100	400–1100	780–1700	800–1650	400–1650
Linearity				±0.5%			
NEP @ 5 Hz and 1 A/W	50 fW/√Hz	50 fW/√Hz	50 fW/√Hz	3 pW/√Hz	4 pW/√Hz	30 fW/√Hz	3 pW/√Hz(3)

1) At calibration temperature maintained to ± 0.2°C, -20 dBm level having 99% encircled energy on detector with no optical attenuator.

2) -70 to +3 dBm for 818-F-IR

3) 0.01 A/W for the 818-IS-1

Digital Real-time Oscilloscope (TDS220)

Appendix Table B5 Vertical specification

	Measurement Type	*Accuracy*
DC Measurement Ac- curacy Average Ac- quisition Mode	Average of ≥ 16, waveforms with vertical position at zero	(± 4% × reading + 0.1 div + 1 mV)
	. Average of ≥ 16 waveforms with vertical position not at zero	± 3% × (reading + vertical position) + 1% of vertical position + 0.2 div] Add 2 mV for settings from 2 mV/div to 200 mV/div. Add 50 mV for settings from > 200 mV/div to 5 V/div.
Delta Volts Measurement Accuracy, Aver- age Acquisition Mode	Delta volts between any two averages of ≥ 16 waveforms acquired under same setup and ambient conditions	(± 3% × reading + 0.05 div)

Appendix Table B6 Horizontal specification

Sample Rate Range	50 S/s to 1 GS/s	
Waveform Interpolation	(sin x)/x	
Record Length	2500 samples for each channel	
SEC/DIV Range	5 ns/div to 5 s/div, in a 1, 2.5, 5 sequence	
Sample Rate and Delay lime Accuracy	ppm over any ± 1 ms time interval	
Delta Time Measurement Accuracy (Full Bandwidth)	*Conditions*	*Accuracy*
	Single-shot, Sample mode	± (1 sample interval + 100 ppm × reading + 0.6 ns)
	> 16 averages	± (1 sample interval + 100 ppm × reading + 0.4 ns)
	Sample interval = s/div ÷ 250	
Position Range	5 ns/div to 10 ns/div	(-4 div × s/div) to 20 ms
	25 ns/div to 100 is/div	(-4 div × s/div) to 50 ms
	250 ns/div to 5 s/div	(-4 div × s/div) to 50 s

Appendix C

Calculation of Rotation Rate and Uncertainty

Calculation of Rotation Rate and Uncertainty

Rotation rate can be determined by measure pulse per round and pulse width at the moment from encoder. To measure pulse per round, experiment is set as show in figure 00.

Appendix Table C1 Measurement of pulse per round using MT101 board

Run	Pulse/round
1	942
2	945
3	940
4	944
5	942

Mean = 942.6, Standard deviation = 1.949,
Standard deviation of mean (Uncertainty) =$1.949 \big/ \sqrt{4} = 0.9745 \cong 1$.

From table C1, encoder generated $\approx 943 \pm 1$ pulses while main gear rotates 360 degree. Then

$$\frac{\deg ree}{pulse} = \frac{360}{943 \pm 1}$$

if $R = \frac{x}{y}$, first norm calculation for uncertainty is $\frac{\Delta R}{R} = \frac{\Delta x}{x} + \frac{\Delta y}{y}$, so

$$\frac{\Delta R}{0.38176} = \frac{0}{360} + \frac{1}{943}$$

$$\Delta R = 0.0004°$$

$$\therefore \quad \text{degree/pulse} = 0.38 \pm 0.0004°$$

1 count from MT101 includes positive and negative pulse that generated from encoder. Then, time between counts is equal to 1 period.

$$\text{degree/pulse} = \text{degree/period} = 0.38 \pm 0.0004°$$

1 degree = 0.01745 radian, then

$$\text{radian/period} = (0.38 \pm 0.0004) \times 0.01745 = 0.00663 \pm 6.98 \times 10^{-6}$$

Using time cursor measurements function of oscilloscope (Tektronix TDS220) to analyze and measure the period time and collect data of period at every rotation rate.

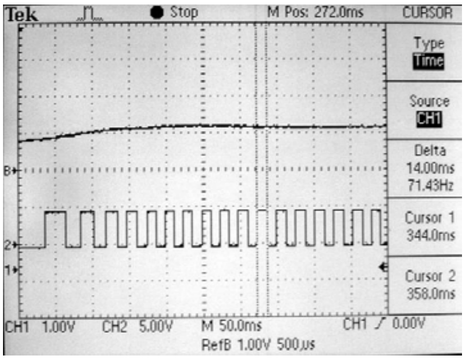

Appendix Figure C1 Measure period time with time cursor function of oscilloscope.

Example calculation of uncertainty at rotation rate No.3.

- Statistical (Type A) uncertainty

Mathematical model of measurement is defined as follows

$$f(x_i) = x_i \pm U \tag{1}$$

where x_i = period time

U = uncertainty of measurement

Average value ($\bar{x}$)

$$\bar{x} = \frac{1}{n}\sum_{i=1}^{n} x_i \tag{2}$$

$$= \frac{(28+28+28+24+28)}{5}$$

$$= 27.2 \text{ ms}$$

Standard deviation ($S(x_i)$)

$$S(x_i) = \sqrt{\frac{1}{(n-1)}\sum_{i=1}^{n}\left(x_i - \bar{x}\right)^2} \tag{3}$$

$$= \sqrt{\frac{(28-\bar{x})^2+(28-\bar{x})^2+(28-\bar{x})^2+(24-\bar{x})^2+(28-\bar{x})^2}{(5-1)}}$$

$$= \ 1.8 \text{ ms}$$

Standard deviation of mean (S($\bar{x}$))

$$S(\bar{x}) \ = \ \left(\frac{S(x_i)}{\sqrt{n}}\right) \tag{4}$$

$$= \ \frac{1.8}{\sqrt{5}} \ = \ \pm 0.8 \text{ ms}$$

The standard uncertainty (U_A) is equal to 0.8 ms

Degree of freedom: $\upsilon_1 = n - 1 = 5 - 1 = 4$

Appendix Table C2 Measurement of period time result.

Rotation Rate No.	Period time (ms)					Mean	STDEV	STDEV of Mean
	Run 1	Run 2	Run 3	Run 4	Run 5			
1	56	56	48	56	48	52.8	4.4	1.96
2	40	44	44	40	44	42.4	2.2	0.98
3	28	28	28	24	28	27.2	1.8	0.80
4	18	18	18	16	18	17.6	0.9	0.40

- Systematic (Type B) uncertainty

From specification, the uncertainty of the digital oscilloscope (Tektronix TDS220) is ± (1 sample interval + 100 ppm × reading + 0.6 ns). Sample interval is equal s/div $\div 250$. Assuming rectangular distribution, the standard uncertainty of oscilloscope is,

$$U_B \ = \ \frac{\left[\left(50ms/250\right) + \left(100 \times 10^{-6} \times \left(27.2ms + 0.6ns\right)\right)\right]}{\sqrt{3}} \tag{5}$$

$$= \ 0.117 \text{ ms} \ \cong \ 0.12 \text{ ms}$$

Degree of freedom: $\upsilon_1 = \infty$

- Combine standard uncertainty evaluation

$$U_C \ = \ \sqrt{U_A^2 + U_B^2} \tag{6}$$

$$= \ \sqrt{0.8^2 + 0.12^2}$$

$$= 0.418 \cong 0.42 \text{ ms}$$

- Effective degree of freedom

$$\nu_{eff} = \frac{(U_C)^4}{\frac{(U_A)^4}{4} + \frac{(U_B)^4}{\infty}} \tag{7}$$

$$= \frac{(0.42)^4}{\frac{(0.8)^4}{4} + \frac{(0.12)^4}{\infty}}$$

$$= \infty$$

- Expand uncertainty

The degree of freedom fro combined standard uncertainty is equal to infinity. This give a coverage factor (k) approximately equals to two at a level of confidence of 95%. Therefore expand uncertainty,

$$U = kU_C \tag{8}$$

$$= 2 \times 0.42 = 0.84 \text{ ms}$$

Appendix Table C3 Uncertainty budget

Source of Uncertainty	Type	U_i	Uncertainty Value (ms)	Probability Distribution	Coverage factor	Standard Uncertainty (ms)	ν_i
Repeatability	A	U_A	0.4	t-distribution	1	0.4	4
Digital Oscilloscope	B	U_B	0.2	Rectangular	$\sqrt{3}$	0.12	∞
Period time measurement	Combined	U_C	-	Normal	-	0.42	∞
Period width measurement	Expanded	U	0.84	Normal	2	-	∞

Appendix Table C4 Period time and uncertainty

Rotational Rate No.	Period time (ms)	Uncertainty (ms)
1	52.8	± 1.97
2	42.4	± 1.01
3	27.2	± 0.84
4	17.6	± 0.46

Using measurement of two experiments above, rotation rate can be calculated by chain rules.

$$\frac{Radian}{period} \times \frac{period}{\sec} = \frac{Radian}{\sec} \tag{9}$$

Then rotation rate No.3 is equal

$$\frac{0.00663 \pm 6.98 \times 10^{-6}}{(27.2 \pm 0.84) \times 2} = 0.0002437 \pm \left[\left(\frac{6.98 \times 10^{-6}}{0.00663} + \frac{0.84}{27.2} \right) \times 0.0002437 \right]$$

$$= 0.0002437 \pm 7.8 \times 10^{-6} \text{ radian/ms}$$

$$\cong 0.24 \pm 0.008 \text{ radian/s}$$

Appendix Table C5 Rotation rate and uncertainty

Rotation Rate No.	radian/s
1	0.13 ± 0.005
2	0.16 ± 0.005
3	0.24 ± 0.008
4	0.38 ± 0.011

Appendix D

Calculation of Uncertainty of Fiber Optic Gyroscope

Calculation of Uncertainty of Fiber Optic Gyroscope

The measurement configuration is shown in appendix figure D1. Using photo detector and optical meter to detect output signal from FOG and transfer measurement result as a voltage to display at oscilloscope. Collect data log from oscilloscope with wave star software via RS232 port.

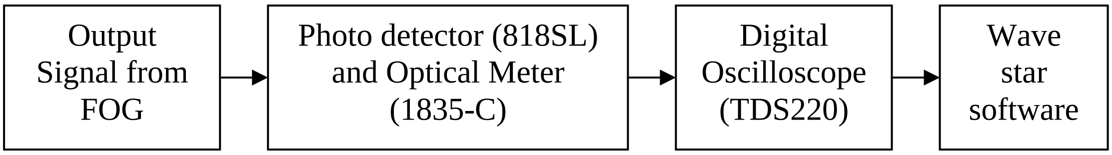

Appendix Figure D1 Measurement configuration.

1. Measurement Record

When all environments meet the condition from design of experiment, the readings were taken at stable rotation rate. Ten measurements were taken at every rotation rate and direction (CW and CCW) as recorded in table D1 and D2.

Appendix Table D1 Measurement records at counter clockwise direction.

ω	Voltage (V) at counter clockwise direction									
(rad/s)	Run 1	Run 2	Run 3	Run 4	Run 5	Run 6	Run 7	Run 8	Run 9	Run 10
0.00	3.45	3.45	3.44	3.44	3.45	3.44	3.44	3.46	3.45	3.44
0.13	3.53	3.64	3.63	3.61	3.67	3.63	3.66	3.66	3.68	3.60
0.16	3.69	3.66	3.69	3.73	3.77	3.79	3.73	3.78	3.80	3.82
0.24	3.86	3.84	3.93	3.94	3.97	3.91	3.94	3.95	3.95	3.96
0.38	4.12	4.33	4.22	4.21	4.29	4.30	4.31	4.25	4.24	4.22

Appendix Table D2 Measurement records at clockwise direction.

ω	Voltage (V) at clockwise direction									
(rad/s)	Run 1	Run 2	Run 3	Run 4	Run 5	Run 6	Run 7	Run 8	Run 9	Run 10
0.00	3.45	3.45	3.44	3.44	3.45	3.44	3.44	3.46	3.45	3.44
0.13	3.29	3.29	3.27	3.31	3.31	3.33	3.33	3.34	3.34	3.29
0.16	3.13	3.00	3.10	3.17	3.16	3.16	3.17	3.19	3.11	3.17
0.24	2.99	3.05	3.07	3.08	3.07	3.06	3.05	3.08	3.07	3.06
0.38	2.92	2.87	2.80	2.91	2.92	2.91	2.92	2.91	2.90	2.90

2. Mathematical Model

The mathematical model is represented as follows:

$$V = D + \text{Correction}$$

where,

V	=	Voltage measured
D	=	Displayed voltage of oscilloscope via wave star software
Correction	=	Correction due to the optical meter with photo detector and digital oscilloscope

3. Uncertainty Equation

The combined standard uncertainty (u_c) includes uncertainties of the repeatability of displayed reading, optical meter with photo detector and digital oscilloscope. This can be represented in the equation below.

$$u_c = \sqrt{u_1^2 + u_2^2 + u_3^2}$$

where,

u_c	=	combined standard uncertainty of the measurement
u_1	=	standard uncertainty of repeatability of measured readings
u_2	=	standard uncertainty of optical meter with photo detector
u_3	=	standard uncertainty of digital oscilloscope

4. Analysis of Measurement Uncertainty Component

4.1 Type A evaluation (example calculation at 0.24 rad/s in CCW direction)

4.1.1 Standard uncertainty of reading, u_1

Mean value, $\bar{V}$ $= \dfrac{1}{10}\sum_{i=1}^{10} V_i$

$$= \frac{(3.86 + 3.84 + 3.93 + 3.94 + 3.97 + 3.91 + 3.94 + 3.95 + 3.95 + 3.96)}{10}$$

$$= 3.93$$

Where V_i are mean of data logs from wave star software as listed in table D1.

The variance is calculated as follows:

$$s^2(V_i) = \frac{1}{n-1}\sum_{i=1}^{n}\left(V_i - \bar{V}\right)^2$$

$$= \frac{1}{9}(0.387105)$$

$$= 0.043 \text{ V}^2$$

Standard deviation

$$s(V_i) = 0.043 \text{ V}$$

Standard deviation of mean is as follow:

$$s(\overline{V}) = \frac{s(V_i)}{\sqrt{n}}$$

$$= \frac{0.043\text{V}}{\sqrt{10}}$$

$$= 0.0136 \text{ V}$$

The standard uncertainty (u_1) is equal to 0.0136 V.
Degree of freedom: υ_1 = n - 1 = 10 - 1 = 9

Appendix Table D3 Mean, standard deviation and standard deviation of mean at CCW direction

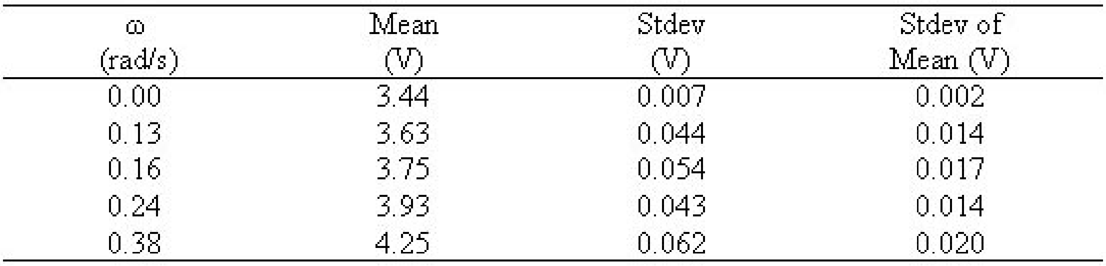

ω (rad/s)	Mean (V)	Stdev (V)	Stdev of Mean (V)
0.00	3.44	0.007	0.002
0.13	3.63	0.044	0.014
0.16	3.75	0.054	0.017
0.24	3.93	0.043	0.014
0.38	4.25	0.062	0.020

Appendix Table D4 Mean, standard deviation and standard deviation of mean at CW direction

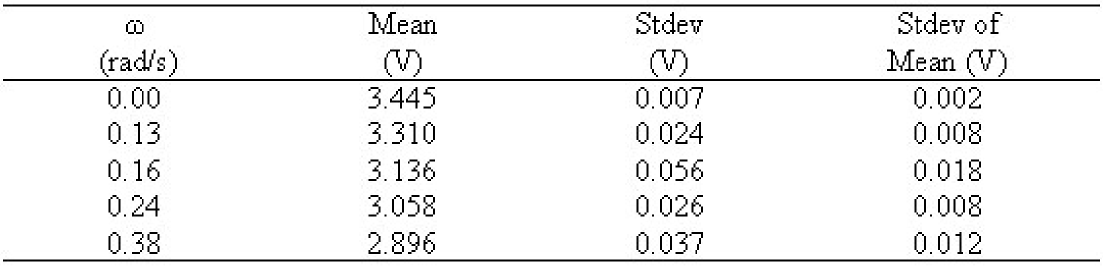

ω (rad/s)	Mean (V)	Stdev (V)	Stdev of Mean (V)
0.00	3.445	0.007	0.002
0.13	3.310	0.024	0.008
0.16	3.136	0.056	0.018
0.24	3.058	0.026	0.008
0.38	2.896	0.037	0.012

4.2 Type B evaluation

4.2.1 Standard uncertainty of optical meter with photo detector, u_2

From system specification the uncertainty of optical meter (1835-c) with photo detector (818SL) is ± 2% of reading. Assuming rectangular distribution, the standard uncertainty of optical meter with photo detector (u_2) is,

$$u_2 = \frac{0.079}{\sqrt{3}}$$

$$= 0.045 \text{ V}$$

Degree of freedom: $\upsilon_2 = \infty$

4.2.2 Standard uncertainty of digital oscilloscope, u_3

From specification, the vertical DC measurement uncertainty of digital oscilloscope is $\pm\left(4\% \times \text{reading} + 0.1\text{div} + 1\text{mV}\right)$ V. Assuming rectangular distribution, the standard uncertainty of digital oscilloscope (u_3) is,

$$u_3 = \frac{\left[4\% \times 3.93 + (0.1 \times 1) + 1\text{mV}\right]}{\sqrt{3}}$$

$$= 0.149 \text{ V}$$

Degree of freedom: $\upsilon_3 = \infty$

5. Combined Standard Uncertainty Evaluation

The combined standard uncertainty of the indicated voltage is:

$$u_c = \sqrt{u_1^2 + u_2^2 + u_3^2}$$

$$= \sqrt{(0.0136)^2 + (0.045)^2 + \left(0.149^2\right)}$$

$$= 0.156 \text{ V}$$

6. Effective Degree of Freedom

Effective degree of freedom of the combined standard uncertainty is given by:

$$\nu_{eff} = \frac{(u_c)^4}{\frac{(u_1)^4}{\upsilon_1} + \frac{(u_2)^4}{\upsilon_2} + \frac{(u_3)^4}{\upsilon_3}}$$

$$= \frac{(0.156)^4}{\frac{(0.0136)^4}{9} + \frac{(0.045)^4}{\infty} + \frac{(0.149)^4}{\infty}}$$

$$= \infty$$

7. Expanded Uncertainty

The degree of freedom fro combined standard uncertainty is equal to infinity. This give a coverage factor (k) approximately equals to two at a level of confidence of 95%. Therefore expand uncertainty,

$$U = kU_C$$

$$= 2 \times 0.156$$

$$= 0.313 \text{ V}$$

8. Uncertainty Budget

Source of Uncertainty	Type	u_i	Uncertainty Value (ms)	Probability Distribution	Coverage factor	Standard Uncertainty (ms)	v_i
Repeatability	A	u_1	0.0136	t-distribution	1	0.0136	9
Optical meter with photo detector	B	u_2	0.079	Rectangular	$\sqrt{3}$	0.045	∞
Digital Oscilloscope	B	u_3	0.258	Normal	$\sqrt{3}$	0.149	∞
Voltage measurement	Combined	u_c	-	Normal	-	0.156	∞
Pulse width measurement	Expanded	u	0.313	Normal	2	-	∞

9. Report of Result

The voltage output from fiber optic gyroscope was measured at rotation rate 0.24 radian/s. The measurement uncertainty is ± 0.313 V. The report of measurement uncertainty is estimated at a level of confidence of approximately 95% with a coverage factor k of 2.

Appendix Table D5 Report of result

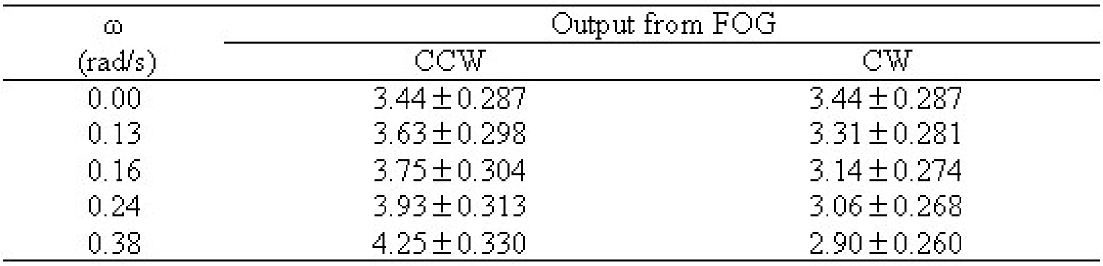

ω (rad/s)	Output from FOG	
	CCW	CW
0.00	3.44 ± 0.287	3.44 ± 0.287
0.13	3.63 ± 0.298	3.31 ± 0.281
0.16	3.75 ± 0.304	3.14 ± 0.274
0.24	3.93 ± 0.313	3.06 ± 0.268
0.38	4.25 ± 0.330	2.90 ± 0.260